Georgios Lagiotis

Green Templeton College (GTC)

Plant Sciences Department

University of Oxford

MicroRNA regulation of axial patterning during Arabidopsis embryogenesis

Michaelmas Term 2013

Thesis submitted for the degree of Doctor of Philosophy

Georgios Lagiotis
Green Templeton College (University of Oxford)
Thesis submitted for the degree of Doctor of Philosophy
Michaelmas Term 2013

MicroRNA regulation of axial patterning during Arabidopsis embryogenesis

Abstract

Pattern formation is the process by which undifferentiated cells divide and differentiate to generate complex tissues and organs. In plants, pattern formation begins in embryogenesis and continues post-embryonically with the function of the meristems. microRNAs (miRNAs), which are small regulatory RNAs that repress gene expression, are involved in a variety of patterning processes in plants, including the formation and function of the meristems and establishment of polarity. For example, regulation of the class III HOMEODOMAIN-LEUCINE ZIPPER (HD-ZIP III) transcription factors by miR165/6 is not only involved in the formation and function of the meristems, but also in polarity establishment in the leaf, and in axial patterning during embryogenesis. To gain a better understanding of the role of miRNAs in embryonic patterning, I investigated the tissue-specific functions of the miRNA biogenesis protein SERRATE (SE), which is required for the regulation of the HD-ZIP IIIs via miR165/6. By expressing SE in various domains in *se-5* null mutant embryos, I revealed that although SE is expressed throughout the embryonic body, tissue-specific expression of SE from either the upper or lower tier of the embryo is sufficient for correct patterning. This observation suggests a SE-dependent non-cell autonomous and bi-directional mechanism that influences patterning in Arabidopsis embryos. Furthermore, through a suppressor screen of a *se-3* loss-of-function mutant allele, I identified mutants in genes that likely function upstream of *SE*, and downstream or in parallel of the *HD-ZIP IIIs*. One of those *se-3* suppressors is likely to be a mutant in the *BELL* homeobox gene *POUND-FOOLISH* (*PNF*).

Acknowledgements

Firstly, I would like to thank my supervisor Professor Dr. Miltos Tsiantis for the opportunity he gave me to work in his lab on a very interesting project. His supervision, guidance, immense knowledge, and patience, were essential for my personal development as a scientist, as well as the development of my project. I would like to thank Dr. Ian Moore, my second supervisor, for his advice and recommendations on my project. I would also like to thank BBSRC (Biotechnology and Biological Sciences Research Council) and Marie Curie ITN-SIREN (Initial Training Network-SIgnal and REgulatory Networks in early plant embryogenesis) for the generous funding that made this study possible.

I am grateful to all members of the ITN-SIREN network for the opportunities they gave me to present my work, improve my communication and scientific skills, for fruitful discussions on plant embryogenesis and the exchange of knowledge and materials. I would especially like to thank Professor Dr. Dolf Weijers and Professor Dr. Ben Scheres who provided materials for cloning and several transgenic strains. I would also like to thank NASC (Nottingham Arabidopsis Stock Centre) for providing seed stocks, and BGI TECH SOLUTIONS (HONGKONG) CO., LIMITED for the whole genome sequencing experiment of the *se-3* suppressors.

I am thankful to my previous supervisors for taking me under their wing during the early stages of my scientific career. Emeritus Professor Dr. Kalliopi Roubelakis-Angelakis for igniting my interest in plant biology, and Assistant Professor Dr. Kalantidis Kriton for patiently teaching me molecular biology techniques. I am really grateful that I was able to work with an amazing group of people in Milto's lab: Ester, Pauline, Zara, Ursula, Claudia, Huw, Gemma, Carla, Maria, Jonathan, Madlen, Raffo and Dana. I am especially thankful to Dr. Carla Galinha for her supervision and the big help in proofreading my thesis, Dr. Daniela Vlad for her invaluable contribution in the *se-3* suppressor screen and mapping, and Dr. Raffaele Dello Ioio for his expertise in genetics and helping me with the cytokinin-treatment experiments. I thank Dr Angela Hay and her group for fruitful discussions and exchange of materials and knowledge. Special thanks to Mr. John Baker for his excellent photo-capturing skills.

Most importantly, I would like to thank my family in Greece and my friends in Oxford/ Cologne. To my parents, Katerina and Dimitri, thank you for bringing me into this world, for loving me unconditionally, and for supporting any of my decisions. To my siblings Chrysoula and Theologis, thanks for being the best siblings in the world, for understanding, and supporting me in difficult times. To Giannis thanks for the happy times and the delicious cooking. Last but not least, to my best friends Dana, Madlen, and Raffo, thank you for putting up with me all these years and for making my life less miserable.

Abbreviations

ACR4	ARABIDOPSIS CRINKLY4
AGO	ARGONAUTE
AHK3	HISTIDINE KINASE3
ALE	ABNORMAL LEAF SHAPE
AMP1	ALTERED MERISTEM PROGRAM1
AP2	APETALA2
ARF	AUXIN RESPONSE FACTOR
ARR	ARABIDOPSIS RESPONSE REGULATOR
ARS2	ARSENIC RESISTANCE PROTEIN2
AtHB8	A. *thaliana* HOMEOBOX GENE8
AtML1	A. *thaliana* MERISTEM LAYER1
AUX/IAA	AUXIN/INDOLE-3-ACETIC ACID
BDL	BODENLOSS
BLH8	BEL1-LIKE HOMEODOMAIN8
BLR	BELLRINGER
BP	BREVIPEDICELLUS
bp	Base pairs
CAP	Cleaved amplified polymorphic sequence
CALS3	CALLOSE SYNTHASE3
CK	Cytokinin
CLSM	Confocal laser scanning microscopy
cM	Centimorgan
CNA	CORONA
Col-0	Columbia-0
CRC	CRABS CLAW
CUC3	CUP-SHAPED COTYLEDONS3
dCAP	Derived cleaved amplified polymorphic sequence
DCL	DICER-LIKE
DHz	Dihydrozeatin
DIC	Differential interference contrast
DSE1	DECREASED SIZE EXCLUSION LIMIT1
dsRNA	Double-stranded RNA
EMS	Ethyl methanesulfonate
ER	Entoplasmic Reticulum
Gal4	Yeast transcription activator protein
GFP	GREEN FLUORESCENT PROTEIN
GNM	GNOM
GUS	β-Glucuronidase
hc-siRNAs	Heterochromatic siRNAs
HD-ZIP III	Class III HOMEODOMAIN- LEUCINE ZIPPER
HD-ZIP IV	Class IV HOMEODOMAIN- LEUCINE ZIPPER
HUA1	HUA ENHANCER1

HYL1	HYPONASTIC LEAVES1
IAA13	AUXIN-INDUCED PROTEIN 13
ISE1	INCREASED SIZE EXCLUSION LIMIT1
ISE2	INCREASED SIZE EXCLUSION LIMIT2
KAN	KANADI
kb	Kilobase
KNOX I	Class I KNOTTED1-LIKE HOMEOBOX
Ler	Landsberg *erecta*
LIC	Ligation independent cloning
MAPK	MITOGEN ACTIVATED PROTEIN KINASE
MAPKK	MITOGEN-ACTIVATED PROTEIN KINASE KINASE
Mb	Megabase
miR165/6	MicroRNA165 and microRNA166
miRNA	MicroRNA
MP	MONOPTEROS
nat-siRNAs	Natural antisense siRNAs
nosT	Nopaline synthase terminator
nt	Nucleotides
OC	Organizing centre
PD	Plasmodesmata
PDF2	PROTODERMAL FACTOR 2
PHB	PHABULOSA
PHV	PHAVOLUTA
PIN	PINFORMED
PLT	PLETHORA
PNF	POUND-FOOLISH
pre-miRNA	Precursor miRNA
pri-miRNA	Primary miRNA
QC	Quiescent centre
RDR	RNA-dependent RNA polymerases
REV	REVOLUTA
RISC	RNAi silencing complex
RM	Root meristem
SAM	Shoot apical meristem
SCR	SCARECROW
SE	SERRATE
SHR	SHORT ROOT
SEL	Size Exclusion Limit
siRNA	Small interfering RNA
SNP	Single nucleotide polymorphism
SPL3	SQUAMOSA PROMOTER BINDING PROTEIN LIKE3
sRNA	Small RNA
SSP	SHORT SUSPENSOR
STM	SHOOT MERISTEMLESS

SUO	“SHUTTLE” IN CHINESE
ta-siRNAs	Trans-acting siRNAs
T-DNA	Transfer DNA from A. tumefaciens
TMO	TARGET OF MONOPTEROS
TPL	TOPLESS
UAS	Upstream activator sequence
vYFP	"VENUS" YELLOW FLUORESCENT PROTEIN
WGS	Whole genome sequencing
WOX	WUSCHEL-related HOMEOBOX
WUS	WUSCHEL
YAB	YABBY
YDA	YODA
ZLL	ZWILLE

Table of contents

Abstract	**1**
Acknowledgements	**2**
Abbreviations	**4**
Table of contents	**7**

Chapter 1: Introduction	**10**
1.1 The unique nature of pattern formation in plants	11
1.2 Embryonic patterning in Arabidopsis	13
1.2.1 Establishment of the apical-basal axis	19
1.2.2 Radial patterning	21
1.3 Organization along the apical-basal axis	24
1.3.1 The basal region of the embryo and initiation of the RM	26
1.3.2 The apical region of the embryo and initiation of the SAM	28
1.3.3 Defining central and peripheral domains	29
1.4 RNA silencing in plants	32
1.4.1 miRNA biogenesis and function	34
1.4.2 Plant miRNAs regulate gene expression by transcriptional and post-transcriptional mechanisms	38
1.5 The role of miRNAs in early embryogenesis	40
1.6 SERRATE: a general regulator of miRNA biogenesis regulating the *HD-ZIP IIIs*	42
1.7 Repression of the HD-ZIP III: a single patterning event in the specification of multiple embryonic axes	45
1.8 The role of plasmodesmata in embryonic patterning	50
1.9 Second-site modifier genetic screens: a powerful tool in the identification new genes in pathways	53
1.9.1 Genetic screens	53
1.9.2 Second-site modifier screens	54
1.10 Aims of this study and main findings	55

Chapter 2: Materials and methods	**59**
2.1 General methods and materials	60
2.1.1 Plant materials	60
2.1.2 Plant growth conditions	60
2.1.3 Bacterial strains	60
2.1.4 Primer sequences	61
2.2 Genetic methods	64
2.2.1 Generation of strains used in this thesis	64
2.2.2 Plant transformation: “Floral dipping”	65
2.2.3 Selection of transgenic plants	66

2.2.4 Cross-pollination 66
2.3 Molecular biology 66
2.3.1 Construct design 66
2.3.2 Ligation, BP/ LR recombination, and LIC cloning protocols 69
2.3.3 Transformation of E. *coli* cells by heat shock 70
2.3.4 DNA extraction for PCR (quick-prep) 70
2.3.5 DNA extraction and Whole Genome Sequencing 71
2.4 Microscopy, histology and histochemistry 72
2.4.1 Confocal microscopy 72
2.4.2 Light microscopy 73
2.4.3 Embryo clearings 73
2.4.4 GUS analysis 73
2.4.5 CK treatment 74

Chapter 3: SE regulates axial embryonic patterning in a bi-directional and non-cell autonomous fashion **75**

3.1 Introduction 76
3.2 Results 81
3.2.1 Expression of SE in the *PLT2* domain is sufficient to rescue embryonic patterning 81
3.2.2 Expression of SE in the *PLT2* domain permits *se-5* embryos to proceed to post-embryonic development 89
3.2.3 Expression of SE in subdomains of the *PLT2* expression domain does not fully rescue *se-5* embryos 95
3.2.4 SE functions in a bi-directional and non-cell autonomous fashion in regulation of axial patterning during embryogenesis 102
3.4 Discussion 106

Chapter 4: *se-3* suppressor screen: identification of new genes in the *SE*/*HD-ZIP III* pathway **112**

4.1 Introduction 113
4.2 Results 115
4.2.1 *se-3* suppressor screen: isolation of 51 independent *se-3* suppressor lines 115
4.2.2 Analysis of *se-3* suppressors crossed with *SE::GUS* reveals genes upstream of *SE* 124
4.2.3 A *se-3* suppressor functioning downstream or as a cofactor of the *HD-ZIP III* 128
4.2.4 *se-3* suppressors resistant to hormonal treatments reveal a possible role in CK pathways 132
4.3 Discussion 136

Chapter 5: Whole genome sequencing (WGS) and mapping of selected *se-3* suppressors	**139**
5.1 Introduction	140
5.2 Results	141
5.2.1 Whole Genome Sequencing (WGS): a rapid method for identifying putative mutations	141
5.2.2 Mapping of the *se-3* suppressor lines [1] and [3]	149
5.3 Discussion	153
Chapter 6: General discussion	**155**
6.1 Introduction	156
6.2 Investigation of cell-specific SE activities reveals its non-cell autonomous functions	157
6.3 Novel genetic interactions in the SE/HD-ZIP III pathway revealed by a *se-3* suppressor screen	162
6.3.1 Upstream and downstream genes in the SE/HD-ZIP III pathway	162
6.3.2 PNF, a novel component of the SE/HD-ZIP III pathway, plays a role in CK signalling	164
6.4 Future work and perspectives	165
References	**169**

Chapter 1

Introduction

1.1 The unique nature of pattern formation in plants

Pattern formation is the process by which simple structures self-organize in complex patterns in space and time. In developmental biology, patterning involves the division and differentiation of undifferentiated cells into complex tissues and organs. Although animal and plant lineages have evolved multicellularity independently, there are remarkable similarities in how they elaborate axial patterning, especially in early embryonic stages. In both cases, development begins with a simple cell, the zygote, which divides and differentiates into the various cell types of the embryonic body. The different cell types of the embryonic body are polarized along axes of growth. Polar/axial patterning is a characteristic of multicellular development and is shared by both animal and plant lineages. However, due to their distinct evolutionary history, animals and plants also show striking differences in their development (Walbot, 1985; Willemsen and Scheres, 2004).

In contrast to animal cells, plant cells are constrained by rigid cell walls that hinder cell movement during pattern formation. Development in plants is based on cell position rather than lineage, and organogenesis is the outcome of polar growth and direction of cell divisions. Animal cells, on the other hand, which are not constrained by rigid cell walls, are able to change position during organogenesis. As such, cell migration is common during patterning in animals. Another striking difference between animal and plant development is the formation of the plant meristems. Plant meristems are “reservoirs” of pluripotent cells that are formed at the tips of the embryo. The Shoot Apical Meristem (SAM) is formed at the top and the Root Meristem (RM) at the bottom of the embryonic body. During embryogenesis, a simple body plan of the plant is laid

down and most of the post-embryonic patterning results from the function of the meristems. The SAM will generate the aerial organs of the adult plant and the RM will generate the rooting system. These pluripotent populations of cells confer remarkable developmental plasticity, permitting plants to dynamically change their development in response to external stimuli, forming new organs throughout their life cycle. In contrast, in most animal lineages patterning is limited to embryonic development. Animal embryos form the complete set of organs of the adult organism, and post-embryonic development is primarily governed by growth of pre-existing sets of tissues and organs (Walbot, 1985; Willemsen and Scheres, 2004).

Axial embryonic patterning is quite variable even amongst different plant lineages. For example, in the dicot plant Arabidopsis, embryonic patterning is characterized by a series of stereotypic cell divisions that take place at specific stages during embryogenesis. In contrast, in other lineages, such as the monocot plant maize (*Zea mays*), only the first cell division of the zygote is predictable and subsequent cell divisions are random. Despite the differences in early embryonic patterning, both lineages eventually form similar embryonic bodies and meristems that will facilitate patterning in the adult plant (Chandler et al., 2008).

1.2 Embryonic patterning in Arabidopsis

Although the final form of the adult plant is quite complex, it can be considered simply as a vascular cylinder that interconnects the two meristems (Figure 1.1). This simple body plan is laid down by patterning events that take place during embryogenesis. Embryonic patterning in the model plant Arabidopsis results in the establishment of key patterning elements of the sporophytic body plan, including the formation of an apical-basal axis, central-peripheral axis (radial patterning) (Figure 1.2), and the programmes that will generate the lateral organs. These patterns are propagated post-embryonically, giving rise to all aerial and below ground parts of the plant.

Embryogenesis in Arabidopsis begins after the fertilization of the ovule by the pollen cell and formation of the zygote, the first sporophytic cell. The zygote elongates and divides asymmetrically into a larger basal cell and a smaller apical cell. With the asymmetric division of the zygote, apical-basal axial patterning is already established. The apical cell and its daughters continue to divide isotropically forming the 8-cell pro-embryo. The basal cell and its daughters divide and expand longitudinally giving rise to the hypophysis and the suspensor. At this stage, four different cell types can be distinguished: 1) the upper tier cells, 2) the lower tier cells, 3) the hypophysis, and 4) the suspensor (Figure 1.2). The events that will take place from the 16-cell stage (dermatogen stage) onwards will become the basis for all post-embryonic patterning processes. At the 16-cell stage, formation of the protoderm, the epidermis primordium, marks the onset of central-peripheral patterning (Figure 1.2). Radial patterning is further illustrated by formation of the provasculature, the vascular tissue primordium, in the central domain of the globular embryo (Figure 1.2). It is at this stage that shoot and root cell identities are spatially

separated at the opposite poles of the pro-embryo, where the respective meristems will form. Bilateral symmetry emerges with the formation of the cotyledons at the heart stage of embryogenesis (Figure 1.2). In subsequent stages, after the torpedo stage, the embryo completes its growth primarily by cell expansion and enlargement. Eventually the mature embryo enters the dormant phase until the environmental conditions become favorable for seed germination (Chandler et al., 2008).

Figure 1.1: The basic body plan of the plant is a vascular cylinder that interconnects the plant meristems

Graphical representation of a heart stage embryo (left) and a young seedling (right) highlighting the central vascular cells (red), shoot meristem cells (yellow), and root meristem cells (blue) in both ontogenetic stages. During embryogenesis in plants, a basic body plan is laid down, which can be simply considered as a vascular cylinder that interconnects the shoot and root meristems. This pattern is propagated in post-embryonic development.

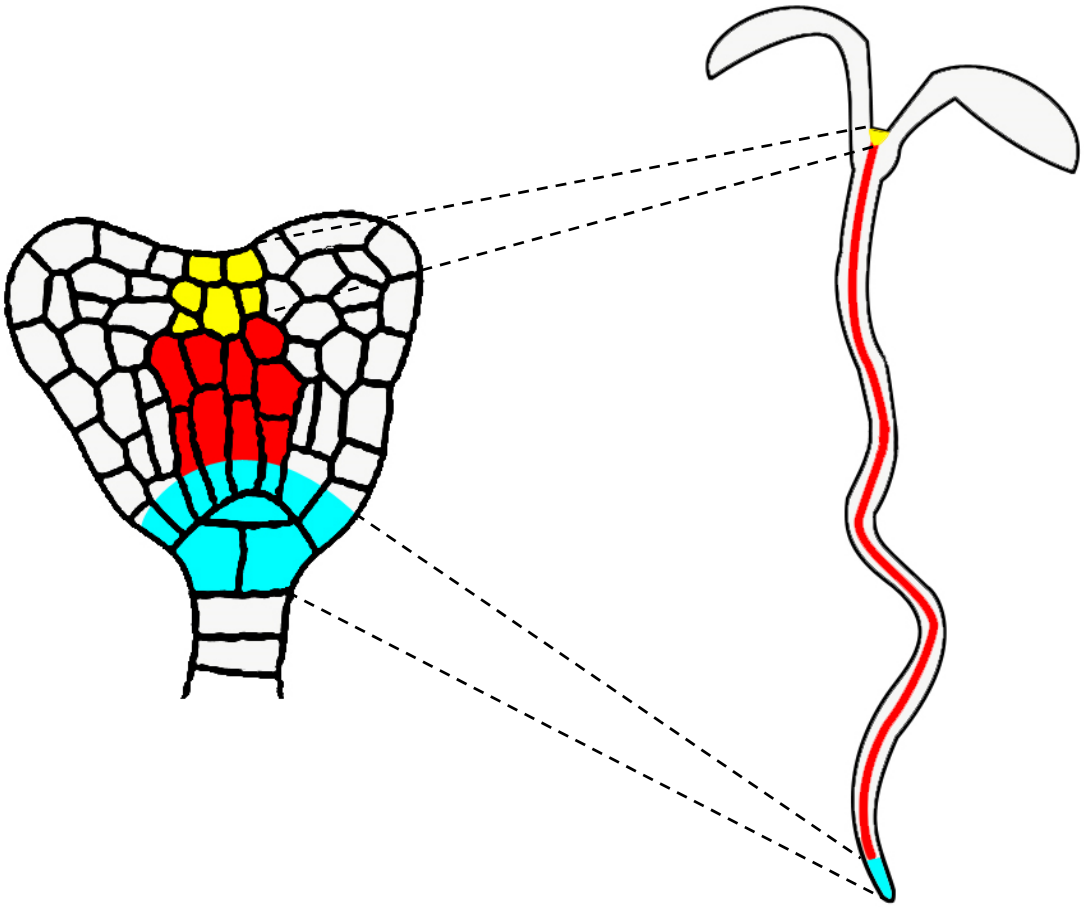
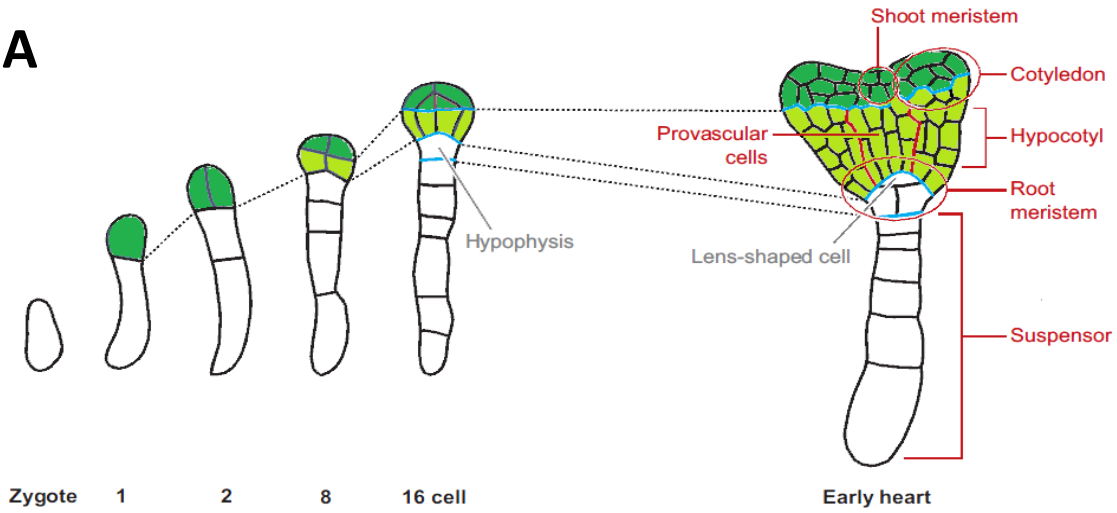


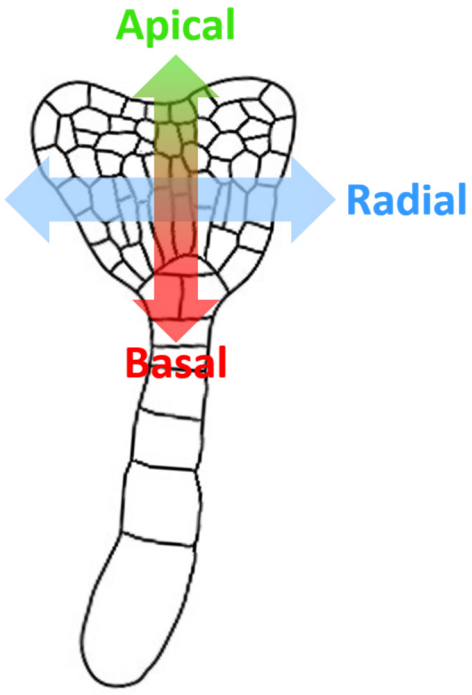
Figure 1.2: Axial embryonic patterning in Arabidopsis

(A) Graphical representation of the developmental stages of Arabidopsis embryogenesis from the zygote to the heart stage. The upper tier cells and their daughters are marked in dark green, the lower tier cells and their daughters in light green. Red markings indicate the position of the respective organs and tissues on the embryonic body (Jenik et al., 2007). (B) Graphical representation of an Arabidopsis heart stage embryo depicting the main axes of embryonic development.

A


Shoot meristem
Cotyledon
Hypocotyl
Provascular cells
Root meristem
Hypophysis
Lens-shaped cell
Suspensor
Zygote
1
2
8
16 cell
Early heart

B


Apical
Radial
Basal

1.2.1 Establishment of the apical-basal axis

Following fertilization and elongation of the zygote, the asymmetric division of the zygote produces daughter cells that will acquire fundamentally different fates. The smaller apical cell and its daughters divide twice longitudinally and once transversely forming the 8-cell stage embryo (Figure 1.2). These cells will give rise to most of the cells of the pro-embryo and the SAM. In contrast, the larger basal cell and its daughters continue to expand longitudinally and divide transversely to produce the filamentous suspensor. The uppermost cell of the suspensor, the hypophysis, will eventually become part of the RM at the basal pole of the embryo (Figure 1.2).

Although our knowledge of the genetic mechanisms underlying the establishment of the apical-basal axis is still scarce, there are several candidate pathways that seem to govern these early patterning events. Amongst those, the *WUSCHEL*-related *HOMEOBOX* (*WOX)* genes have been implicated in axial patterning during early embryogenesis, mainly due to their characteristic expression profiles. These distinct expression profiles begin with the first division of the zygote, with WOX2 being confined in the apical cell, and WOX8 and 9 in the basal cell (Haecker et al., 2004). At the 16-cell stage embryo, their expression pattern parallels the four morphologically distinguishable cell types, with *WOX2* gene being expressed in the apical tier promoting apical cell fate, whereas *WOX8* and *9* are expressed in the lower tier, basal pole, and suspensor promoting basal cell fate (Haecker et al., 2004; Wu et al., 2007; Breuninger et al., 2008).

In addition to *WOX8* and *9*, the MITOGEN-ACTIVATED PROTEIN KINASE KINASE (MAPKK) kinase gene *YODA* (*YDA)* is also associated with the basal cell fate, marking the basal cell and its daughters. After the asymmetric division, YDA is down-regulated in the apical cell

which acquires embryonic identity, whereas it is still expressed in the basal cell. Loss-of-function mutants of *YDA* form zygotes that are unable to elongate, and after the first division the basal cell usually ceases to divide (Lukowitz et al., 2004). In contrast, gain-of-function mutants have the opposite effect of elongated basal cells dominating the apical cells (Lukowitz et al., 2004). Similar effects, albeit to a lesser extent, are also observed in knockouts of the MITOGEN ACTIVATED PROTEIN KINASE (MAPK) genes *MPK3* and *MPK6* (Wang et al., 2007), and the receptor-like kinase gene *SHORT SUSPENSOR (SSP)* (Lukowitz et al., 2004), indicating a possible involvement of kinase-cascade signalling in the establishment of the apical-basal axis. This involvement of YDA and MAPKK signalling in the establishment of the basal cell identity is further suggested by the finding that the zinc-finger protein WRKY2, which positively regulates WOX8 at the basal pole, has several MAP kinase phosphorylation sites, and loss-of-function mutants in this gene fail to perform correct zygote division (Ueda et al., 2011). Although this hypothesis requires further investigation, it is possible for *WRKY2* to function as an intermediate between the *WOX* and *YDA* pathways in the establishment of the apical-basal axis.

Apart from transcription factors and MAP kinases, the phytohormone auxin is also involved in early polarization events. The apical-basal fate is marked by the differential expression of the PINFORMED (PIN) auxin efflux facilitators (Galweiler et al., 1998; Petrasek et al., 2006; Wisniewska et al., 2006). PIN7, one member of the PIN protein family, is preferentially localized at the apical side of the basal daughter of the zygote, probably providing the apical daughter with auxin (Friml et al., 2003). Although *pin7* mutants have minor effects on axis establishment in the zygote, higher order mutants of *PIN* family members, such as *pin1;pin3;pin4;pin7*, are strongly depolarized forming only one file of suspensor cells, implying that auxin polarity at the daughters of the zygote is

essential for apical cell fate (Friml et al., 2003; Blilou et al., 2005; Vieten et al., 2005). These observations hint towards an antagonistic model, with an apical auxin concentration instructing apical cell fate, and the YDA/MAPKK at the basal pole instructing suspensor fate.

Although our knowledge of the factors that are involved in early embryonic patterning is increasing, it is unclear how the apical-basal axis is established along the zygote cell in the first place. After fertilization, within the zygote the nucleus is polarized at the future apical pole and the large vacuole is localized at the future basal pole (Faure et al., 2002). This clearly indicates the presence of polarity, even from the zygote stage. However, it is still unknown how such polarity arises. The best hypothesis is that the zygote polarity is instructed by hormonal signals, mainly auxin. Auxin gradients have been shown to determine egg and synergid fate versus antipodal fate during ovule development (Pagnussat et al., 2009). Thus, it is possible that such signals also affect establishment of the apical-basal axis in the zygote.

1.2.2 Radial patterning

Radial patterning during Arabidopsis embryogenesis begins with the formation of the epidermis primordium, the protoderm. Between the 8- and 16-cell stage of embryogenesis, several transcription factors show polar expression profiles in a radial pattern along the Arabidopsis pro-embryo. The paralogous Class IV HOMEODOMAIN-LEUCINE ZIPPER (HD-ZIP IV) transcription factors A. *thaliana* MERISTEM LAYER 1 (AtML1) and PROTODERMAL FACTOR 2 (PDF2) are expressed in the periphery of the pro-embryo within the protoderm, whereas ZWILLE (ZLL) and WUSCHEL (WUS) are expressed in the

tissues internally of the protoderm (Lu et al., 1996; Abe et al., 2003). Although *atml1;pdf2* double mutants form a protoderm, they fail to differentiate and maintain a functional epidermis (Abe et al., 2003). This observation suggests that AtML1 and PDF2 are not required for protoderm development, but they are essential for epidermis differentiation. Although it is still unclear how AtML1 and PDF2 are retained in the protoderm layer, maintenance of their expression and epidermis development are dependent on cell-to-cell communication mechanisms that are coordinated by the receptor-kinase ARABIDOPSIS CRINKLY 4 (ACR4), and the ABNORMAL LEAF SHAPE (ALE) proteins, the protease ALE1, and the receptor-like kinase ALE2 (Tanaka et al., 2001; Tanaka et al., 2002; Tanaka et al., 2007; San-Bento et al., 2013). Although single mutants in those genes show relatively weak defects, higher order mutations result in abnormal protoderm division and reduced expression of protoderm-specific markers (Tanaka et al., 2007). Remarkably, *ALE1* mRNA accumulates in the endosperm that surrounds the embryo, suggesting that the endosperm may instruct patterning of the embryo (Tanaka et al., 2001).

Patterning in the central domain of the embryo becomes morphologically apparent with the differentiation of the provascular cells, the vasculature primordium, at the globular stage. In order to understand vascular development, it is important to discuss how auxin and auxin flow are involved in axial patterning, because many of the genes that are polarly expressed in the central domain of the embryo are regulated by auxin and/ or are components of auxin signalling pathways.

After the initial establishment of auxin maxima at the apical daughter of the zygote, the apical cell continues to divide isotropically, while auxin is continuously transported to the developing pro-embryo (Friml et al., 2003). At the early globular stage, apical to basal

flow of auxin is established, as PIN1 is preferentially localized at the basal side of the central cells and PIN7 reverts to basal polarity in the suspensor cells. As a consequence, auxin is drained from the pro-embryo and concentrates basally. At the late globular stage, auxin flows upwards through the protodermal layer and downwards through the central tissues, which will elongate forming the initials of the provasculature. The apical to basal auxin flow has been established. From late globular stage onwards PIN1 polarity is reverted towards the apical part of the embryo, concentrating auxin at the tips of the developing cotyledons, the embryonic leaves (Jenik et al., 2007; Bowman and Floyd, 2008).

The flow of auxin and the formation of maxima are critical for correct embryo development. Mutations in genes in auxin-dependent pathways result in embryos with defective patterning and abnormal auxin flow (Jenik et al., 2007; Bowman and Floyd, 2008). For example, loss-of-function mutants of the *GNOM* (*GNM*) gene, which regulates vesicle budding, an important process for the recycling of PINs (Steinmann et al., 1999; Geldner et al., 2003), show depolarized PIN patterns at the central domain of the globular embryo and fail to properly pattern provasculature, similarly to higher-order *pin* loss-of-functions mutants (Liu et al., 1993; Hadfi et al., 1998; Friml et al., 2003). Thus, the apical to basal auxin flow is important for correct patterning of the vasculature along the central domain of the embryo.

The signals from the flow of auxin are perceived by the AUXIN RESPONSE FACTOR (ARF) transcription factors. In a steady state, ARFs are bound by the AUXIN/ INDOLE-3-ACETIC ACID (AUX/ IAA) proteins in the cytosol, which renders them inactive. Upon auxin signalling the AUX/ IAA proteins are degraded and the ARFs are free to activate

transcription of auxin responsive genes in the nucleus (Dharmasiri and Estelle, 2004). As expected, polarization is also affected by mutations in genes that encode such factors, including the ARF MONOPTEROS (MP) and the AUX/IAAs BODENLOSS (BDL) and the AUXIN-INDUCED PROTEIN 13 (IAA13). MP, BDL and IAA13 are initially expressed in the apical daughter of the zygote and by the mid-globular stage of embryogenesis they are restricted to the provascular cells (Hardtke and Berleth, 1998; Hamann et al., 2002; Weijers et al., 2005). Mutations in these genes abolish apical-basal polarity, and also central-peripheral patterning (Hardtke et al., 2004).

MP is required for the transcription of the *A. thaliana HOMEOBOX GENE 8* (*AtHB8)* gene, which is the earliest known marker of provascular identity (Mattsson et al., 2003). AtHB8 belongs to the plant-specific family of the class III HOMEODOMAIN- LEUCINE ZIPPER (HD-ZIP III) transcription factors, which contains five members in Arabidopsis: the REVOLUTA (REV), PHABULOSA (PHB), PHAVOLUTA (PHV), CORONA (CNA), and AtHB8 proteins. All members, except *PHV*, are expressed along the provasculature, and higher order loss-of-function mutants in these genes show significantly reduced vasculature development (McConnell et al., 2001; Emery et al., 2003; Prigge et al., 2005).

1.3 Organization along the apical-basal axis

The main goal of plant embryogenesis is the formation of distinct cell fates that will generate the pluripotent organs of the plant, the SAM and RM, which will facilitate the subsequent post-embryonic development. These stem-cell pools are formed at the tips of

the embryonic body, using as a reference the apical-basal axis, which has been established very early in embryogenesis (Figure 1.2). As post-embryonic development is mostly based on the formation and function of the embryonic meristems, investigation of the embryonic patterning mechanisms that form the SAM and RM is of fundamental importance.

Major anatomical and transcriptional differences between these cell fates are initiated at the 16-cell stage embryos, originating the distinctly separated upper tier, lower tier, and hypophyseal cell identities (Figure 1.2). Afterwards, each domain will follow distinct patterns of cell division and gene expression. The lower tier cells and the hypophysis, which will give rise to hypocotyl and root through highly stereotypic cell divisions (Scheres et al., 1994), express *PLETHORA* (*PLT*) transcription factors (Aida et al., 2004; Galinha et al., 2007), whereas the upper tier cells will generate the apical shoot fates marked mainly by the expression of *WOX2* and *CUP-SHAPED COTYLEDONS3* (*CUC3)* genes (Vroemen et al., 2003; Haecker et al., 2004).

Nonetheless, it becomes increasingly clear that interaction between apical and basal fates is essential for integrated developmental processes (Souter and Lindsey, 2000). For example, maintenance of shoot fates requires the expression of TOPLESS (TPL), as indicated by *tpl-1* mutants that exhibit loss of apical meristem, lack of hypocotyl, and formation of root in both poles of the embryo (Long et al., 2002; Long et al., 2006). *tpl-1* mutants develop normally until approximately the globular stage. Thus, TPL is probably required to fix shoot fates after the apical-basal axis is established (Long et al., 2006). This fixation of shoot fate could involve either epigenetic regulation (Long et al., 2006), regulation of auxin-dependent transcription (Szemenyei et al., 2008), or direct

transcriptional downregulation of basal fate determinants, the *PLT* genes (Smith and Long, 2010).

1.3.1 The basal region of the embryo and initiation of the RM

Development of the basal fate and root initiation is the outcome of differentiation of the lower tier cells and that of the hypophysis. The initials of the embryonic hypocotyl can be distinguished at the midglobular stage, with the protoderm that will give rise to the epidermis, the innermost elongated cells that will form the stele, and the in-between cells that will give rise to the ground tissue (Scheres et al., 1995). The RM, on the other hand, is initiated by an asymmetric division of the hypophysis at the globular stage, giving rise to the smaller lens-shaped cell (progenitor of the quiescent center (QC)) and a larger basal daughter cell (Scheres et al., 1994). Although formation of the QC involves processes that happen in the hypophysis, it also requires the establishment of the apical-basal auxin flow, function of the CK signalling pathway, and activity of transcription factors active in surrounding tissues.

The function of MP, BDL and IAA13 in the provasculature at the globular stage is required for the division of the hypophysis, even before the asymmetric division occurs (Hamann et al., 2002; Weijers et al., 2005; Weijers et al., 2006). Localized expression of MP in the central domain of the *mp* loss-of-function mutant is sufficient to drive division of the hypophysis (Weijers et al., 2006). MP and BDL expression is confined to the provasculature cells, which indicates that they may act non-cell-autonomously in the specification of the QC. Given that MP and BDL are components of the auxin signalling pathway and that there is a polarized flow of auxin towards the hypophysis during its

division, suggest that auxin is likely implicated in this patterning process. However, the fact that external auxin application is not sufficient to drive correct development of the RM in *mp* mutants (Weijers et al., 2006), implies that this is probably not an auxin-specific patterning process. This process has been recently linked to the function of the small bHLH TARGET OF MONOPTEROS (TMO) transcription factors, which are direct targets of MP (Schlereth et al., 2010). Specifically, *TMO7* mRNA is produced in the provasculature and TMO7 protein moves to the hypophysis to promote RM initiation (Schlereth et al., 2010). Indeed confined expression of TMO7 in the hypophysis of *mp* mutants is sufficient to restore RM defects in this background (Schlereth et al., 2010).

In addition to ARFs and auxin, the phytohormone cytokinin (CK) has been also shown to play a role in the patterning of the hypophysis, preceding formation of the RM. The function of CK is mediated by the ARABIDOPSIS RESPONSE REGULATOR (ARR) transcription factors, which are classified in the type-A *ARR* genes that negatively regulate CK responses, and the type-B *ARR* genes that promote CK responses. At the early globular stage, CK activity is detected in the hypophysis and the suspensor, but soon after the division of the hypophysis CK activity drops in the basal daughter cell of the hypophysis but remains in the lens-shaped cell and the suspensor (Muller and Sheen, 2008). This polar pattern is mediated by the type-B *ARR* genes *ARR7* and *ARR15*, which are expressed in the basal daughter of the hypophysis, to repress CK signalling (Muller and Sheen, 2008). Because these genes are regulated by ARF transcription factors, it has been proposed that the auxin/CK interplay in the early globular embryo may be involved in the correct patterning of the hypophysis and consequently in RM development (Muller and Sheen, 2008).

Further specification of the lens-shaped cell and QC is mediated by the independent function of two regulatory pathways, the *SHORT ROOT* (*SHR*)/ *SCARECROW* (*SCR*) and the Auxin/*PLT* pathways (Wysocka-Diller et al., 2000; Sabatini et al., 2003; Aida et al., 2004; Blilou et al., 2005). The mobile transcription factor SHR is expressed in the provasculature and non-cell autonomously activates transcription of the QC determinant *SCR* in the lens-shaped cell and its daughters, as well as in the initials of the ground tissue (Helariutta et al., 2000; Nakajima et al., 2001; Sabatini et al., 2003; Heidstra et al., 2004). The *PLT1* and *PLT2* genes are expressed at the basal tier of the 8-cell embryo and later in embryogenesis become restricted to the provascular cells and lens-shaped cell, except *PLT2* which is also expressed in some cells of the ground tissue (Aida et al., 2004). *PLT* genes act downstream to auxin in QC specification (Aida et al., 2004; Blilou et al., 2005). The QC forms where auxin maxima, *SCR* and *PLT* expressions coincide (Aida et al., 2004). By the heart stage the QC has already been established.

1.3.2 The apical region of the embryo and initiation of the SAM

Patterning events that specify the SAM share many similarities with those that generate the RM. For example, the maintenance of both is dependent on functionally interchangeable members of the WOX family of transcription factors, WOX5 being expressed in the root and WUS in the shoot (Laux et al., 1996; Mayer et al., 1998; Sarkar et al., 2007). WUS is initially expressed in the four inner cells of the upper tier at the 16-cell stage embryo, and in later embryonic stages it is restricted to a few cells in the organizing centre (OC) of the SAM (Mayer et al., 1998). In addition to *WUS*, the homeobox gene *SHOOT MERISTEMLESS* (*STM*) is also implicated in the specification and

maintenance of SAM, and consistent with its role, is expressed in all cells that form the SAM (Barton and Poethig, 1993; Long et al., 1996; Lenhard et al., 2002). Nonetheless, WUS and STM seem to be independently required for the generation of SAM, as supported by the distinct *stm* and *wus* mutant phenotypes (Willemsen and Scheres, 2004).

Expression of genes responsible for the patterning of SAM begins much earlier than any anatomical change and it coincides with patterning events that form the cotyledons. Key regulators in these processes are the CUC transcription factors, which are involved in SAM formation and cotyledon separation, important for the activation of *STM* in the SAM (Aida et al., 1997; Aida et al., 1999; Takada et al., 2001; Vroemen et al., 2003). Consistently, *cuc* mutants form fused cotyledons around the apex and fail to form the SAM (Aida et al., 1997). After the globular stage, STM downregulates *CUC* expression in the incipient SAM, and concurrent downregulation mediated by auxin in the emerging cotyledons, restricts *CUC* gene expression to a ring around the SAM separating it from the lateral cotyledons (Aida et al., 1999; Aida et al., 2002; Furutani et al., 2004; Treml et al., 2005). Nevertheless, SAM and cotyledon fates are not dependent on each other, as inferred from *stm* and *wus* mutants that fail to establish SAM, but do form cotyledons (Barton and Poethig, 1993; Laux et al., 1996).

1.3.3 Defining central and peripheral domains

Because cotyledons and lateral organs are formed in the boundary between central and peripheral domains, with an adaxial domain deriving from central cells and an abaxial domain deriving from peripheral cells, it has been proposed that central/adaxial and

peripheral/abaxial domains are interconnected (Kerstetter et al., 2001; McConnell et al., 2001). The central cell identity is mainly marked by the expression of the *HD-ZIP III* genes, whereas the peripheral cells are marked by the expression of the *KANADI* (*KAN)* and *YABBY* (*YAB)* genes.

Very early in embryogenesis, the *HD-ZIP III* are expressed throughout the pro-embryo, whereas from the mid-globular stage onwards they are restricted to the center of the upper tier, the adaxial side of the cotyledons, and the provasculature (McConnell et al., 2001; Emery et al., 2003; Prigge et al., 2005). Loss of function of the *PHB*, *PHV*, and *REV* genes in triple *phb;phv;rev* mutants results in severe phenotypes of loss of meristematic identity in the SAM and malformed cotyledons with abaxialized nature (Emery et al., 2003; Prigge et al., 2005). Apart from *REV*, single mutants in genes of this family do not show any defects, indicating a redundancy between the various members (Prigge et al*.,* 2005). Clearly, loss of HD-ZIP III function results in loss of central as well as apical identities.

KAN genes are initially expressed throughout the early globular embryo, but soon are restricted abaxially to the hypocotyl and lateral organs (Eshed et al., 2001; Kerstetter et al., 2001). Higher order *KAN* mutants have the opposite phenotype to those of *HD-ZIP III* mutants, implying an antagonistic relationship between the adaxial/central *HD-ZIP III* and the abaxial/peripheral *KAN* genes (Kerstetter et al., 2001; Eshed et al., 2004; Izhaki and Bowman, 2007). However, the ectopic hypocotyl leaves in *kan* mutants do not form in *HD-ZIP III* gain of function mutants (Izhaki and Bowman, 2007). These formations are correlated to ectopic auxin maxima in *kan* mutants at the base of the globular embryo, suggesting that one of the primary roles of *KAN* genes is to antagonize auxin responses

(Izhaki and Bowman, 2007). However, the fact that normal auxin maxima are formed in *phb;phv;rev;kan1;kan2;kan4* mutant embryos and that bilateral symmetry is restored in these embryos, implies that the function of *HD-ZIP III* and *KAN* genes is not absolutely required for the establishment of bilateral symmetry or central-peripheral axis (Izhaki and Bowman, 2007). Rather, antagonism of these fates probably delineates the area of correct auxin flow.

Confinement of the *HD-ZIP IIIs* in the adaxial side of the developing cotyledons is also mediated via a miRNA silencing mechanism, with miR165/6 targeting all the Arabidopsis *HD-ZIP III* gene transcripts (Byrne, 2006). As a consequence, in the developing leaf and embryos the *HD-ZIP IIIs* are restricted to the central and adaxial side, whereas miR165/6 are expressed complementary to this pattern (Kidner and Martienssen, 2004; Williams et al., 2005). Validation of the involvement of miRNA silencing to the developmental confinement of *HD-ZIP III* genes, could be inferred from the observation that *PHB* and *PHV* dominant gain-of-function mutations (*phb-d* and *phv-d*, respectively), which alter the miRNA binding site, and also mutant versions of *PHB*/*PHV* with altered miRNA binding site but not altered amino acid sequence, result in misexpression of the HD-ZIP III to the abaxial side of lateral organs (McConnell et al., 2001; Emery et al., 2003; Mallory et al., 2004). These mutants have increased embryonic SAM size and adaxialized cotyledons (McConnell and Barton, 1998).

The SE/HD-ZIP III regulation is also implicated in the patterning of the post-embryonic root. The miR165/6, which are expressed in the root endodermis, move towards the stele to delineate the boundary of the *HD-ZIP III* expression along the stele, thus providing positional information for xylem differentiation (Carlsbecker et al., 2010; Miyashima et

al., 2011). Such observations suggest that miRNA and RNA silencing may play important roles in developmental patterning by delineating expression domains of developmentally important transcription factors.

1.4 RNA silencing in plants

RNA silencing or RNAi is a regulatory mechanism of gene expression that plays important roles in development, genome stability, and defense against viruses (Fusaro et al., 2006; Dunoyer and Voinnet, 2008; Djupedal and Ekwall, 2009). This mechanism is triggered by double-stranded RNA (dsRNA), which derives from external viral sources, as well as endogenous transcripts. Specifically in plants, these dsRNA molecules are recognized by the DICER-LIKE (DCL) RNAse III endonucleases, which cleave dsRNA into small RNA (sRNA) duplexes. These sRNAs are subsequently loaded into ARGONAUTE (AGO)-containing protein complexes that will perform sequence-specific gene inactivation, guided by the loaded sRNA molecule.

Specifically, in Arabidopsis there are four different DCL orthologous genes and ten AGO genes (Vazquez, 2006; Vaucheret, 2008). The sRNAs produced by each member of the DCL family differ in size and downstream functions. For example, DCL1 and DCL4 produce 19-24 nt long and 21 nt long sRNAs, respectively, which are subsequently loaded in AGO1-containing protein complexes to drive regulation of complementary RNAs (Dunoyer et al.; Bartel, 2004). In contrast DCL3 produces 24 nt long sRNAs that are

incorporated in AGO4- and AGO6-containing protein complexes to drive RNAi-based chromatin modifications.

sRNAs, based on their biogenesis and molecular function, are broadly classified into two groups, the microRNAs (miRNAs) and the small interfering RNAs (siRNAs). miRNAs are 20-24 nt long sRNAs that are processed from longer hairpin RNA precursor molecules by the function of DCL1. miRNAs have been involved in many biological processes, including developmental patterning, stress responses, and metabolism (Bartel, 2004; Jones-Rhoades et al., 2006; Meyers et al., 2008; Voinnet, 2009). On the other hand, siRNAs derive from dsRNA that is either produced by the function of the RNA-dependent RNA polymerases (RDR), or by transcription of inverted repeats (Mette et al., 2000; Lippman et al., 2004; Borsani et al., 2005; Gendrel and Colot, 2005; Yoshikawa et al., 2005). siRNAs are further classified into trans-acting siRNAs (ta-siRNAs), heterochromatic siRNAs (hc-siRNAs), and natural antisense siRNAs (nat-siRNAs). ta-siRNAs biogenesis is triggered by the cleavage function of miRNA-loaded AGO complexes and RDR enzymes. Their roles are similar to that of miRNAs. Specifically in development, ta-siRNAs target members of the ARF and MYB transcription factors, consequently regulating developmental patterning (Fahlgren et al., 2006; Rajagopalan et al., 2006; Vazquez, 2006). The hc-siRNAs most likely derive from transposable element sequences and DNA repeats, are mainly processed by DCL3 into 24 nt siRNA, and are incorporated in AGO4 and AGO6 complexes to drive the sequence-specific DNA methylation and chromatin modification (Zilberman et al., 2003; Zheng et al., 2007). Finally, biogenesis of the nat-siRNAs requires the function of DCL1 and/or DCL2, as well as several RDR polymerases (Borsani et al., 2005; Ramachandran and Chen, 2008). nat-siRNAs may play important roles in stress responses (Borsani et al., 2005).

It is apparent that the RNA silencing mechanism is complex and involves many unique and overlapping pathways that are implicated in a variety of biological processes. Despite the complexity, understanding how sRNAs are produced and how they function is essential to understand biological processes such as metabolism, stress responses and, especially, development in plants.

1.4.1 miRNA biogenesis and function

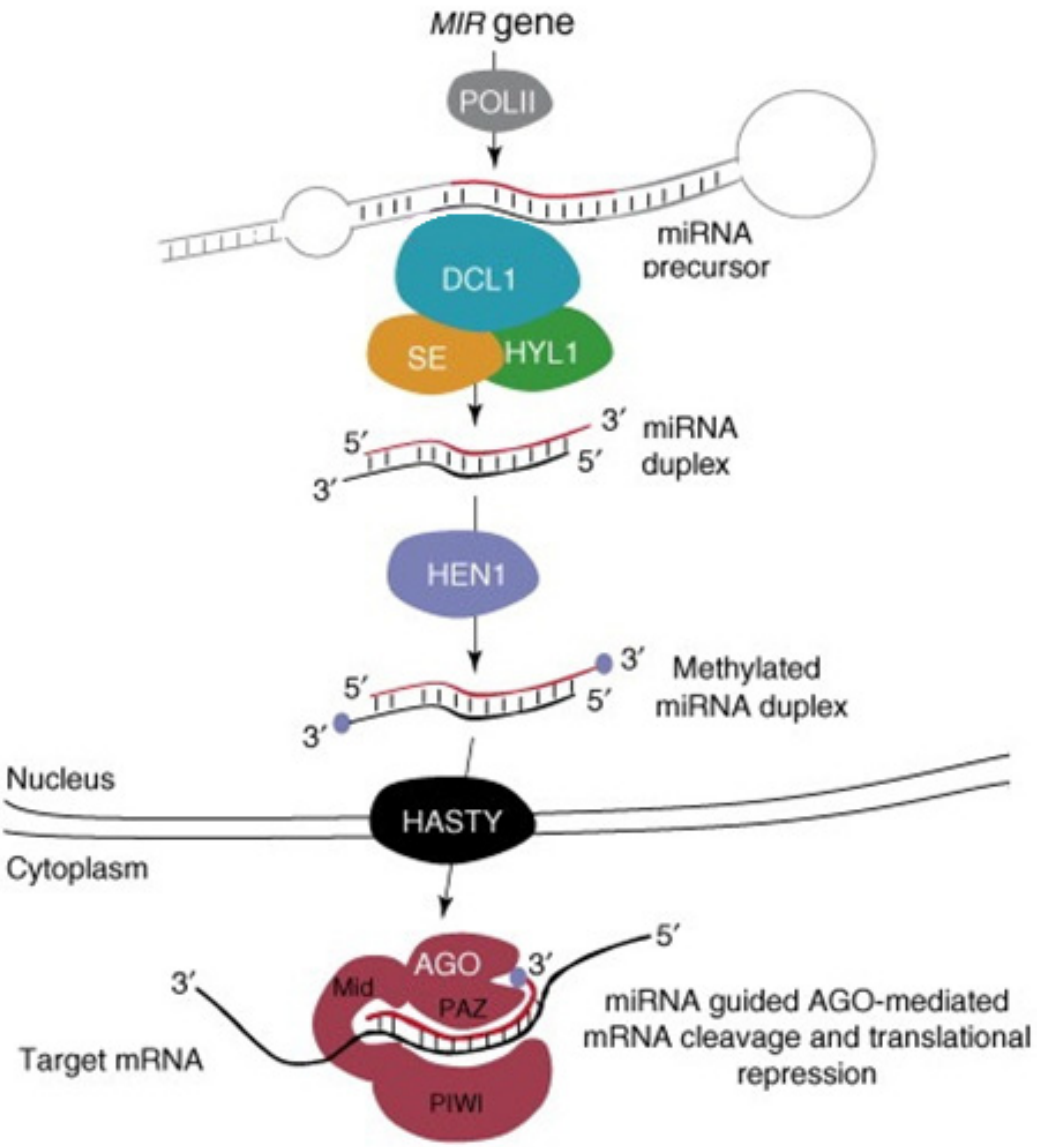
miRNAs are a unique type of sRNAs, which derive from endogenous long transcripts that form hairpin (stem-loop) structures (Figure 1.3). Most *MIR* genes have their own promoter sequence and they are transcribed by the RNA polymerase II (Xie et al., 2005; Kim et al., 2011). The stem-loop transcripts, also known as pri-miRNA, are processed into shorter double stranded dsRNAs (pre-miRNA) by the dicing complex, which includes the Rnase III DCL1 and several RNA binding proteins, such as SERRATE (SE) and HYPONASTIC LEAVES1 (HYL1) (Figure 1.3). The pre-miRNA is further processed by the dicing protein complex into the mature miRNA/miRNA* duplex, and after several modifications, it is exported to the cytoplasm for incorporation into the AGO1-containing silencing complex (Figure 1.3). Only the mature strand of the miRNA/miRNA* duplex is incorporated into the AGO-containing protein complex, forming the RNAi silencing complex (RISC) (Figure 1.3). The RISC guided by the mature miRNA strand, recognizes complementary transcripts and facilitates RNA regulation, either by cleavage or translational repression (Rogers and Chen, 2013), (Figure 1.3).

The miRNA dicing complex

The formation and function of the dicing complex is integral for miRNA biogenesis and function. The core proteins that constitute this complex, apart from the RNAse III DCL1, include the RNA binding proteins SE, and HYL1 (Dong et al., 2008), (Figure 1.3). These proteins bind to dsRNA at different positions along the pri-miRNA hairpin structure and facilitate accurate pri-miRNA processing by DCL1 (Kurihara et al., 2006; Dong et al., 2008; Manavella et al., 2012). The DCL1, HYL1, and SE proteins have been shown to physically interact with each other (Kurihara et al., 2006; Lobbes et al., 2006; Yang et al., 2006; Machida et al., 2011), but it is not clear whether they form a stable microprocessor complex. Although all members in this complex are required for correct miRNA processing, it seems that different miRNA/mRNA target modules are differentially affected by loss of any of the components in the complex (Grigg et al., 2005; Grigg et al., 2009; Laubinger et al., 2010; Nodine and Bartel, 2010). This is clearly demonstrated in the work of Laubinger *et al.,* 2010, who performed whole-genome tilling array analysis of mutants impaired in the miRNA machinery in several tissues and different stress conditions. Although many miRNA genes and their targets are similarly affected by loss of either DCL1, HYL1 and/or SE, there are many miRNA/mRNA target modules that require specific members of the dicing complex (Laubinger et al., 2010). However, it is still unclear how such specificity is acquired.

Figure 1.3: miRNA biogenesis and function

Simplified schematic representation of the miRNA biogenesis and function pathways in Arabidopsis. Transcription of *MIR* genes by RNA polymerase II generates the hairpin (stem-loop) pri-miRNA transcripts (here miRNA precursor). The pri-miRNAs are processed into shorter miRNA duplexes by a protein complex that includes the Rnase III DCL1 and the RNA binding proteins SE and HYL1 (dicing complex). The miRNA duplexes are subsequently methylated by the methyltransferase HUA ENHANCER1 (HUA1), and exported to the cytoplasm by the nuclear exporter HASTY for incorporation into AGO-containing protein complexes. Only the mature strand of the miRNA duplex (marked in red) is incorporated into the AGO-containing protein complexes to form the RISC complex. The miRNA-guided RISC complex regulates expression gene expression, either by cleavage or translational repression of complementary transcripts (image modified from Mallory and Bouché, 2008).


MIR gene
POLII
miRNA precursor
DCL1
SE
HYL1
5′
3′
3′
5′
miRNA duplex
HEN1
5′
3′
3′
5′
Methylated miRNA duplex
Nucleus
HASTY
Cytoplasm
AGO
Mid
PAZ
PIWI
3′
5′
3′
Target mRNA
miRNA guided AGO-mediated mRNA cleavage and translational repression

1.4.2 Plant miRNAs regulate gene expression by transcriptional and post-transcriptional mechanisms

a. miRNAs regulate gene expression via cleavage or translational inhibition of complementary transcripts

Plant miRNAs show high complementarity towards their target transcripts, and since high complementarity is essential for effective AGO slicing, most plant miRNAs guide mRNA cleavage of complementary transcripts instead of translational inhibition (Mallory et al., 2004). In contrast, complementarity is mainly limited to the 5‘-prime end of the animal miRNAs, thus slicing is less common and translational inhibition of target transcripts is a more common mechanism (Lewis et al., 2003; Zeng et al., 2003; Brennecke et al., 2005; Karginov et al., 2010; Shin et al., 2010). However, several observations suggest that translational repression might be a more common mechanism in plants than initially thought. For example, several studies in flower development involving the APETALA2 (AP2) and SQUAMOSA PROMOTER BINDING PROTEIN LIKE3 (SPL3) transcription factors show miRNA-dependent regulation of the respective proteins without any effect in the mRNA levels (Aukerman and Sakai, 2003; Chen and Kaiser, 2003; Gandikota et al., 2007). Furthermore, recent work identified mutations affecting miRNA silencing at the protein level, but not at the post-transcriptional level (Brodersen et al., 2008; Yang et al., 2012; Li et al., 2013). These collectively suggest that translational inhibition is more common in plants, and also that this mechanism is most likely to be independent of miRNA cleavage.

Although, the exact molecular mechanism by which plant miRNAs guide translational inhibition of complementary transcripts is still unknown, recent work gives insights into putative components that could facilitate such a mechanism. Yang *et al*., 2012 show that

the membrane protein ALTERED MERISTEM PROGRAM1 (AMP1) is required for miRNA translational inhibition but not miRNA cleavage (Yang et al., 2012). AMP1 protein physically interacts with AGO1 and the endoplasmic reticulum. *amp1* loss-of-function mutants show a pleotropic phenotype (Yang et al., 2012), which is common amongst the mutants with impaired miRNA silencing. These collectively suggest that translational inhibition is an important aspect of miRNA silencing and reveals a previously unknown function of the endoplasmic reticulum.

b. Several miRNAs regulate gene expression via DNA methylation

A novel role for miRNAs in epigenetic gene silencing derives from the work of Bao *et al.,* 2004, who reported that miR165/6 direct DNA methylation of the *HD-ZIP III* genes *PHB* and *PHV* on exons located downstream of the miRNA binding site (Bao et al., 2004). In *phb-d* and *phv-d* gain-of-function mutants, which produce transcripts that are resistant to miR165/6 binding and mRNA cleavage, CG methylation at the *PHB* and *PHV* loci is heavily reduced (Bao et al., 2004). This observation indicates that the miRNA-directed *PHB* and *PHV* methylation requires binding of miR165/6 and possibly mRNA cleavage. The miRNA-directed regulation of target genes via DNA methylation has been also recently reported for other miRNA families. For example, miR2883 and miR2328 regulate gene expression by DNA methylation around the miRNA binding site of their target genes (Chellappan et al., 2010). These findings collectively reveal that at least some plant miRNAs may regulate gene expression in two different ways, via DNA methylation or mRNA cleavage silencing mechanisms.

1.5 The role of miRNAs in early embryogenesis

miRNA regulation has been shown to play important roles in many developmental processes, including cell differentiation and developmental timing (Bartel, 2004; Jones-Rhoades et al., 2006; Chen, 2009; Voinnet, 2009). Although such roles of miRNAs during post-embryonic development have been extensively studied, less is known about such roles in embryonic patterning. Several observations suggest that miRNAs may have a central role during Arabidopsis embryogenesis. Firstly, many transcription factors that are important for embryonic patterning, such as the ARFs, CUCs, and HD-ZIP IIIs, are miRNA regulated (Aida et al., 1997; Dharmasiri et al., 2005b; Prigge et al., 2005). Additionally, null mutants in the core enzymes of the miRNA biogenesis machinery, such as SE and DCL1, result in severe patterning defects and embryo lethality (Lobbes et al., 2006; Grigg et al., 2009; Nodine and Bartel, 2010). These clearly indicate that miRNAs are not only required for correct elaboration of the embryonic patterning, but also without miRNAs the organism is not able to develop past the embryonic stage.

Despite its importance for development, we have only just started to understand how miRNA regulation is implicated in axial embryonic patterning. Several studies in animal embryogenesis suggest that miRNAs are required for correct embryogenesis by triggering developmental transitions (Wightman et al., 1993; Moss et al., 1997; Reinhart et al., 2000; Farh et al., 2005; Giraldez et al., 2006; Lund et al., 2009). In these studies, it is shown that miRNAs sharpen boundaries and/or clear expression of genes in precursor cells to allow them to differentiate and transition to the next embryonic stage. Such mode of function has also been observed in several cases of plant miRNAs. For example, the miR172 and the miR156 have been shown to facilitate organ transitions by regulating

the AP2 and SPL3 transcription factors, respectively (Aukerman and Sakai, 2003; Wu et al., 2009). However, these studies are focused on specific regulatory modules and are limited to post-embryonic development.

Recent work on that front suggests that plant miRNAs may have a different role during embryogenesis. Studies of loss-of-function mutants of *SE* and *DCL1* indicate that miRNAs are required as early as the globular stage, or even in earlier stages (Grigg et al., 2009; Nodine and Bartel, 2010). Indeed, *dcl1* null mutants fail to properly establish several cell divisions from the 8-cell stage of embryogenesis (Nodine and Bartel, 2010). This aberrant patterning is also observed in early globular *se-5* embryos (Grigg et al., 2009). Furthermore, DCL1 is required for the repression of approximately 50 genes in early embryonic stages. Most of those genes are transcription factors and most of them are required for patterning in later embryonic stages (Nodine and Bartel, 2010). Specifically, *dcl-1* mutants prematurely express genes that are required during the maturation phase of embryogenesis (Nodine and Bartel, 2010). These collectively suggest that plant miRNAs are required in early embryonic stages to prevent expression of differentiating transcription factors, in contrast to animal miRNAs that allow differentiation.

Nevertheless, it is unclear whether this is a global function of miRNAs or it is limited to specific miRNA/mRNA target regulatory modules. Nodine *et al.,* 2010 suggest that defective patterning in *dcl1* mutants is primarily attributed to misregulation of the *SPL* genes, *SPL10* and *SPL11*, which show the highest levels amongst the genes that are upregulated in this mutant background (Nodine and Bartel, 2010). Given that *SPL* genes are known to promote developmental phase changes, it is possible that this novel

function of miRNAs is limited to the mir165/SPL regulation, revealed only in the *dcl1* mutant background.

This association of miR156/SPL with DCL1 function further supports the work of Laubinger *et al*., 2010, who show that the various components of the miRNA biogenesis machinery are required for different sets of miRNAs (Laubinger et al., 2010). However, this is not unique to DCL1. .Other components of the miRNA biogenesis machinery show similar specificities. For example, phenotypes observed in *se* loss-of-function mutants are largely attributed to misexpression of the HD-ZIP III transcription factors, which are regulated by miR165/6 (McConnell et al., 2001; Emery et al., 2003; Grigg et al., 2005; Grigg et al., 2009). This suggests that the miRNA regulation of the HD-ZIP III primarily requires the function of SE. Assuming that this novel role of DCL1 in preventing precautious gene expression during early embryogenesis is a global function of miRNAs, it would be intriguing to reveal similar functionalities for SE and HD-ZIP IIIs.

1.6 SERRATE: a general regulator of miRNA biogenesis regulating the *HD-ZIP IIIs*

It is clear that miRNA regulation is an important aspect of developmental patterning. Thus, understanding how miRNAs are produced and function is integral in understanding how patterning is elaborated in plants. The pleotropic phenotypes observed in mutants impaired in miRNA biogenesis, such as *se* and *dcl1*, suggest that miRNAs affect multiple developmental processes, possibly involving a large number of different miRNAs. Even though many miRNA pathways are perturbed in these mutants, it is surprising that a large

proportion of the patterning defects is attributed to misregulation of a few transcription factors. One such example involves the HD-ZIP III transcription factors and the miRNA biogenesis protein SE.

The miR165/6-regulated HD-ZIP III transcription factors are involved in SAM development and establishment of leaf polarity during post-embryonic development (McConnell et al., 2001; Emery et al., 2003). The regulation of the HD-ZIP III by miRNA is facilitated by SE (Grigg et al., 2005). Indeed, in *se-3* loss-of-function mutants, the *PHB* and *PHV* expression domains are expanded (Grigg et al., 2005). The *se-3* mutants also show larger SAM and leaf polarity defects, reminiscent of *HD-ZIP III* gain-of-function alleles (McConnell and Barton, 1998; McConnell et al., 2001; Bao et al., 2004; Grigg et al., 2005). Furthermore, miRNA165/6 processing is impaired in this mutant background (Grigg et al., 2005). These observations collectively indicate that SE is required for the miRNA regulation of the HD-ZIP III, and via this regulation SE is implicated in axial patterning and SAM development.

This involvement of SE in miRNA regulation of the *HD-ZIP III* genes is expected, given that SE is one of the main components of the miRNA biogenesis machinery. However, the fact that patterning defects observed in *se-3* loss-of-function mutants are alleviated in *se-3;phb-6;phv-5* triple mutants strongly suggests that the developmental defects observed in *se-3* mutants are predominantly attributed to *PHB* and *PHV* misexpression (Grigg et al., 2005). Knocking down *PHB* and *PHV* in the null *hyl1-1* allele and the hypomorphic *dcl1-7* allele does not rescue patterning defects observed in these mutant backgrounds (Grigg et al., 2009). These observations further indicate that regulation of *PHB* and *PHV* requires the function of SE, and further supports the notion that specific miRNA-regulatory pathways require different components of the miRNA biogenesis machinery, in line with

the work of Laubinger *et al*., 2010 (Laubinger et al., 2010), and Nodine *et al.,* 2010 (Nodine and Bartel, 2010).

If SE is specifically required for regulation of the HD-ZIP IIIs, especially PHB and PHV, then this raises the question of how SE as a general regulator of miRNA biogenesis acquires such specificity. One possibility of such SE-specific functions derives from the observation that CG methylation in the *PHB* locus is also reduced in the *se-3* loss-of-function mutant background (Grigg et al., 2005), similar to the *phb-d* allele (Bao et al., 2004). This observation suggests that SE may also play a role in epigenetic gene silencing via DNA methylation, which is a novel function attributed to a few miRNA families, including miR165/6 (Bao et al., 2004; Chellappan et al., 2010). Involvement of SE in other molecular mechanisms of mRNA processing gives further insights into possible ways by which SE might differentiate its function from other members of the miRNA biogenesis machinery. For example, SE was shown to physically interact with the cap-binding complex proteins facilitating pre-mRNA splicing (Laubinger et al., 2008). A recent study on the animal homolog of SE (*ARSENIC RESISTANCE PROTEIN2* (*ARS2*)) revealed a role of ARS2 as a transcriptional activator of the *SOX2* gene in maintenance of the neuronal stem-cell identity (Andreu-Agullo et al., 2011). Although we lack evidence supporting that SE also functions as a transcription factor in plants, it would be interesting to test this hypothesis.

1.7 Repression of the HD-ZIP III: a single patterning event in the specification of multiple embryonic axes

The SE/*HD-ZIPIII* regulation is also active during embryonic development. In *se-5* null mutants, the expression of *PHB* and *PHV* is severely expanded to the basal pole of the embryo, whilst in wild-type embryos it is restricted apically (Grigg et al., 2009). *se-5* mutants are characterized by aberrant divisions at the basal pole of the embryo and eventually by embryonic lethality, likely associated with the expansion of *PHB* and *PHV* expression, which interferes with basal cell fate. Strikingly, both embryo lethality and patterning along the apical-basal axis are restored in *se-5;phb-13;phv-11* triple mutants (Grigg et al., 2009). QC is absent in *se-5* embryos, supported by the absence of cells expressing the QC determinant *SCR* and the marker *WOX5* (Grigg et al., 2009). Additionally, expression of genes that determine abaxial and peripheral fates is missing, whereas apical fate determinants are expanded, implying that in *se-5* mutants the expansion of the *HD-ZIPIIIs* is associated with expansion of the apical fate (Grigg et al., 2009). Thus, SE-mediated restriction of *PHB* and *PHV* apically is required for embryonic root development and apical-basal patterning (Grigg et al., 2009).

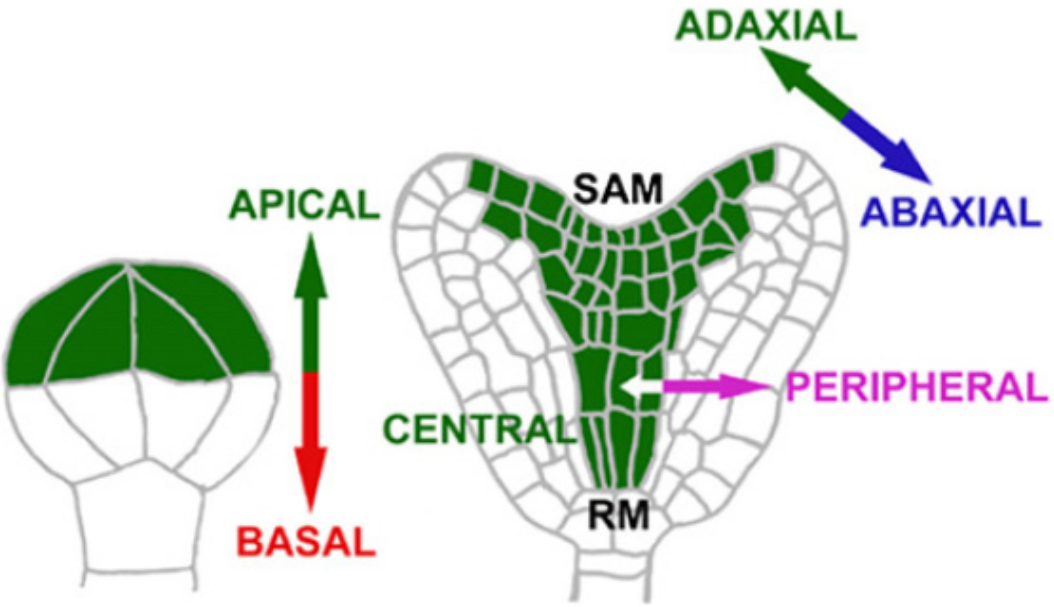
It becomes increasingly clear that mutual repression between the apical and basal fates is required for correct embryonic patterning. This notion is supported by two observations. First, failure to restrict expression of the SAM promoting HD-ZIPIIIs apically interferes with embryonic root patterning (Grigg et al., 2009). Even more dramatic is the conversion of the root into a second shoot, when miRNA-resistant versions of HD-ZIP III are ectopically expressed in the basal pole of the embryo (Smith and Long, 2010). Second, failure to restrict expression of the RM promoting *PLT* genes basally perturbs shoot

development (Long et al., 2002; Long et al., 2006). These observations raise the question of what the molecular mechanisms underlying this repression are. Apical HD-ZIPIII restriction requires redundant action of miR165/6 and PLTs, while PLT restriction to the base requires activity of a repressor complex containing AUX/IAAs and the co-repressor TPL (Long et al., 2002; Long et al., 2006; Szemenyei et al., 2008; Grigg et al., 2009; Smith and Long, 2010). The significance of HD-ZIP III regulation for these interactions is further underlined by the observation that dominant *HD-ZIPIII* alleles suppress the *tpl-1* phenotype that results from inappropriate *PLT* expression (Smith and Long, 2010). These observations suggest that PLTs may act as transcriptional repressors of HD-ZIP IIIs. However, PLTs and HD-ZIP IIIs co-localize in the vasculature (McConnell et al., 2001; Emery et al., 2003; Aida et al., 2004; Blilou et al., 2005; Galinha et al., 2007), and *PLT2* expression is not perturbed in *se-5* mutants in which *HD-ZIP IIIs* are misexpressed (Grigg et al., 2009), arguing against such direct interactions. Thus, it seems that the role of PLT in repressing the HD-ZIP IIIs is indirect and only revealed in the context of cell-fate transformations occurring when *HD-ZIP III* genes are misexpressed, such as in the *tpl-1* background. Furthermore, it is noteworthy that while this antagonism between apical and basal fates is critical for correct patterning and meristem function from the globular stage onwards, it is unlikely to be influential in the establishment of the apical-basal axis early in embryogenesis. This idea is supported by observations that both *se-5* and *tpl-1* mutants develop normally until the globular stage (Grigg et al., 2009; Smith and Long, 2010). Therefore the role of these interactions, involving HD-ZIP III regulation, may be to maintain and translate the initial apical-basal polarity established in the zygote, into developmentally important information that facilitates meristem establishment.

It is apparent that a single patterning process mediated by repression of *HD-ZIP III* contributes to the establishment and further refining of all embryonic developmental axes: apical-basal, central-peripheral, adaxial-abaxial (Figure 1.4). Given that one of the main regulators of *HD-ZIP IIIs* is the miRNA biogenesis protein SE, it is essential to elucidate the spatiotemporal fashion in which the SE/*HD-ZIP III* regulatory pathway functions during embryonic pattern formation.

Figure 1.4: A patterning mechanism involving repression of *PHB* contributes to the establishment of all embryonic developmental axes

Graphical representation of Arabidosis 16-cell stage (left) and heart stage (right) embryos depicting the major axes of development at each stage. The expression domain of the HD-ZIP III transcription factor PHB is marked in green. A single patterning process involving repression of *PHB* contributes to the establishment and further refining of all embryonic developmental axes: apical-basal, central-peripheral (radial), adaxial-abaxial. Model derived from (Grigg et al., 2009), and preceding related literature (McConnell et al., 2001; Emery et al., 2003). Image was modified from (Grigg et al., 2009).


ADAXIAL
ABAXIAL
APICAL
BASAL
SAM
PERIPHERAL
CENTRAL
RM

1.8 The role of plasmodesmata in embryonic patterning

Cell-to-cell communication is pivotal for the orchestration of biological processes across the body of a multicellular organism. For plant cells, communication is facilitated either by diffusion of molecules across the cell walls and the plasmalema (apoplastic route), or via the plasmodesmata (PD) (symplastic route). PD are subcellular cytoplasmic channels traversed by strands of ER that connect the cytoplasm of neighboring cells, forming a symplast. They are divided in primary PD that are formed during cytokinesis by strands of ER trapped within the developing cell plate, and secondary PD that are *de novo* formed between neighboring cells , which may not necessarily share the same lineage (Raven et al., 2005).

PD allow the trafficking of minerals, small metabolites, and small proteins, but they are impermeable to large proteins and metabolites. The effectiveness of molecules to cross the PD channels is primarily limited by the size exclusion limits (SEL) of the plasmodesmal aperture (Raven et al., 2005). There are two prevalent pathways via which PD facilitate exchange of molecules between cells. The first involves simple diffusion of molecules based on their size (Gate Opened/Gate Closed pathway), and the second involves protein-protein interactions and manipulation of the size of the plasmodesmal aperture to facilitate trafficking of specific molecules (Lucas and Lee, 2004). A third transport pathway derives from a combination of diffusion and selective mechanisms, which could operate in a more flexible manner in different developmental and/or physiological conditions (Lucas and Lee, 2004).

Given that PD are required for cell-to-cell communication, it is conceivable that they should also play an essential role in developmental patterning by facilitating the

trafficking of morphogens. It is well accepted that mobile proteins and hormones regulate a variety of developmental processes, from tissue patterning to the formation and maintenance of the meristems (Han et al., 2013). For example, the maize homeodomain transcription factor KNOTTED1 (KN1), which was the first non-cell autonomous protein to be discovered in plants, is expressed in the L2 layer of the meristem and KN1 protein/mRNA complexes travel to the L1 layer via PD to maintain the meristematic activity of SAM (Lucas et al., 1995). A well-studied process that integrates patterning cues from a variety of molecules, such as mobile proteins, miRNAs and hormones, is the radial patterning of the root. In this network of interactions the mobile transcription factor SHR, which is produced in the stele, moves to the endodermis to activate the transcription factor SCR and control ground-tissue patterning (Helariutta et al., 2000; Nakajima et al., 2001; Cui et al., 2007). The SHR/SCR complex activates the expression of miR165/6, which reciprocally move from the endodermis to the stele to instruct the differentiation of the vasculature by regulating the HD-ZIP III transcription factors (Carlsbecker et al., 2010; Miyashima et al., 2011; Marin-Gonzalez and Suarez-Lopez, 2012). An additional layer of complexity derives from the function and interaction of hormones and proteins. For example, within the stele SHR promotes CK function and the HD-ZIP IIIs promote both CK and auxin functions (Izhaki and Bowman, 2007; Cui et al., 2011; Dello Ioio et al., 2012). In turn, CKs negatively regulate auxin, which is integral for embryonic as well as post-embryonic patterning events (Dello Ioio et al., 2007; Dello Ioio et al., 2008; Muller and Sheen, 2008; Ruzicka et al., 2009; Zhang et al., 2011).

Although PD are required for morphogen mobility, it is still ambiguous how their function affects developmental patterning. Due to the fundamental involvement of PD in cell-to-cell communication, one would expect that all cells and tissues should develop PD with

similar properties. However, recent work in the field suggests that the formation and function of PD is a highly regulated process. Several studies using GFP fusions of variable size demonstrated that the PD conductivity is not only different between different cell types and tissues, but it is also quite variable between different developmental stages and physiological conditions (Liarzi and Epel, 2005; Stadler et al., 2005; Werner et al., 2011). Furthermore, the size reduction of the plasmodesmal aperture by callose deposition in gain-of-function mutants of the *CALLOSE SYNTHASE3* (*CALS3*) gene, causes reduced intercellular trafficking and defective root patterning (Werner et al., 2011). This observation strongly supports the notion that PD are essential for correct cell-to-cell communication and developmental patterning. Nevertheless, how cell-to-cell connectivity via PD contributes to embryonic patterning is still poorly understood.

During early embryogenesis, all cells of the embryo share more and larger PD forming a common symplast (Kim et al., 2005b; Kim et al., 2005a; Kim, 2005). These PD connections are considerably reduced as embryogenesis proceeds, especially during the mid-torpedo stage of embryogenesis (Kim et al., 2005b; Kim et al., 2005a). However, in the *ise1* (*increased size exclusion limit1*) and *ise2* (*increased size exclusion limit2*) loss-of-function mutants this decrease in PD connections fails to take place, which culminates in defective embryonic patterning and embryo lethality (Burch-Smith and Zambryski; Kobayashi et al., 2007). Decrease in the size and number of PD connections during early embryogenesis, which is observed in *dse1* (*decreased size exclusion limit1*) loss-of-function mutants, results in similar defects (Xu et al., 2012). These observations suggest that cell-to-cell communication has to be dynamically regulated during embryogenesis to allow correct patterning and embryo viability. This notion is further supported by the pioneering work of Kim *et al*., 2005, where it is clearly demonstrated that cell-to-cell communication

conveys positional information required for correct axial patterning (Kim et al., 2005a). The early-embryo symplast permits for a relatively free exchange of molecules (Kim et al., 2005b; Kim et al., 2005a; Kim and Zambryski, 2005). From the heart stage onwards, this symplast is divided in PD-isolated subdomains that form along the apical-basal axis and allow for a relatively free exchange of molecules amongst the cells within a subdomain, but not as effectively between subdomains (Kim et al., 2005b; Kim et al., 2005a). These collectively suggest that PD development is not only a highly regulated process, but it also plays an important role in embryonic patterning.

1.9 Second-site modifier genetic screens: a powerful tool in the identification of new genes in pathways

1.9.1 Genetic screens

Genetic and molecular studies rely on organisms that can be easily manipulated. Utilization of the small mustard plant A. *thaliana* revolutionized plant sciences and especially plant genetics and development, permitting the use of genetic screens as a powerful tool for identification of new gene functions. Genetic screens can be grouped in forward and reverse screens. In forward genetic screens (the traditional approach) plants with an interesting phenotype are selected for identification of new gene(s) in the process of interest. Reverse genetic screens follow the opposite approach, in which the screen aims to identify phenotypes that arise as a result of a particular genetic sequence.

The success of a forward genetic screen is based on the genetic background that is used, and the screening procedures followed to identify mutants of interest. Of course, selection of the appropriate background is of the utmost importance. Although a wild-type background is suitable for identifying mutants with obvious phenotypes, using mutant backgrounds is more beneficial in cases were the function of the gene of interest is masked by the function of other genes. The screening process is also important for the success of the screen. An easily scorable phenotype or rapid selection method considerably improves the effectiveness of the genetic screen.

Once the mutants of interest have been isolated, they are backcrossed to the parental strain and outcrossed with a polymorphic ecotype (typically Col-0/L*er*). The causal mutation is subsequently identified by map-based cloning.

1.9.2 Second-site modifier screens

A modifier screen is a powerful genetic tool that allows the identification of additional components in a genetic pathway that is perturbed by the mutation of interest. The screen, basically, requires secondary mutagenesis of a characterized mutant. There are two types of second site modifier screens, the enhancer and suppressor screens. Enhancer screens facilitate identification of new genes that function in parallel pathways or encode co-factors. The enhancer mutation enhances the mutant phenotype of the original mutation. This screen is extremely useful in identifying genes with overlapping functions, such as the ones in multigenic families. In contrast, the suppressor screens are useful in revealing “negative” genetic interactions between the suppressor mutation and

the original mutation. In this case, the suppressor mutation alleviates the effects of the phenotype of the original mutation.

Given that modifier screens are really powerful tools in the unbiased identification of novel genetic interactions in known genetic pathways, they have been extensively used in a plethora of developmental studies. For example, a modifier screen on the *crc* loss-of-function mutant of the *YABBY* gene *CRABS CLA*W (*CRC)* furthered our understanding of how polarity is established in carpels (Eshed et al., 1999). Phenotypes observed in the single *crc* mutant do not directly hint at polarity defects in the carpels (Alvarez and Smyth, 1999; Eshed et al., 1999). However, enhancer mutations in the *crc* mutant background result in carpels with characteristic perturbation in axiality (Eshed et al., 1999). In a more recent study, a modifier screen identified the GW-repeat protein "SHUTTLE" IN CHINESE (SUO) as a component of miRNA silencing, giving insights into the poorly understood translational inhibition miRNA silencing mechanism (Yang et al., 2012). These are a few of the examples that showcase how effectively modifier screens can be utilized to improve our understanding of complex developmental pathways.

1.10 Aims of this study and main findings

In this study, my aim was to understand how SE, and by implication miRNAs, contribute to patterning events that take place during Arabidopsis embryogenesis. Analysis of loss-of-function mutations in genes that are required for miRNA biogenesis, such as *SE* and *DCL1*, suggests that miRNAs are essential for correct embryonic patterning and embryo

viability (Lobbes et al., 2006; Grigg et al., 2009; Nodine and Bartel, 2010). The importance of miRNAs in embryonic patterning is further supported by the fact that many miRNA-regulated genes, such as *ARFs*, *CUCs*, and *HD-ZIP IIIs*, are central in patterning events that take place during embryogenesis (Aida et al., 1997; Dharmasiri et al., 2005b; Prigge et al., 2005). Nevertheless, how miRNAs function in a tissue-specific context and how this affects axial patterning during embryonic development remains largely unknown.

To understand the tissue specificity of miRNAs during embryogenesis, I investigated how localized expression of the miRNA biogenesis protein SE affects embryonic patterning. I chose SE due to the fact that SE was shown to have an essential role in patterning along all embryonic axes, via regulation of the HD-ZIP III transcription factors (Grigg et al., 2009). Thus, I expressed SE in different domains, either at the lower tier and/or the upper tier, in *se-5* null embryos and assessed to what extent such tissue-specific expression is able to rescue *se-5* patterning and embryo lethality (Chapter 3). I demonstrated that activity of SE in the lower tier/basal pole of the embryo, within the *PLT2* domain, is sufficient to permit correct patterning throughout the embryonic body (Chapter 3). I also showed that expression of SE in sectors of the *PLT2* expression domain did not fully rescue *se-5* embryogenesis (Chapter 3). In contrast, expression of SE in the upper tier, within the *CUC2* domain, could also rescue *se-5* embryos, indicating that SE can function in a non-cell autonomous and bi-directional fashion during embryogenesis (Chapter 3). The fact that both *PLT2* and *CUC2* promoters are active from early embryonic stages, in contrast to other domains used in this study, also suggests a temporal aspect to this non-cell autonomous patterning mechanism.

The second aim of my thesis was to identify new genes that are involved in SE-dependent patterning processes. To this end, I performed a second site suppressor screen of the non-embryo lethal *se-3* allele. With this screen I aimed to isolate and identify mutants in genes that function either upstream or downstream of the SE/HD-ZIP III regulatory pathway, which was shown to have important patterning roles during and after embryogenesis (Grigg et al., 2005; Grigg et al., 2009). One could argue that because *se-3* is not embryo lethal, it is unlikely for the suppressor genes to have a prominent role in embryonic development. However, given that the SE/HD-ZIP III regulation is required in both ontogenetic stages and that the *se-3* allele also shows some mild embryonic defects (Grigg et al., 2005; Grigg et al., 2009), suggests that the same patterning mechanisms are active in embryonic and post-embryonic development and justifies the decision to conduct the suppressor screen on *se-3*.

The *se-3* suppressor screen yielded 51 independent suppressor lines. I selected 24 of those lines for further analysis (Chapter 4). To reveal the level at which the "suppressor genes" function in the *SE/HD-ZIP III* pathway, I performed genetic tests by crossing the 24 suppressors with the *SE::GUS* and *phb-d/+* strains (Chapter 4). Analysis of the *SE::GUS* strains revealed four suppressors upstream of SE, and analysis of the *phb-d/+* strains revealed a single suppressor as a putative mutant in a gene downstream of *PHB* or a gene encoding for PHB co-factor. Given that *PHB* and *MIR165* are implicated in CK-dependent pathways (Dello Ioio et al., 2012), I treated the 24 *se-3* suppressors with CK, to reveal putative mutants in CK-dependent pathways. These assays and treatments informed my selection of three candidate lines for mapping, and analysis of their Single Nucleotide Polymorphism (SNP) context by whole genome sequencing (Chapter 5). These strains are

currently undergoing further verification and complementation tests to confirm the causal mutation.

The main findings and conclusions of this work are summarized below:

Patterning

- Expression of SE in the *PLT2* domain (lower tier and basal pole of the embryo) is sufficient to rescue *se-5* patterning and embryo lethality.
- Expression of SE in sub-domains of the *PLT2* expression domain can not fully rescue *se-5* patterning and embryo lethality.
- Expression of SE in the *CUC2* domain (upper tie and apical pole of the embryo) is also sufficient to rescue *se-5* patterning and embryo lethality.
- SE influences embryonic patterning in a non-cell autonomous and bi-directional fashion.

se-3 suppressor screen

- Isolated 51 independent lines that suppress the short root of *se-3* and selected 24 of those lines for further analysis.
- Identified four *se-3* suppressors upstream of *SE*, and one downstream/co-factor of *HD-ZIP IIIs*.
- Identified three *se-3* suppressor lines resistant to CK application (putative mutants in CK-dependent pathways).
- The CK-resistant *se-3* suppressor [3] is a putative mutant in the *BELL* gene *PNF*.

Chapter 2

Materials and methods

2.1 General methods and materials

2.1.1 Plant materials

Arabidopsis *thaliana* accession Columbia-0 (Col-0) was used as wild type. The *se-3* (NASC line SALK_083196) and *se-5* (NASC line SALK_101046) strains are described in Grigg *et al.*, 2005 (Grigg et al., 2005), and Grigg *et al*., 2009 (Grigg et al., 2009), respectively. The *ahk3-3* strain, which was used for the CK treatment experiments, is described in Dello Ioio *et al.*, 2007 (Dello Ioio et al., 2012).

2.1.2 Plant growth conditions

Plants were grown on soil and 0,5 X Murashige and Skoog medium (MS) supplemented with 1% sucrose. Specific MS recipes were followed for the selection of transgenic plants and treatment with CK, which are described in the sub-chapters below. Plants were grown either in the greenhouse or in growth cabinets in a "long days" photoperiodic cycle of 16 hours light/8 hours dark at 20-22°C.

2.1.3 Bacterial strains

The E*. coli DH5α* and *DB3.1* strains were used for plasmid amplification. The A. *tumefaciens GV3101* strain was used for plant transformations. *E.coli* strains were grown at 37^{o}C, overnight, in Luria Broth (LB) medium supplemented with the respective antibiotics. The *GV3101* strain was grown at 28^{o}C, for 2 days, in LB medium supplemented with gentamycin and the plasmid specific antibiotic selection.

2.1.4 Primer sequences

Primers used for *PLT2::vYFP:SE, SHR::vYFP:SE,* and *CUC2::vYFP:SE*constructs		
Oligo Name	**Sequence**	**Description**
attB4_pSHR_F	GGGGACAACTTTGTATAGAAAAGTTGCGCGAGAAATTACATAAGAAACTG	Primers used to amplify 2.5 kb of the *SHR* promoter with the *attB4* and *attB1r* sites for gateway cloning
attB1r_pSHR_R	GGGGACTGCTTTTTTGTACAAACTTGGGGAGACCCACAATATCTAAG	
attB1_GFP/YFP_F	GGGGACAAGTTTGTACAAAAAAGCAGGCTGGATGGTGAGCAAGGGCGAGGAG	Primers used to amplify the *vYFP::SE* fusion sequence with the *attB1* and *attB2* sites for gateway cloning
attB2_SE_R	GGGGACCACTTTGTACAAGAAAGCTGGGTGCTACAAGCTCCTGTAATCAATAACG	
LIC-vYFP_F	TAGTTGGAATGGGTTCGAAATGGTGAGCAAGGGCGAG	Primers used to amplify the *vYFP::SE* fusion sequence with the LIC adaptors for LIC cloning
LIC-gSE_R	TTATGGAGTTGGGTTCGAACTACAAGCTCCTGTAATCAATAACG	
pSHR_F	ACTCACAAATCCACCAAACC	Primers used for colony screening
pSHR _R	CACCTGAGGACTTATTATTC	
pPLT2_screen_F	GAGATGATTTGCGGAGTGTG	
pPLT2_F	TCTCTTCCTCTTCTCAATCC	
nosT_R	CAAGACCGGCAACAGGATTC	
nosT_F	TTTATGATTAGAGTCCCGCA	
pCUC2-3F	CTGCTTTGGCTTTGCTCTCT	

Primers used for mapping		
Oligo Name	**Sequence**	**Description**
R1_F	GTAGGACAAAACCAAGTACA	Chromosome I markers
R1_R	TAATAAAGTTCCAGCTTTGA	
R2_F	CACTGCAACAAAGTGGAAAT	
R2_R	ATCCGTTTCAATATCCACAA	
ATHS0392_F	TTTGGAGTTAGACACGGATCTG	
ATHS0392_R	GTTGATCGCAGCTTGATAAGC	
T27K12_F	GGAGGCTATACGAATCTTGACA	
T27K12_R	GGACAACGTCTCAAACGGTT	
R3_F	TGCGGGAGTGTGATAGAATA	
R3_R	TCCTCGAAAGATTCATTGAT	
NGA280_F	CTGATCTCACGGACAATAGTGC	
NGA280_R	GGCTCCATAAAAAGTGCACC	
F11P17-4615_F	CGCAATCGATTTTATTTAAATCC	
F11P17-4615_R	TTTCAGTTTGATGATTTATTCGC	
F19K23_F	GGTCTAATTGCCGTTGTTGC	
F19K23_R	GAATTCTGTAACATCCCATTTCC	
R5_F	GGACCGACGGTTACGAGAG	
R5_R	TAACGGGCCGTTGCAAGA	
R6_F	CGTGTTTACCGGGTCGGA	Chromosome II markers
R6_R	AAAACCCTTGAAGAATACG	
MSAT2.26_F	TCTCCGATTGAGCCCCAAAG	
MSAT2.26_R	CGGGGAAAGATGGGTTTTGA	
MSAT2.18_F	TAGTCTCTTTTGGTGCGCATA	
MSAT2.18_R	AGCCTCTCCAAGCTTAGGTCT	
MSAT2.28 _F	AATAGAAATGGAGTTCGACG	
MSAT2.28 _R	TGAACTTGTTGTGAGCTTTG	
MSAT2.11_F	GATTTAAAAGTCCGACCTA	
MSAT2.11_R	CCAAAGAGTTGTGCAA	
A007019-4706_F	ATAGTGGGTGATCTTTGAATG	
A007019-4706_R	ACTTGTCTCGTCGCACTGTT	
R8_F	TCCGATTCGATTAAACTC	
R8_R	TTATTTCCTATTTCAAGACT	
R9_F	ATGAACGGAGTAGCTATC	
R9_R	CGCGTAGAACATAATCTGTA	

Primers used for mapping		
Oligo Name	**Sequence**	**Description**
R18_F	CTCTGTTGGGGCAAAACC	Chromosome V markers
R18_R	GATGCTGGAGAGTAGCTTAG	
R20_F	CACAGGCCATTGGATGTA	
R20_R	TGTTAGAACCCACCATTTG	
R21_F	CCTGTTCCAATGAATATG	
R21_R	TGTAGCTGCTGAGTTGTC	
MSAT5.10_F	GTTGCTTCTTTTGCTAACT	
MSAT5.10_R	ATCGTTCACGCAATAAG	
JV61/62 _F	CGCTTTCCTTGTGTCATTCC	
JV61/62 _R	AAATGCAAATATTGATGTGTGAAA	
JV75/76 _F	CACAATCAGAGGGGGTTGAT	
JV75/76 _R	AAATTTTGGGGGAAATGAAA	
R22_F	AAAAGGCGACTACTAGCA	
R22_R	GCCATTTATTTGGTCAAC	
MSAT5.19_F	AACGCATTTGCTGTTTCCCA	
MSAT5.19_R	ATGGTTATCTCATCTGGTCT	
MSAT2.18_F	TAGTCTCTTTTGGTGCGCATA	
MSAT2.18_R	AGCCTCTCCAAGCTTAGGTCT	

Other oligos		
Oligo Name	**Sequence**	**Description**
SE-3_F	TCCTCCACCGCCTTCTTCTTC	Primers used to genotype *se-3* T-DNA insertion (SALK_083196). SE-3F/ LbB1 primers amplify the mutant band. The SE-3F/3R amplify the wild type.
SE-3_R	CCATAACCTCCACGTCCTCCC	
SE-5_F	TTGTCTTTTTCCTATGGCGTG	Primers used to genotype *se-5* T-DNA insertion (SALK_101046). SE-5F/ LbB1 primers amplify the mutant band. The SE-5F/5R amplify in wild type
SE-5_R	TGTCCCGCTTTGTAAATCAAG	
LbB1	GCGTGGACCGCTTGCTGCAACT	Used for genotyping of SALK T-DNA lines
phb-1d_CAP_MboII_F	CAAATCCTCAGCATCAGCAA	CAP marker used to genotype *phb-1d*
phb-1d_CAP_MboII_R	TCAGACACAACTAAAGAATAGAAATCA	
M13(-20)F	TGTAAAACGACGGCCAGT	Primers used for colony screening and sequencing of various of the constructs used in this thesis
M13R	CAGGAAACAGCTATGACC	
ocs-R	CGCTCGGTGTGTCGTAGATA	
SP6	ATTTAGGTGACACTATAG	
T7	TAATACGACTCACTATAGGG	

2.2 Genetic methods

2.2.1 Generation of strains used in this thesis

PLT2::vYFP:SE;se-5/+, CUC2::vYFP:SE;se-5/+, and SHR::vYFP:SE;se-5/+

The *PLT2::vYFP:SE;se-5/+*, *CUC2::vYFP:SE;se-5/+*, and *SHR::vYFP:SE;se-5/+* transgenic lines were generated by transformation of the respective fusion constructs in *se-5/+* heterozygous plants. *PLT2::vYFP:SE;se-5/+* and *SHR::vYFP:SE;se-5/+* T1 lines were selected with hygomycin, and the presence of the *se-5* T-DNA was tested by genotyping. *CUC2::vYFP:SE;se-5/+* lines were selected with BASTA and genotyped for the presence of the *se-5* T-DNA insertion. All lines were checked and analyzed for *vYFP* expression by confocal microscopy. Careful analysis of *vYFP* expression patterns and phenotypic characterization of embryonic development were carried out in the T2 generation. Details about these constructs are described in sub-chapters below.

p7>>UAS::SE;se-5/+ and p19>>UAS::SE;se-5/+

The *p7>>UAS::SE;se-5/+* and *p19>>UAS::SE;se-5/+* strains were generated by crossing the *p7* and *p19 Gal4*-driver lines (Moller, B. and Weijers, D. unpublished materials) with the *UAS::SE;se-5/+* transgenic strains. The *UAS::SE;se-5/+* strain was generated by transformation of the *UAS::SE-pMLBART* plasmid (harboring the *SE* coding sequence under the *UAS* enhancer) in the *se-5/+* strain. These lines function in a two component transcriptional mechanism in which transcription of the *Gal4* mRNA is activated in the *p7* and *p19* domains (see Chapter 3, Table 3.1, and Figure 3.6) and the Gal4 protein transiently activates expression of the *UAS::SE* in these domains. Individual F2 lines were genotyped for the presence of the *se-5* T-DNA insertion. These lines were also checked

for GFP expression (the driver-line fluorescent reporter) in confocal microscope. Details about these constructs are described in sub-chapters below.

Other strains

The *phb-d* strain derives from the introgression of the original *phb-1d (*L*er)* mutation (see ref. McConnell et al., 2001) into Col-0. Transformation in Col-0 of a construct harboring the *GUS* coding sequence under the *SE* promoter generated the *SE::GUS* strain. The *se-3* (L*er*) strain was generated by introgression of the *se-3* (Col-0) T-DNA insertion (SALK_083196) into the L*er* ecotype. The *se-3* suppressor mapping populations were generated by outcrossing of the suppressor strains with the *se-3* (L*er*) strain.

2.2.2 Plant transformation: "Floral dipping"

Plasmids containing T-DNA were introduced in the *GV3101* strain by electroporation. A 5 ml Luria Broth (LB) pre-culture from a single transformation colony was used to inoculate a 1 L transformation culture. These cultures were grown to an optical density of OD600nm = 0.8. Cells were re-suspended in transformation buffer (5% sucrose, 1 X Gamborg's vitamins (Sigma), 0,03% silwet-77). Inflorescences were submerged in this solution for five minutes, after which plants were stored laid on the side of the pots, overnight at 4°C. The next day the plants were returned to the greenhouse, placed upright and fertilized.

2.2.3 Selection of transgenic plants

Transgenic plants were selected by spraying with 400 µM BASTA herbicide (commercial name "Kaspar" from Aventis) or with antibiotics diluted in 1X MS without sucrose (hygrogromycin selection 25 mg/L). For hygromycin selection, seeds were sterilized for 10 min with a solution containing 70% ethanol, 0,1% Triton X-100, followed by a 10 min wash with 100% ethanol. After ethanol evaporation, seeds were re-suspended in 0,01% agarose solution and directly plated on the selection plates.

2.2.4 Cross-pollination

To cross the different strains, pollen from mature flowers of the donor plant was transferred onto the stigma of the acceptor plant. All floral organs, except for the carpel, were removed from the acceptor flower before pollination. Hybrid seeds were then collected from individual siliques.

2.3 Molecular biology

2.3.1 Construct design

PLT2::vYFP:SE and SHR::vYFP:SE

The *PLT2::vYFP:SE* and *SHR::vYFP:SE* cloning strategies are based on the "Multisite Gateway Three-Fragment Cloning Kit" (Invitrogen/12537-023), modified by Hofhuis, H. and Scheres, B. (system used in (Galinha et al., 2007), and (Hofhuis et al., 1013)). This cloning system utilizes recombination sequences to simultaneously clone multiple DNA

fragments in one recombination step. In the modified version the commercially provided *pDONR* and *pDEST* vectors have been replaced with the commonly used *pGEM-TEasy* and *pGREEN* cloning vectors, respectively. These plasmids were modified by the addition of the corresponding recombination sequences and generated the, *pGEM-TP4P1R*, *pGEM-T221*, *pGEM-TP2RP3* entry vectors and the *pGII0227* (Hyg^r) destination vector. Each of the entry and destination vectors has different *att* recombination sites, so recombination can only happen in one direction. The *pGEM-TP4P1R* plasmid is used for the recombination of 5'- sequences, usually promoter sequences. The *pGEM-T221* is used for the cloning of the main sequence, usually coding sequences. The *pGEM-TP2RP3* plasmid is used for cloning of 3'- sequences, such as terminators or fluorescent fusion tags.

For both the *PLT2::vYFP:SE* and the *SHR::vYFP:SE* constructs, I amplified the fusion of the genomic sequence of *SE* with the *vYFP* fluorescent tag sequence from the *SE::vYFP:SE* (*pEGAD*) plasmid described in Grigg *et al*., 2009 (Grigg et al., 2009). The primers used for this amplification contained *attB1* and *attB2* sites. This facilitated the recombination of the *vYFP:SE* fusion in the *pGEM-T221*, generating the *vYFP:SE-L1L2* plasmid. Concerning the 5' sequences, a 2.5 kb sequence upstream of the start codon of the *SHR* gene was amplified with the respective *attB4* and *attB1r* sequences and cloned by recombination in the *pGEM-TP4P1R* vector. This generated the *pSHR-L4R1* entry vector. The *pPLT2-L4R1* plasmid, containing a 5.8kb fragment of the *PLT2* promoter cloned in the *pGEM-TP4P1R* vector, was given to us by Hofhuis, H. and Scheres, B (plasmid used in Galinha *et al*., 2007). For the 3'-sequence, I utilized the *nosT-L2R3* plasmid (provided by Hofhuis, H. and Scheres, B., system used in Galinha *et al*., 2007, and Hofhuis *et al*., 2013), which contains the *NOS* terminator sequence. LR recombination of the respective components of the construct in the *pGII0227* (Hyg^r) vector generated the *PLT2::vYFP:SE:nosT* and

SHR::vYFP:SE:nosT constructs, here referred to as *PLT2::vYFP:SE* and *SHR::vYFP:SE*. These plasmids are based on the *pGREEN* vector, so they confer kanamycin resistance in bacteria and hygromycin resistance in plants.

CUC2::vYFP:SE

The 3.2kb fragment of the *CUC2* promoter was excised from the *pCUC2-pBJ36* plasmid (generated by Dello Ioio R., unpublished material) with *EcoRI* digest. This fragment was sub-cloned in the *EcoRI* site in front of the ligation independent cloning (LIC) site of the *pPLV01* (Ba^r) vector. This generated the *pCUC2-pPLV01* plasmid. The *pPLv01* (Ba^r) vector is part of a versatile set of vectors generated by De Rybel *et al.*, 2011 (De Rybel et al., 2011) to facilitate high-throughput analysis of multiple genes in plants. This cloning system provides a fast alternative to the conventional ligation and recombination cloning strategies. The *vYFP:SE* fusion sequence was amplified by the *SE::vYFP:SE* (*pEGAD*) plasmid (used in (Grigg et al., 2009)) with primers containing the corresponding LIC adaptors. The *pCUC2-pPLV01* plasmid was subsequently digested with *HpaI*, which linearizes the vector within the LIC site. Both *LIC-vYFP:SE* and the linearized *pCUC2-pPLV01* DNA fragments were treated with the T4 DNA polymerase to create the complementary "overhangs". The fragments were incubated at 22^{o}C to hybridize. This resulted in the generation of the *CUC2::vYFP:SE-pPLV01* plasmid, here known as *CUC2::vYFP:SE*. The protocols I followed are described in detail in (De Rybel et al., 2011). The *CUC2::vYFP:SE* plasmid is based on the *pPLV01* vector, thus it confers kanamycin resistance in bacteria and BASTA resistance in plants.

p7 and p19 driver lines

The *p7* and *p19* driver lines were provided by Moller, B. and Weijers, D. (unpublished materials). These promoter-trap lines were generated using the LIC vector *pPLV04* (Kan^r) described in De Rybel *et al*., 2011. *pPLV04* harbors the *SV40* nuclear localization signal followed by a triple repetition of the *GFP* coding sequence and the *Gal4* trans-activator protein sequence.

2.3.2 Ligation, BP/LR recombination, and LIC cloning protocols

Ligation by T4 DNA Ligase

Insert and vector DNAs were mixed in a 1.5 ml eppendorf tube in the typical 3:1 (insert:vector) ratio. 1 µl of Ligation Buffer 10 X and 1 µl T4 DNA Ligase (Promega) were added to the DNA mixture. The ligation reaction was supplemented with water until the final volume of 10 µl is reached. The ligation reaction was incubated at 16^{o}C overnight or at 25^{o}C for 4 hours. Ligation reactions were subsequently transformed in the respective E.*coli* strains.

BP/ LR recombination reaction

For the BP and LR recombination cloning I followed the protocol described in the "Multisite Gateway Three-Fragment Cloning Kit" (Invitrogen/12537-023).

LIC cloning

For the LIC cloning of *CUC2::vYFP:SE* in *pPLV01*, I followed the protocols described extensively in De Rybel *et al*., 2011 (De Rybel et al., 2011).

2.3.3 Transformation of E. *coli* cells by heat shock

Competent cells of the corresponding E. *coli* stain are mixed with the DNA sample to be transformed. The mixture is incubated on ice for 15-30 min. Subsequently, the mixture is heated at 42^{o}C, for 45 sec. After the heat shock, the cells are incubated on ice for 5 min. 1 ml LB is added to the mixture and the culture is then transferred in a 37^{o}C incubator for 1-2h. Cells are subsequently precipitated by mild centrifugation at 2200-2500 rpm, for 2 min. Most of the supernatant is discarded and cells are re-suspended in the remaining volume of LB. The re-suspension is then plated on petri dishes containing solid LB medium, supplemented with the appropriate antibiotics for selection. The transformation plates are incubated overnight, at 37^{o}C. After 12h incubation, single colonies should be visible on the plate.

2.3.4 DNA extraction for PCR (quick-prep)

The tissue from 1-2 leaves was mechanically disrupted in a 1,5 ml eppendorf tube. 400 µl extraction buffer (250 mM Tris-Hcl pH 7.5, 250 mM NaCl, 25 mM EDTA, 0,5% SDS) was added to the disrupted tissue and followed by the immediate vortexing of the mixture. Tubes were centrifuged at 13000 rpm for 10 min. 200 µl of the supernatant were transferred to a fresh eppendorf tube containing 200 µl of isopropanol. Samples were vortexed and incubated at room temperature for 5 min for DNA precipitation. Tubes were subsequently centrifuged at 13000 rpm for 10 min, supernatant was discarded, and DNA was air-dried. The dry DNA was re-suspended in 200 µl dH_2O, and 2-3 µl of this solution were used for PCR reaction.

The protocol was modified for high-throughput DNA extraction of multiple samples. Leaf samples collected in 96-well DNA extraction plates were incubated in -80oC for 10 min to facilitate tissue disruption. The frozen tissue was mechanically disrupted by metallic beads using the TissueLysser (Qiagen) shaker. 400 µl DNA extraction buffer (250 mM Tris-Hcl pH 7.5, 250 mM NaCl, 25 mM EDTA, 0,5% SDS) was added in each sample. The following steps are similar to the small scale protocol described above, with the exception that the 96-well plates were centrifuged at 5000 rpm.

2.3.5 DNA extraction and Whole Genome Sequencing

DNA extraction Protocol

High purity genomic DNA was extracted using the DNAeasy Maxi Kit (Qiagen/68163) from leaf-tissue samples weighing ~1 gr. Depending on the species and the amount of the tissue used, DNA yield can vary from 10-30 µg. Usually, 1 gr of Arabidopsis tissue yields around 20 µg of genomic DNA. DNA was extracted from pools of ~50 individuals with the phenotype of interest (per line) from segregating populations. DNA was extracted from pools of long-root individuals of *se-3* suppressor lines [1], [3], and [23]. DNA extract from a pool consisted of *se-3* individuals was used as a reference. 10 µg of the extracted DNA were send to BGI TECH SOLUTIONS (HONGKONG) CO., LIMITED to perform illumina sequencing and generate the lists of SNPs for each respective sample.

Whole Genome Sequencing

The DNA samples of *se-3* suppressor [1], [3], [23], and the *se-3* reference sample were sent to BGI TECH SOLUTIONS (HONGKONG) CO., LIMITED for the generation of libraries

and illumina sequencing using 30X sequencing depth. The short reads generated by the illumina sequencing were aligned and assembled along the Arabidopsis Col-0 genome, which was used as a scaffold. Comparison of the assembled genomes derived from the samples and the reference generated the lists of unique SNPs detected within each sample but excluded from the reference or any other sample. After sequencing and the initial filtering of sample-unique SNPs by BGI TECH SOLUTIONS (HONGKONG) CO., LIMITED, I was given the SNP data to further filtering of significant SNPs and further analysis (see chapter 5 for further information). This analysis was performed in collaboration with Dr. Xiangchao Gan.

2.4 Microscopy, histology and histochemistry

2.4.1 Confocal microscopy

Root and shoot apices were dissected and mounted in dH_2O. Embryos in different developmental stages were dissected out of the seed and mounted in 7% (w/V) glucose solution. Confocal microscopy was performed using the Leica SP5 or Zeiss 510 LSM Meta systems. To image GFP I used the 458 nm argon laser with a 646-700 nm filter for the chlorophyll channel and a band pass 475-525 nm filter for GFP. To image vYFP I used the 488 nm argon laser with a 657-743 nm filter for the chlorophyll channel and a band pass 505-550 nm filter. Transmitted light was used in both cases for visualization of the embryo structures.

2.4.2 Light microscopy

Imaging of tissue clearings and GUS stained samples was performed using an Olympus BX50 microscope. To enhance the contrast of the specimens, I used differential interference contrast optics (DIC). Pictures were captured with a digital camera using the Image-Pro 6.2 and Infinity Capture1 softwares.

2.4.3 Embryo clearings

To analyze embryonic patterning in the various lines generated in this thesis, intact embryos in different developmental stages were removed from the developing siliques and mounted in chloral hydrate solution (hydrate:glycerol:water/ 8:2:3) on a slide under a coverslip. The samples were incubated overnight at 4°C before observation.

2.4.4 GUS analysis

Tissue was fixed in 90% acetone at -20°C for 1 hour, washed briefly with 100 mM phosphate buffer, and stained for 30 min in freshly prepared 100 mM sodium phosphate buffer, 10 mM sodium EDTA, 1 mM 5-bromo-4-chloro-3-indolyl-ß-D-glucuronic acid (Molecular Probes) supplied with ferrocyanide and ferricyanide salts (2 mM). Reactions were terminated with 95% ethanol, and root tip apices were mounted in 50% glycerol for microscopy.

2.4.5 CK treatment

Seedlings were grown on 0,5 MS + 1% sucrose square plates positioned vertically to allow correct root development. 6 days after germination a subset of seedlings were transferred on 0,5 MS + 1% sucrose+ 5 µM Dihydrozeatin and returned back to the growth chamber for overnight treatment with CK. The root tips from 10 seedlings per sample were dissected and mounted in chloral hydrate solution (hydrate:glycerol:water/ 8:2:3) on a slide under a coverslip. The root meristem size analysis of treated and untreated samples was performed as described in Dello Ioio *et al*., 2007 (Dello Ioio et al., 2012) (see also Chapter 4.2.4).

Chapter 3

SE regulates axial embryonic patterning in a bi-directional and non-cell autonomous fashion

3.1 Introduction

During embryogenesis, a simple body plan of the plant is laid down by coordination of cell division and differentiation. In the model plant Arabidopsis, cell division and differentiation follow stereotypic patterns. Several studies have revealed a central role of miRNAs in regulation of these stereotypic patterning processes. For example, many miRNA-regulated genes, such as the *ARFs*, *CUCs*, and *HD-ZIP IIIs,* are important in patterning events that happen during Arabidopsis embryogenesis (Aida et al., 1997; Emery et al., 2003; Dharmasiri et al., 2005b; Prigge et al., 2005). Furthermore, several loss-of-function mutants of genes that are required for miRNA biogenesis show severe patterning defects and embryo lethality (Lobbes et al., 2006; Grigg et al., 2009; Nodine and Bartel, 2010). These collectively suggest that miRNA regulation is important for correct embryogenesis and embryo viability. Thus, studying the role of miRNAs in development is essential for understanding embryonic patterning.

miRNAs are 21-24 nt RNAs that are processed from longer double-stranded transcripts by a nuclear protein complex containing the RNase III DCL1, and the RNA binding proteins SE and HYL1 (Dong et al., 2008). The mature miRNAs regulate gene expression by guiding degradation and/or translational inhibition of complementary transcripts facilitated by the AGO1 protein (Mallory and Bouché, 2008). During post-embryonic development, the miRNA biogenesis protein SE regulates the expression of the HD-ZIP III transcription factors via miR165/6 (Grigg et al., 2005). Because most of the phenotypes observed in the *se-3* loss-of-function mutant are suppressed by knocking down two *HD-ZIP III* genes (Grigg et al., 2005), this supports the involvement of SE in patterning events that require the function of the HD-ZIP IIIs. These patterning events are the development of the SAM

and the correct establishment of polarity in lateral organs (McConnell et al., 2001; Emery et al., 2003).

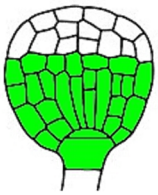
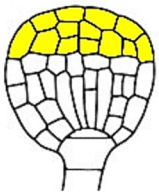
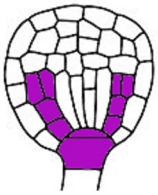
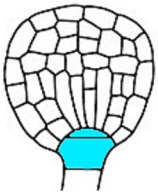
The regulation of the HD-ZIP IIIs by SE is also important for embryonic development(Grigg et al., 2009). Failure to confine the HD-ZIP III transcription factors PHB and PHV in the apical pole of the early globular *se-5* null embryo perturbs patterning in peripheral and basal domains of the embryo leading to developmental arrest (Grigg et al., 2009). Moreover, gain-of-function mutations that render the *HD-ZIP III* mRNAs resistant to miRNA regulation phenocopy patterning defects observed in *se-5* embryos (Grigg et al., 2009). These clearly indicate that miRNA regulation of the HD-ZIP IIIs by SE is a requirement for correct embryonic patterning and further suggest that SE, and by implication miRNAs, are important for embryo development and viability. Similarly to *se-5*, null *dcl1* mutants also show patterning defects and developmental arrest (Nodine and Bartel, 2010). Although both SE and DCL1 are core enzymes of the miRNA processing complex, it seems that regulatory modules such as miR165-6/HD-ZIP IIIs and miR156/SPLs specifically require the function of SE and DCL1, respectively (Grigg et al., 2009; Nodine and Bartel, 2010). However, it is still unclear why specific miRNA regulatory modules are dependent on specific components of the miRNA biogenesis machinery. We still know very little concerning the tissue-specific functions of miRNAs, especially during embryogenesis. Are there specific domains of the embryo in which miRNA regulation is needed more than others?

In this chapter I discuss experiments I performed in order to understand the tissue-specific function of miRNAs in embryonic patterning. More specifically, I expressed SE in various domains in the null *se-5* embryo, aiming to decipher how SE and by implication

miRNAs influence embryonic patterning. Furthermore, I wanted to understand whether production of miRNAs in these domains can influence patterning in other domains of the embryo.

Table 3.1: Table summarizing the experimental set up designed for the tissue-specific expression of SE in various domains chosen for the purposes of this study

The table shows (from left to right) the fusion construct containing the sequence of SE, cartoons depicting the domains in which SE expression was driven, the mutant background in which the transgenes were transformed, and the cloning strategy followed for the generation of each respective promoter-SE combination (direct fusion or two components system). The fusion of the *SE* genomic sequence with *vYFP* was driven under the *PLT2*, *SHR*, and *CUC2* promoters in *se-5/+* heterozygous plants. To drive expression of SE under the *p7* and *p19* promoter-trap driver lines (provided by Moller, B. and Weijers, D., unpublished materials), transgenic lines of SE driven by the *UAS* promoter in the *se-5/+* background (*UAS::SE;se-5/+*) were crossed with the respective *p7* and *p19* driver lines. SE was expressed in the *PLT2* (lower tier and basal pole) and *CUC2* (upper tier and apical pole) domains because they are complementary to each other covering wider domains of the embryo. The *SHR* (central domain of the lower tier), *P7* (peripheral domain of the lower tier and basal pole), and *P19* (basal pole) domains were chosen in order to further dissect the *PLT2* expression domain in smaller subdomains.

Fusion/ Gene	Domain			Genotype	Construct strategy
vYFP:gSE	*pPLT2* 	*pSHR* 	*pCUC2* 	***se-5/+***	**Direct**
UAS::SE	*p7* 	*p19* 		***se-5/+***	**Two component**

3.2 Results

3.2.1 Expression of SE in the *PLT2* domain is sufficient to rescue embryonic patterning

To understand the involvement of SE in embryonic patterning, I analyzed how expression of SE in specific domains in the null *se-5* mutant affects embryonic patterning (Table 3.1). This experimental set up aims to dissect embryonic domains where activity of SE is essential for proper axial patterning, possibly by regulation of the HD-ZIP III transcription factors. The initial strategy involves driving expression of SE in the *PLT2* and *SHR* domains (Table 3.1). I expressed SE under these promoters because they are both active in the root pole of the embryo. *PLT2* has wider expression, whereas *SHR* has more restricted expression (Table 3.1). It is noteworthy that both *PLT2* and *SHR* pathways are involved in the development of the root pole, beginning with the patterning of the hypophysis (Jenik *et al.*, 2007), which is one of the earliest patterning events that fail to take place in *se-5* embryos (Grigg et al., 2009).

I generated direct fusion constructs of the genomic sequence of *SE* with *vYFP* driven by each promoter and transformed those constructs in *se-5/+* heterozygous plants. After transformation and selection of approximately 20 lines per construct, I selected 4-6 independent T1 lines per construct for further analysis. These T1 lines were self-fertilized to generate the T2 generation. The T2 lines were screened for embryonic phenotypes, vYFP expression, and genotyped for the presence of the *se-5* allele. *vYFP* and *se-5* homozygosity were verified in the T3 generation.

Because the *se-5* T-DNA insertion confers embryo lethality, it is not possible to work with homozygous *se-5* strains, making the use of segregating heterozygous *se-5/+* strains obligatory. The progeny of a *se-5/+* plant segregate the *se-5* phenotype in the expected

mendelian ratio of a recessive mutation, 3:1 (wild-type looking embryos : mutant looking embryos). Thus, in the silliques of the *se-5/+* transgenic plants, 25% of the embryos have the *se-5* phenotype of defective patterning and embryo lethality, whilst the remaining 75% have the wild-type phenotype (Figure 3.1 A-B).

Although SE is expressed in all cells of the embryo, expression of SE solely in the *PLT2* domain in the *se-5/+* mutant background (*PLT2::vYFP:SE;se-5/+* transgenic lines) conferred 100% recovery of embryogenesis (Figure 3.1, Table 3.2). The *se-5* phenotype was undetectable in all six independent *PLT2::vFFP:SE;se-5/+* T2 lines that have been analyzed (Table 3.2). These lines were verified for transgene homozygosity in the T3 generation. This observation indicates that activity of SE in the *PLT2* domain is sufficient to rescue patterning defects observed in *se-5* null embryos. Given that the *PLT2* promoter is widely expressed in several different cell types in the root pole of the embryo (Figure 3.1 D), I tested whether more restricted expression of SE in the root pole can confer similar results. Thus, I expressed SE under the *SHR* promoter, which is restricted in the central domain in the lower tier of the embryo (Table 3.1).

Table 3.2: Table summarizing the embryonic phenotypes observed in the *PLT2::vYFP:SE;se-5/+* T2 lines (see also Figure 3.1)

Line	T2.1	T2.2	T2.3	T2.4	T2.5	T2.6
Wt-like embryos	185	190	199	200	200	189
Defective embryos	-	-	-	-	-	1
Total embryos	185	190	199	200	200	190
Defective embryos (%)	**0**	**0**	**0**	**0**	**0**	**0.5**

In contrast to what I observed in the *PLT2::vYFP:SE;se-5/+* transgenic plants, expression of SE in the *SHR* domain in *se-5/+* plants (*SHR::YFP:SE;se-5/+* transgenic lines) did not fully rescue *se-5* embryos (Table 3.3). Similarly, approximately 200 embryos were phenotyped per line from four independent *SHR::YFP:SE;se-5/+* T2 lines. These lines were verified for transgene homozygosity in the T3 generation. Although patterning is improved in the *SHR::vYFP:SE;se-5/+* embryos, in comparison to *se-5*, aberrant divisions are still detectable along the apical-basal axis (Figure 3.2). Thus, activity of SE in the central domain at the lower tier of the embryo (*SHR* domain) is not sufficient to fully rescue patterning in *se-5* embryos.

Table 3.3: Table summarizing the embryonic phenotypes observed in the *SHR::vYFP:SE;se-5/+* T2 lines (see also Figure 3.2)

Line	T2.1	T2.2	T2.21	T2.23
Wt-like embryos	176	160	153	169
Defective embryos	54	50	44	52
Total embryos	220	199	189	210
Defective embryos (%)	24.54	25.12	23.28	24.76

Collectively, these data indicate that activity of SE in the *PLT2* expression domain, but not in the *SHR* domain, is sufficient for proper axial patterning throughout the embryonic body. This further suggests either that expression of SE is required in the full complement of the *PLT2* domain or that a different subset of the *PLT2* domain has stronger contribution to the effectiveness to rescue patterning in *se-5* embryos. Alternatively, such differences in the effectiveness of rescuing *se-5* patterning may be attributed to differences in the developmental timing of these promoters. The *PLT2* promoter is active

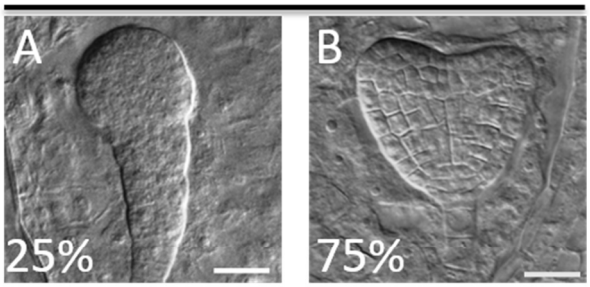
from the zygote stage onwards, whereas *SHR* expression begins at the early globular stage of embryogenesis.

It is noteworthy that although SE was solely active in the lower tier/basal pole of the embryo in the *PLT2::vYFP:SE;se-5* embryos, this was sufficient to promote correct patterning in the apical pole, where *vYFP* is not detectable (Figure 3.1 D). This observation suggests that a patterning mechanism triggered by SE within the *PLT2* domain may non-cell autonomously regulate patterning in the apical pole of the embryo.

Figure 3.1: Expression of SE in the *PLT2* domain is sufficient to fully rescue *se-5* embryos

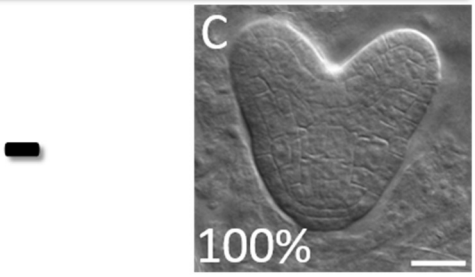
(A-C) Nomarski images of heart stage embryos of *se-5/+* progeny (A-B), and *PLT2::vYFP:SE;se-5/+* progeny (C). Representative images of the various phenotypic classes observed in each strain are shown directly below the labels. The frequency of each phenotypic class is indicated at the bottom left corner of the respective image. Six *PLT2::vYFP:SE;se-5/+* independent T2 lines were analyzed and approximately 200 embryos were phenotyped per line (Table 3.2). (D) CLSM image of *PLT2::vYFP:SE* at heart stage embryo. Scale bars: 20 µm.

se-5/+ progeny



No transgene

PLT2::vYFP:SE; se-5/+ progeny



PLT2::vYFP:SE

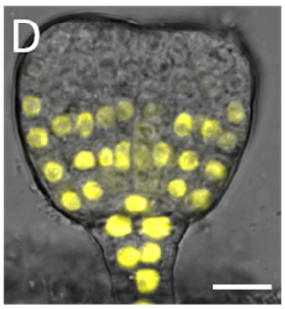
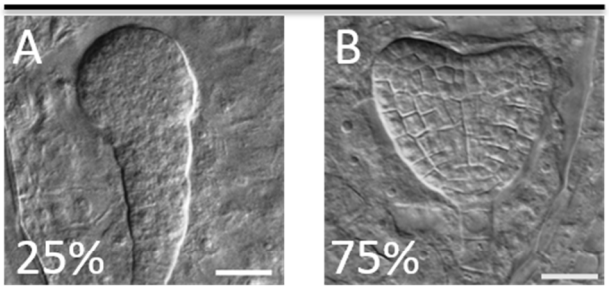


Figure 3.2: Expression of SE in the *SHR* domain partially rescues *se-5* embryos.

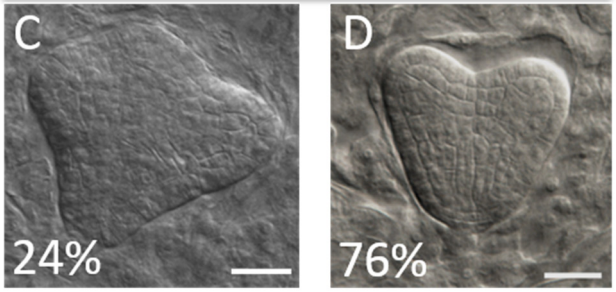
(A-D) Nomarski images of heart stage embryos of *se-5/+* progeny (A-B), and *SHR::vYFP:SE;se-5/+* progeny (C-D). Representative images of the various phenotypic classes observed in each strain are shown directly below the labels. The frequency of each phenotypic class is indicated at the bottom left corner of the respective images. Six *PLT2::vYFP:SE;se-5/+* independent T2 lines were analyzed and approximately 200 embryos were phenotyped per line (Table 3.3). (E) CLSM images of *SHR::vYFP:SE* at heart stage embryo. Scale bars: 20 µm.

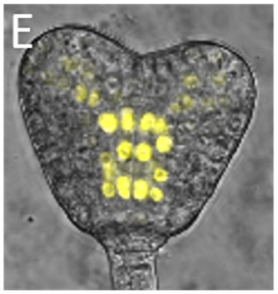
se-5/+ progeny



No transgene

SHR::vYFP:SE; se-5/+ progeny





3.2.2 Expression of SE in the *PLT2* domain permits *se-5* embryos to proceed to post-embryonic development

The analysis of the *PLT2::vYFP:SE;se-5/+* and *SHR::vYFP:SE;se-5/+* T2 lines revealed that tissue-specific expression of SE in the *PLT2* domain is sufficient to fully restore embryogenesis of *se-5* embryos to the extent that *PLT2::vYFP:SE;se-5* embryos were indistinguishable from their wild-type siblings. This observation raises the question of whether the rescued *se-5* embryos can proceed with post-embryonic development. Thus, I analyzed the shoot and root development of T3 individuals from the *PLT2::vYFP:SE;se-5/+* and *SHR::vYFP:SE;se-5/+* T2 lines for any post-embryonic phenotypes that might set apart the rescued *se-5* individuals from their wild-type looking siblings.

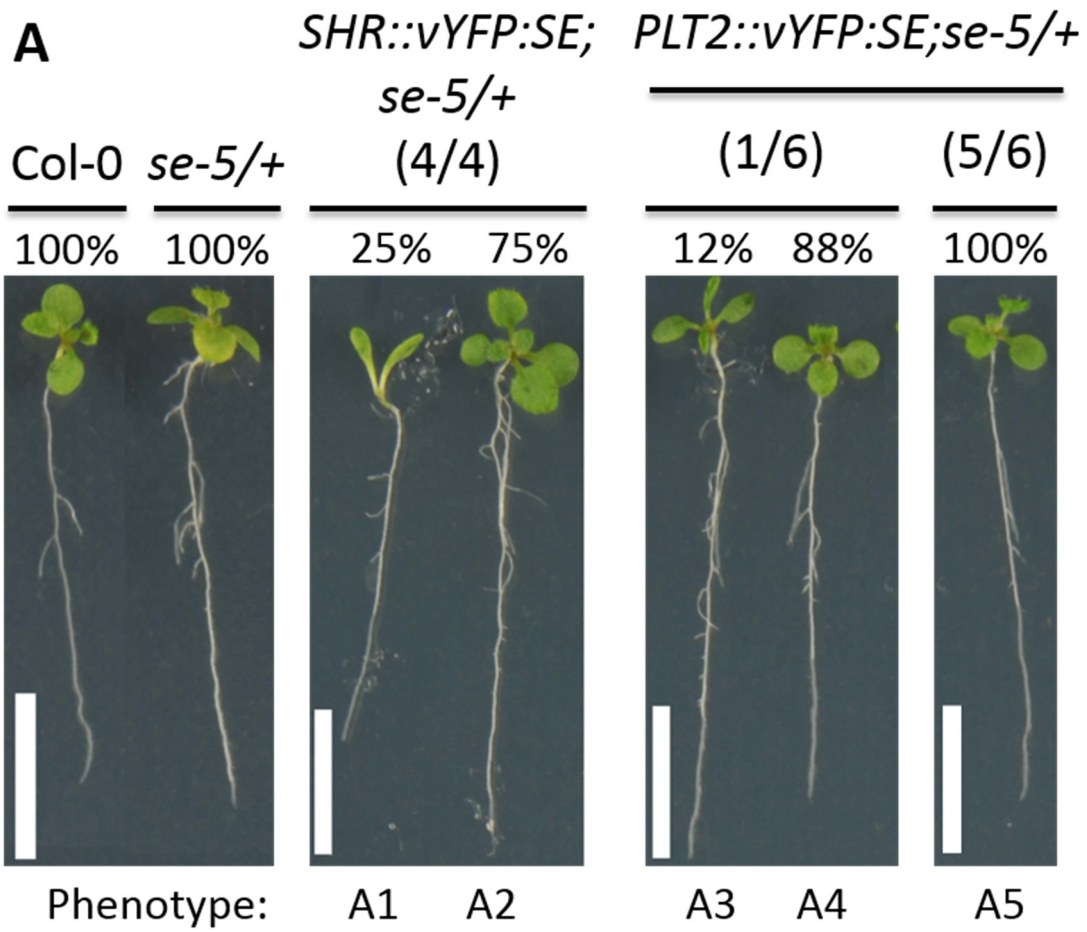
Surprisingly, both *PLT2::vYFP:SE;se-5* and *SHR::vYFP:SE;se-5* individuals proceed to post-embryonic development (Figure 3.3). Although expression of SE in the *SHR* domain is not able to fully rescue *se-5* embryos, it is sufficient to permit post-embryonic development (Figure 3.3). Specifically, 25% of the *SHR::vYFP:SE;se-5/+* T3 individuals show shoot and root phenotypes that are reminiscent of the phenotypes observed in milder loss-of-function alleles of *SE* and *HD-ZIP III* gain-of-function mutants, such as narrow and elongated cotyledons, serrated leaves, and shorter roots (Figure 3.3 A). More importantly, most of the *PLT2::vYFP:SE;se-5/+* T3 lines that have been analyzed (5 out of 6) were indistinguishable in their post-embryonic development from wild-type plants (Figure 3.3). This observation indicates that activity of SE in the *PLT2* domain is sufficient to rescue embryonic patterning of *se-5* mutants and permit post-embryonic development. Nonetheless, it is important to note that in 1 out of the 6 *PLT2::vYFP:SE;se-5/+* T3 lines shoot development was defective in a subset of the 25% rescued *se-5* embryos (Figure 3.3). Although embryogenesis progresses normally in all embryos in this

line, 12% of the individuals showed defective phyllotactic patterns and up-curled leaves that strongly resemble *phb-d/+* gain-of-function mutants (Figure 3.3). The fact that not all rescued *se-5* embryos of this line and most of the *PLT2::vYFP:SE;se-5/+* T3 lines do not show this phenotype, suggests that the observed phenotypes are attributable to line-specific effects.

Analysis of the expression pattern of the fusion constructs during post-embryonic development suggests that a mechanism that acts during embryogenesis, with SE functioning specifically in the root pole and distantly controlling patterning of the apical pole, may also function during post-embryonic development. As expected, *PLT2* promoter is expressed along the root meristem and is excluded from the shoot tip, whereas *SHR* is expressed along the vascular tissue in the root and shoot tips (Figure 3.4). It is noteworthy that the *PLT2* expression pattern was similar in all 6 independent lines that were analyzed. This observation excludes the possibility that the post-embryonic phenotypes observed in one of the *PLT2::vYFP:SE;se-5/+* lines (phenotype A3 Figure 3.3A, and Figure 3.4B-B') are attributive to differential expression patterns amongst the lines. In concordance with the embryonic tissue specific rescue experiments, SE requires the cellular context of the *PLT2* expression domain in order to promote correct patterning. In conclusion, these results suggest that expression of SE solely in the root, within the *PLT2* domain, may affect patterning of the shoot via a long distance mechanism of cell communication.

Figure 3.3: Expression of SE in the root pole permits post-embryonic development of *se-5* embryos

(A) Post-embryonic phenotype of 8 days after germination old seedlings (from left to right) of Col-0, *se-5/+*, *SHR::vYFP:SE;se-5/+*, and *PLT2::vYFP:SE;se-5/+*. The "%" values above the images represent the frequency of each phenotypic class in the population. The ratio in brackets below the labels represents the number of independent lines that show the respective phenotypes to the total number of lines analyzed. The various phenotypic classes are coded below image A (see A1-A5). (B-G) Rosette images of Col-0 (B), A2 (C), A1 (D), A4 (E), A3 (F), and A5 (G) plants. Scale bars: 1 cm.


A
SHR::vYFP:SE; se-5/+
PLT2::vYFP:SE;se-5/+
Col-0
se-5/+
(4/4)
(1/6)
(5/6)
100%
100%
25%
75%
12%
88%
100%
Phenotype:
A1
A2
A3
A4
A5

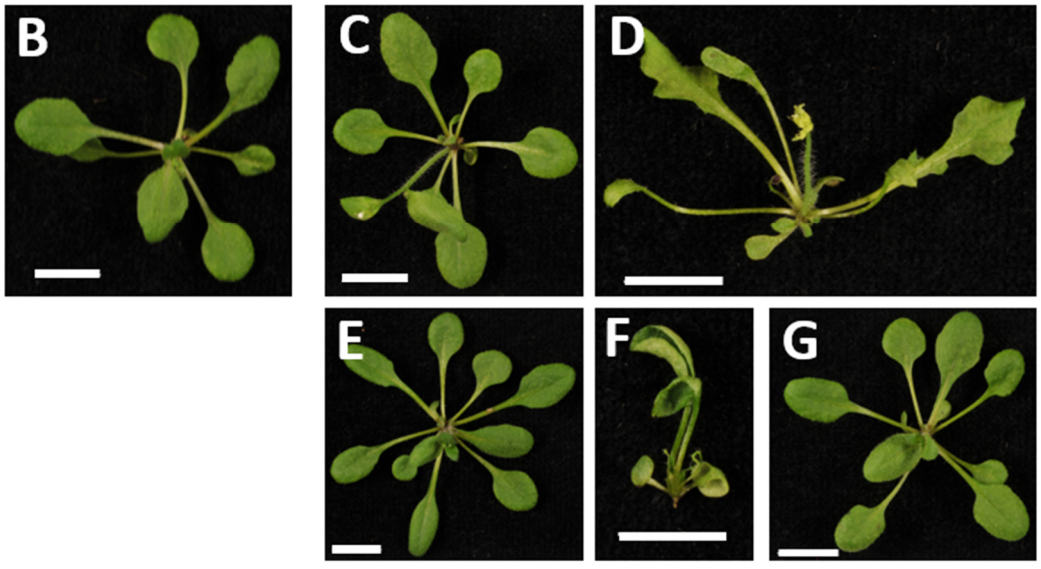
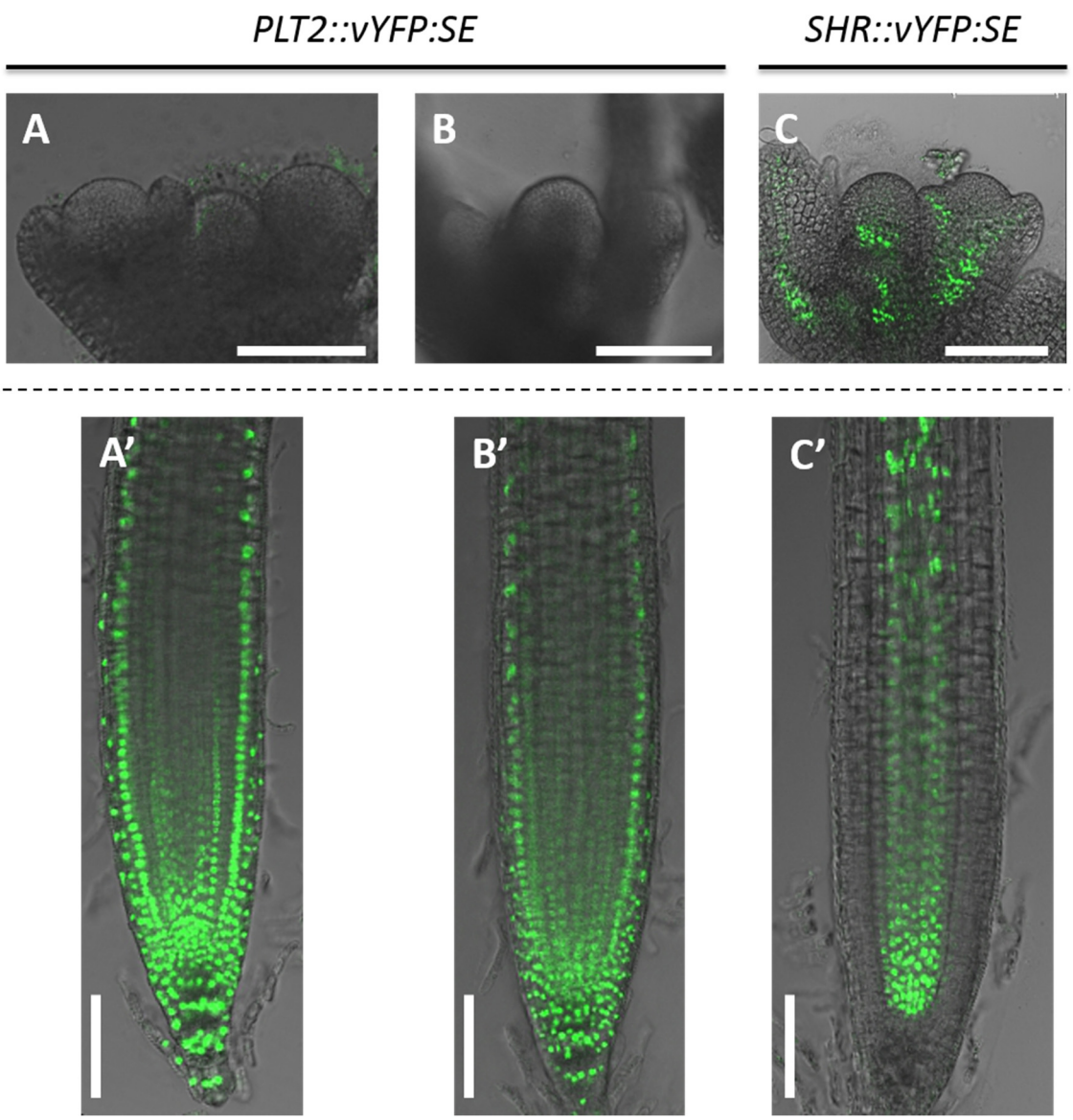

B
C
D
E
F
G

Figure 3.4: Post-embryonic expression of the *PLT2::vYFP:SE* and *SHR::vYFP:SE* transgenes

SAM (A-C) and RM (A'-C') CLSM images of *PLT2::vYFP:SE* (A-B,A'-B'), and *SHR::vYFP:SE* (C,C'). Images A and A' derived from plants of the A4 phenotype (see Figure 3.3), B and B' correspond to plants with the A3 phenotype (see Figure 3.3), and images C and C' derived from plants with the A2 phenotype (see Figure 3.3). Scale bars: 100 μm.


PLT2::vYFP:SE
SHR::vYFP:SE
A
B
C
A'
B'
C'

3.2.3 Expression of SE in subdomains of the *PLT2* expression domain does not fully rescue *se-5* embryos

Detailed comparison of the expression patterns of the *PLT2::vYFP:SE* and *SHR::vYFP:SE* constructs in several embryonic stages showed distinguishable expression patterns from early embryonic stages. Although *PLT2* and *SHR* expression domains overlap at the cells in the central domain of the globular embryo, *SHR* expression at this stage is excluded from cells in the periphery and at the basal pole of the embryo (Figure 3.5). Complementary expression patterns become more pronounced in later embryonic stages (Figure 3.5). These observations strongly suggest that activity of SE is possibly required in the periphery and/ or at the basal pole of the embryo, where *SHR* is not expressed. This hypothesis is also supported by the fact that the miR165/6, which regulate the *HD-ZIP III*, are expressed in these domains of the embryo (Miyashima et al., 2011), assuming that patterning in *se-5* is mainly attributed to misregulation of the *HD-ZIP IIIs*.

To test whether expression of SE in peripheral/basal subdomains of the *PLT2* expression domain is where SE activity is required, I crossed *UAS::SE;se-5/+* lines (homozygous for the *UAS::SE* transgene, but segregating for the *se-5* allele) with the Gal4 promoter-trap strains *p7* and *p19* (transformed in the *se-5/+* strain). Embryos were analyzed in the F1 generation after crossing the two-component strains. The *p7* and *p19* promoter-trap constructs are expressed in peripheral-basal and solely basal cells, respectively (Figure 3.6).

In both cases, tissue-specific expression of SE in *p7* or *p19* was not sufficient to fully rescue embryogenesis of *se-5* mutants (Figure 3.6, Table 3.4). Specifically, expression of SE in the *p7* domain revealed phenotypes of incomplete restoration of embryogenesis

with aberrant patterning along the apical-basal pole and formation of cotyledon-like structures in the periphery of the embryo (Figure 3.6, Table 3.4), similarly to that observed in the *SHR::vYFP:SE;se-5/+* lines (Figure 3.2, Table 3.3). Expression of SE under the basal-specific *p19* promoter had a much stronger effect in suppressing the *se-5* phenotype, with 16% of the embryos showing a *se-5* like phenotype, whereas the rest of the embryos were indistinguishable from wild type (Figure 3.6, Table 3.5). Collectively these data suggest that activity of SE solely at the basal/peripheral pole is not sufficient to completely rescue embryogenesis of *se-5* mutants, and likely requires the full complement of the *PLT2* expression domain.

Table 3.4: Table summarizing the embryonic phenotypes observed in the *p7;se-5/+ x UAS::SE;se-5/+* F1 progeny (see also Figure 3.6)

Line	F1.1	F1.2	F1.3	F1.4
Wt-like embryos	146	149	131	144
Defective embryos	42	46	44	50
Total embryos	188	195	175	194
Defective embryos (%)	22.34	23.58	25.14	25.77

Table 3.5: Table summarizing the embryonic phenotypes observed in the *p19;se-5/+ x UAS::SE;se-5/+* F1 progeny (see also Figure 3.6)

Line	F1.1	F1.2	F1.3	F1.4
Wt-like embryos	167	149	165	165
Defective embryos	33	30	31	32
Total embryos	200	179	196	197
Defective embryos (%)	16.50	16.75	15.81	16.24

Nonetheless, it should be taken into account that the *PLT2* promoter is active from early embryonic stages and *SHR*, *P7*, and *P19* promoters are active in later stages of embryogenesis. Such temporal differences in the expression patterns of these promoters might explain why SE activity in the *PLT2* domain is sufficient to rescue *se-5* embryogenesis, but activity of SE in sub-domains of *PLT2* is not.

Figure 3.5.: *PLT2::vYFP:SE* and *SHR::vYFP:SE* have complementary expression patterns in late embryonic stages

CLSM images of *PLT2::vYFP:SE* (A-C'), and *SHR::vYFP:SE* (D-F') in globular (A,D), heart (B,E), and torpedo (C,F) stage embryos. (C', and F') Magnification of the areas selected in images C and D, respectively. (G-H) CLSM images of *SE::vYFP:SE* in globular (G), and late heart/torpedo (H) stage embryos. Scale bars: 20 µm.

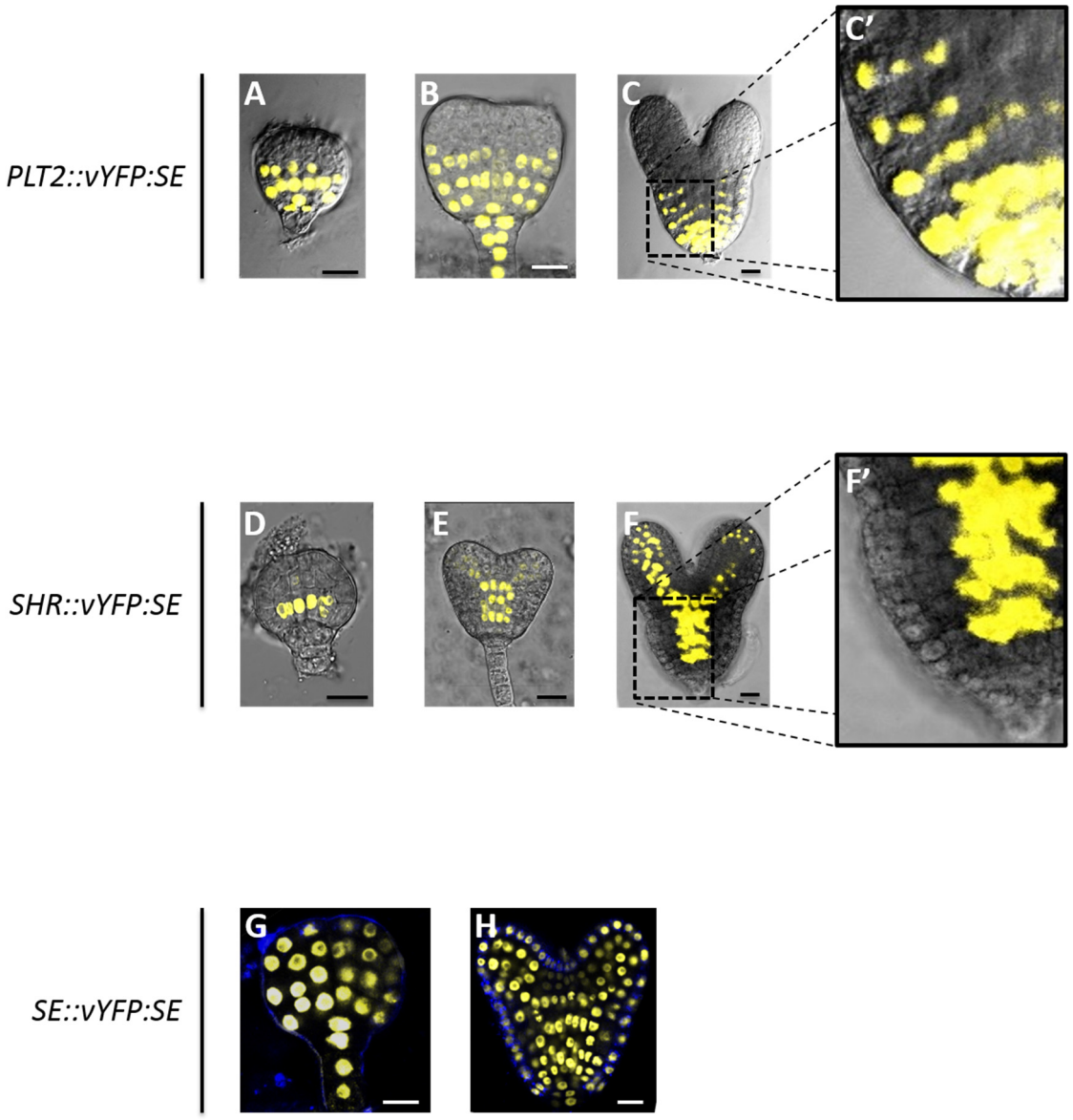
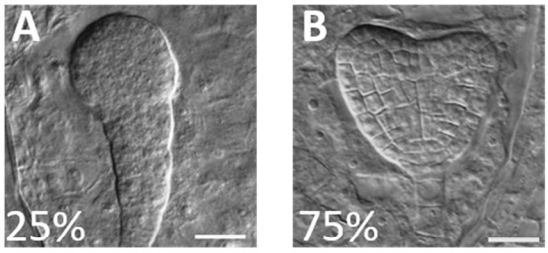

PLT2::vYFP:SE
A
B
C
C'
SHR::vYFP:SE
D
E
F
F'
SE::vYFP:SE
G
H

Figure 3.6: Expression of SE in sub-domains of the *PLT2* expression domain does not fully rescue *se-5* embryos

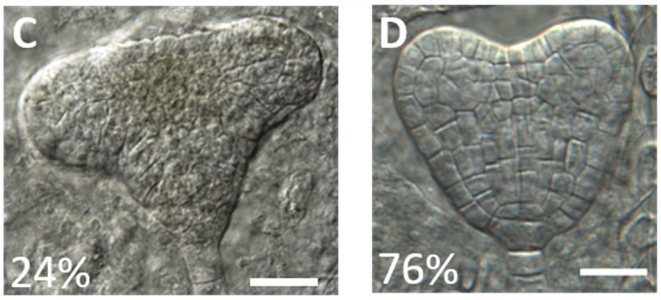
(A-B, C-D, F-G) Nomarski images of heart stage embryos of *se-5/+* (A-B), *P7xUAS::SE;se-5/+* (C-D), and *P19xUAS::SE;se-5/+* plants (F-G). The frequency of each phenotypic class is indicated by a "%" value at the bottom left corner of the respective images. (E, H) CLSM images of transition/heart stage embryos of the *P7* (E) and *P19* (H) *Gal4* reporter lines. 4 independent lines have been analyzed per construct and approximately 200 embryos were phenotyped per line (Tables 3.4-3.5). Scale bars: 20 µm.

se-5/+ progeny



No transgene

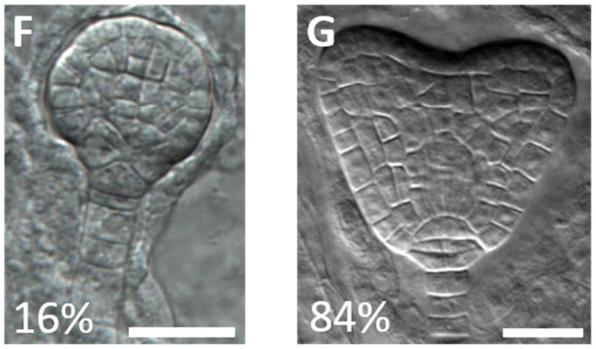
P7 x UAS::SE;se-5/+ progeny



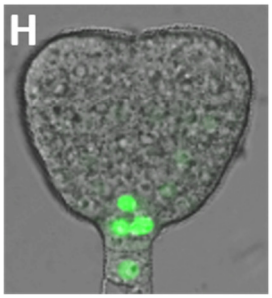
P7 x UAS::SE



P19 x UAS::SE;se-5/+ progeny



P19 x UAS::SE



3.2.4 SE functions in a bi-directional and non-cell autonomous fashion in regulation of axial patterning during embryogenesis

Given that activity of SE in the root pole is sufficient to rescue *se-5* embryogenesis, a question that arises is what will happen if SE is expressed only in the apical pole? To answer this, I generated a direct fusion construct of the *vYFP:SE* with the apically expressed *CUC2* promoter (Table 3.1). This construct was transformed in *se-5/+* plants and four *CUC2::vYFP:SE;se-5/+* independent T2 lines (out of 15 lines, totally) were selected for further analysis. Transgene homozygosity was validated in the T3 generation. Like *PLT2*, *CUC2* promoter is also active during early embryogenesis, though unlike *PLT2*, the *CUC2* promoter is expressed in the upper tier/apical domain of the embryo (Table 3.1).

Surprisingly, expression of SE in the *CUC2* domain was sufficient to completely rescue embryonic patterning of *se-5* mutants (Figure 3.7, Table 3.7). In fact, all globular and heart stage embryos in the *CUC2::vYFP:SE;se-5/+* lines looked like wild-type (Figure 3.7). This result reveals that activity of SE in the apical pole can rescue embryogenesis in *se-5* mutants. Because activity of SE in the root pole is also sufficient to rescue embryogenesis, these data collectively indicate that SE can coordinate axial patterning via a non-cell autonomous and bi-directional mechanism. Although SE is expressed everywhere in the embryo (Figure 3.5 G-H), it seems that restricted activity of SE in broad sub-domains of the embryo, such as that of CUC2 (upper tier) and PLT2 (lower tier), is sufficient to compensate for loss of SE function.

Table 3.6 Table summarizing the embryonic phenotypes observed in the *CUC2::vYFP:SE;se-5/+* T2 lines (see also Figure 3.7)

Line	T2.2	T2.4	T2.6	T2.8
Wt-like embryos	200	199	195	199
Defective embryos	-	2	-	-
Total embryos	200	201	195	199
Defective embryos (%)	**0**	**0.99**	**0**	**0**

However, it should be noted that both *CUC2* and *PLT2* are expressed in cells of the embryonic epidermis, whereas *SHR*, *p7*, and *p19* are not (Figure 3.1 D, 3.2 E, 3.6 E and H, 3.7 G and H). This observation supports a putative role for the embryonic epidermis in SE-dependent patterning processes. Furthermore, both *CUC2* and *PLT2* promoters are active in earlier embryonic stages than the *SHR*, *p7* and *p19* promoters. These collectively suggest that the timing of the SE activity and/ or the tissue-specific expression of SE in the epidermis may contribute to embryonic patterning.

Figure 3.7: Expression of SE in the apical pole fully rescues embryogenesis of *se-5* embryos

(A-F) Nomarski images of globular (A, B, E) and heart stage (C, D, F) embryos of *se-5/+* progeny (A-D), and *CUC2::vYFP:SE;se-5/+* (E-F). The frequency of each phenotypic class is indicated by a "%" value at the bottom left corner of the respective images. (G-H) CLSM images of *CUC2::vYFP:SE* in globular (G) and heart (H) stage embryos. 4 independent lines have been analyzed per construct and approximately 200 embryos were phenotyped per line (Table 3.6). Scale bars: 20 µm.

se-5/+ progeny

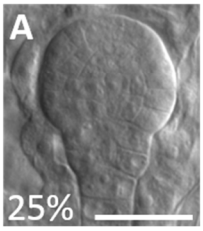
CUC2::YFP:SE;se-5/+ progeny

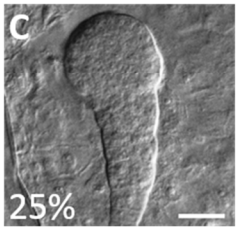
Globular

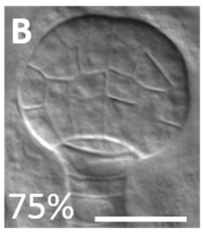
Heart

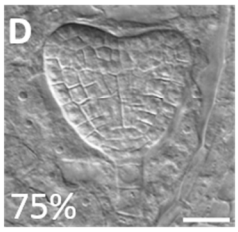
Globular

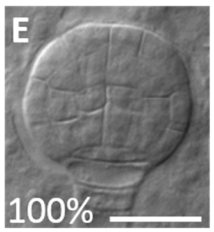
Heart

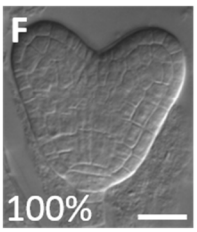




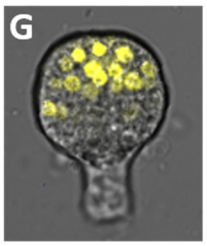


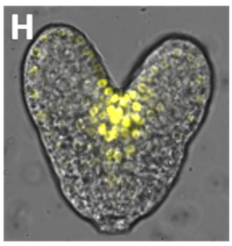






No transgene





3.4 Discussion

Although patterning mechanisms involving miRNAs during post-embryonic development have been extensively studied, little is still known about such mechanisms during embryogenesis. Where does miRNA regulation take place during embryogenesis? How do specific miRNA/mRNA-target modules instruct positional information during embryonic patterning? What is the contribution of miRNA patterning mechanisms in developmental timing during embryogenesis? These are few of the questions that have been poorly investigated. Although our understanding of embryonic miRNA pathways is still limited, it becomes apparent from several observations that they are essential for embryonic patterning and embryo viability. For example, loss-of-function mutations in the miRNA processing proteins SE and DCL1 causes severe patterning defects in early embryonic stages and consequently leads to embryonic arrest (Grigg et al., 2009; Nodine and Bartel, 2010).

The SE/miR165-6/HD-ZIP III regulatory module plays a central role in the establishment of the SAM and polar patterning of lateral organs during post-embryonic development (Grigg et al., 2005). This module is also implicated in embryonic patterning. Misexpression of the apical identity promoting HD-ZIP III transcription factors at the basal pole of the embryo, in the context of *se-5* loss-of-function mutants, leads to patterning defects in this domain, failure to properly establish the RM, and culminates in embryo lethality (Grigg et al., 2009). Although these observations strongly support a SE-specific contribution in axial patterning via regulation of the HD-ZIP III, the tissue specific function of such regulatory modules and more specifically SE and miRNAs still remains a mystery.

Aiming to reveal the tissue-specific requirement of the miRNA biogenesis protein SE, I expressed SE in various embryonic domains either at the root and/or shoot pole in the null *se-5* mutant embryo. My work revealed that expression of SE only at the root pole of *se-5* embryos, within the *PLT2* domain, was sufficient to completely rescue embryonic patterning and lethality in this mutant background (Chapter 3.2.1). This indicates that SE function is required at the root pole of the embryo for correct elaboration of the embryonic patterning. The fact that patterning of the apical pole, which is also defective in *se-5* embryos, is also rescued in these lines, strongly suggests that SE activity in the root pole can non-cell autonomously drive patterning processes in the apical pole of the embryo. Such functions of SE are plausible, given that SE is a central component in the biogenesis of miRNAs, which have been shown to be mobile (Marin-Gonzalez and Suarez-Lopez, 2012). Although SE is also involved in other processes either than miRNA biogenesis (Laubinger et al., 2008), it is conceivable to speculate that the mechanisms that are driven by SE in the *PLT2::vYFP:SE;se-5/+* lines are possibly mediated by mobile miRNA signals.

Although activity of SE in the *PLT2* domain is sufficient to rescue embryogenesis, expression of SE in a different domain of the root pole does not yield the same results. Expression of SE under the *SHR* promoter, which is expressed in the central cells of the root pole along the vasculature (Figure 3.5), results in embryos that are still largely distinguishable from the wild type (Figure 3.2). Collectively these observations indicate that tissue-specific activity of SE in the *PLT2*, but not in the *SHR* domain, is sufficient to rescue overall embryonic patterning. However, because both *PLT2* and *SHR* are expressed in the root pole of the embryo and have overlapping expression patterns in early embryonic stages (Figure 3.5), this further raises the question as to why SE behaves so

differently when it is expressed in either of those domains. There are a couple of plausible hypotheses that could explain this phenomenon. Firstly, although both *PLT2* and *SHR* have overlapping domains, *PLT2* is expressed in cells at the peripheral domain of the root pole, where *SHR* is excluded (Figure 3.5). It is possible that SE activity is required within the peripheral and basal domains of the *PLT2* expression domain and that this is the reason *SHR*-specific expression of SE can not fully rescue embryonic patterning of *se-5* embryos. Secondly, because *PLT2* promoter is active in earlier embryonic stages (1-cell stage) than the *SHR* promoter (early globular stage), strongly suggests a possible temporal role of SE in regulation of embryonic patterning. It can be further extrapolated that SE activity is required in the root pole earlier than the globular stage to drive patterning processes that are important for subsequent patterning events.

Although they are not mutually exclusive, there are several observations that support the latter of the two possibilities. Expression of SE under the peripheral/basal *P7* and the exclusively basal *P19* promoters does not sufficiently rescue *se-5* embryos (Figure 3.6). It should be noted that both of these promoter-trap lines are expressed in cells where *PLT2* is expressed and *SHR* is excluded from (Figure 3.5-3.6). However, in contradiction to the *PLT2* expression, both of those promoters are activated in later embryonic stages, coinciding with the activation of the *SHR* promoter. Strikingly, the *p7>>SE* tissue-specific *se-5* embryos strongly resemble the partially rescued *se-5* embryos from the *SHR::vYFP:SE;se-5/+* lines (Figures 3.2, 3.6). These collectively suggest that SE may have an important role in early patterning events that are required for patterning processes in subsequent stages. This is also supported by the fact that the *HD-ZIP III* mRNAs are polarly expressed in the apical pole of the 8-cell stage embryo, a pattern that is perturbed

in *se-5* embryos, which precedes any phenotypic aberration in this mutant background (Grigg et al., 2009).

Since expression of SE specifically in the root pole can rescue patterning of the shoot pole, I wondered whether expression of SE in the apical pole can also rescue patterning of the root pole. Surprisingly, expression of SE under the apical *CUC2* promoter is sufficient to fully rescue *se-5* embryos, similar to what has been observed in the *PLT2::vYFP:SE;se-5/+* lines (Figure 3.7). All *se-5* embryos were indistinguishable from wild-type and *se-5/+* siblings. This indicates that although SE is expressed everywhere in the embryo, restricted function of SE either from the apical or the basal pole is sufficient to drive correct embryonic patterning in a bi-directional fashion. The fact that both *PLT2* and *CUC2* promoters are expressed in earlier embryonic stages than the *SHR*, *P7*, and *P19* promoters, further supports the hypothesis that the SE-dependent patterning processes may have a strong temporal aspect. In other words, it seems that having SE active in early embryonic stages, independent of the domain, is more critical for embryogenesis than having SE active in specific domains in later embryonic stages.

Nevertheless, we can not disregard a possible role of the embryonic epidermis in these patterning processes, given that both the *PLT2* and CUC2 promoters are also active in epidermal cells, where none of the other promoters are activated (Table 3.1 and Figure 3.5-3.7). This may explain why expression of SE in the *PLT2* and *CUC2* but not in the other domains can rescue *se-5* patterning defects. However, the fact that the expression of the protoderm-specific *AtML1* gene is not perturbed in the *se-5* background (Grigg et al., 2009), suggests that protoderm development is possibly not affected in this mutant and less likely to contribute to the SE-dependent patterning.

Another valid argument in the interpretation of the tissue-specific expression data derives from the fact that the *PLT2* and *CUC2* domains are much larger domains than *SHR*, *p7*, and *P19*, and that the effectiveness in rescuing *se-5* may lie in the capacity to produce more SE. This argument can be supported by the fact that although expression of SE in *SHR*, *p7*, and *p19* does not fully rescue *se-5* embryos, it is still sufficient for partial rescue (Chapter 3.2.1 and 3.2.3).

In summary, the data in this chapter indicate that SE functions in non-cell autonomous and bi-directional patterning mechanism(s) that are possibly required in early embryogenesis to permit embryos to proceed with development in later stages. However, this raises the question as to what extent timing is important in these patterning events. A possible experimental approach to elucidate this, would be to induce expression of SE in the *PLT2* and/or *CUC2* domains in the *se-5* embryos, from the globular stage onwards, and to assess how important the timing of the SE expression is in these domains for correct patterning.

Another open point that requires further investigation is to what extent the SE-dependent non-cell autonomous mechanism(s) are dependent on miRNA regulation, given that SE is primarily a miRNA biogenesis protein, miRNA molecules are mobile, and that miRNA regulation has also been involved in regulation of developmental timing during embryogenesis (Nodine and Bartel; Nodine and Bartel, 2010). Because SE is not solely involved in miRNA processing and because many miRNAs are dependent on SE, the question arises as to what exactly is the mechanism(s) in which SE non-cell autonomously coordinates patterning? Does it involve miR165/6 and HD-ZIP IIIs or is it dependent on a different regulatory module? Such questions can be addressed by expressing miR165/6

GFP sensor constructs (Carlsbecker et al., 2010) in the various *se-5* rescue lines, in order to assess whether the miR165/6 activity is altered amongst those lines. Additionally, tissue-specific expression of constructs that block miR165/6 activity, such as the mimicry construct *MIM165/6 (Todesco et al., 2010)*, in the *PLT2* and *CUC2* domains in wild-type embryos, will decipher whether sequestration of SE activity specifically in these domains is responsible for the defects observed in *se-5* embryos.

Given that the mobile phytohormone CK has been recently linked to the SE/HD-ZIP III pathway (Dello Ioio et al., 2012), it is likely that CK signalling may also play a patterning role during embryogenesis. Analyzing the expression pattern of the *TCS::GFP* reporter, which is responsive to CK activity, in the various lines will clarify whether CK activity is perturbed in these tissue specific expression lines. Additionally, tissue-specific perturbation of the CK balance in the *PLT2* and *CUC2* domains, either by catabolism or biosynthesis, will clarify whether this SE-dependent bi-directional mechanism is mediated by CKs.

Chapter 4

se-3 suppressor screen:

Identification of new genes in the *SE/HD-ZIP III* pathway

4.1 Introduction

Genetic screens have been extensively utilized in developmental genetics, because they can provide valuable insights into the function of genes. Particularly after the introduction of Arabidopsis as a model organism for plant sciences, genetic screens have become the core for most developmental, genetic, and molecular studies. A genetic screen requires the mutagenesis of a genetically amenable organism and screening for individuals with the phenotype of interest. The screen aims at the identification and isolation of the mutated gene that causes the phenotype of interest. This is the case for the most commonly used forward genetic screen. A forward genetic screen in its basic form is a very powerful tool in identifying novel genes associated with a characteristic phenotype. However, they are limited by the fact that a strong and distinguishable plant phenotype is a pre-requisite for the success of the screen. To surpass such obstacles, variations to the original forward genetic screen have been invented. One of those variations includes the second site modifier screen.

A second site modifier screen is a powerful genetic tool that can be used to identify novel genetic interactions with characterized genes and genetic pathways. A modifier screen begins by mutagenizing a characterized mutant, which perturbs the process of interest. The aim of such a screen is to identify mutated genes that modify the initial mutation. There are several types of modifier screens, amongst the most commonly used are the enhancer and suppressor screens. In the first case, one screens for mutants that enhance the phenotype of the initial mutation. In the latter, one screens for mutants that alleviate/suppress the phenotype of the initial mutation. Both screen varieties ultimately

lead to identification of new genes that directly or indirectly interact with the gene of the original mutation in regulation of the process of interest.

Because SE has been implicated in regulation of the *HD-ZIP III* genes, via miR165/6, I decided to perform a second site suppressor screen on the *se-3* loss-of-function mutant, in order to identify new genes in the *SE/HD-ZIP III* regulatory pathway. The *se-3* mutation, which in contrast to *se-5* is not an embryo lethal mutation, has short root phenotype and defective shoot development, reminiscent of *HD-ZIP III* gain-of-function mutations. Because both *se-3* and the embryo lethal *se-5* mutants have defective root and shoot development, and *se-3* embryos also show mild embryonic defects (Grigg et al., 2005; Grigg et al., 2009), I decided to perform the second site suppressor screen on the *se-3* mutant, scoring for extragenic suppressors that alleviate the short root phenotype of the parental *se-3* mutation. Because SE has residual activity in this mutant background (Grigg et al., 2005), this experimental set up facilitates the identification of new genes that may function either upstream of *SE*, regulating *SE* transcription, and downstream or as cofactors of the *HD-ZIP III* (Figure 4.1).

In this chapter I discuss the screening process of the ethyl methanesulfonate (EMS) generated suppressor line collection, which aims to identify lines that suppress the short root phenotype of *se-3*. I also address genetic and hormonal tests that I performed to gain insights into the nature of the gene(s) that underlies the *se-3* suppressors.

4.2 Results

4.2.1 *se-3* suppressor screen: isolation of 51 independent *se-3* suppressor lines

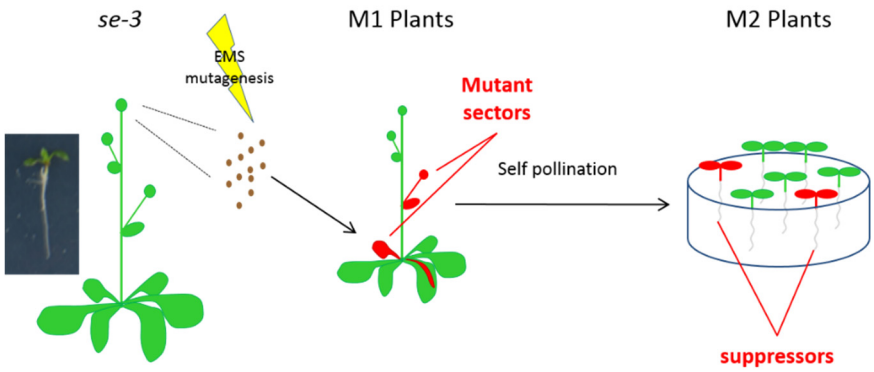
The screen, as depicted in Figure 4.1, involves the mutagenesis of *se-3* seeds (M0 generation) with the alkylating agent EMS. The M1 plants that derive from those seeds are chimeras of mutagenized and non-mutagenized sectors. Seeds collected from pools of the M1 plants generated the M2 seed pools. The M2 pools were subsequently screened for individuals that suppress the short root phenotype of *se-3*. These individuals were selected for further analysis. Although there are several nodes in the *SE/HD-ZIP III* pathway in which the mutated genes in the suppressors may be functioning, I have been interested in identifying genes that may function either upstream of *SE* (like gene X), and/or downstream (gene Y) or as co-factors (gene Z) of the *HD-ZIP IIIs* (see Figure 4.1C). This is further discussed in the following sections.

Figure 4.2 shows the specific number of plants utilized for this EMS screen and the various steps in the screening process. Specifically, 1125 M1 EMS *se-3* plants were pooled in 225 M2 groups. From these 225 M2 pools, 190 M2 pools have been screened and 51 independent lines that suppress the short root phenotype of *se-3* have been identified. These 51 *se-3* suppressor lines derived from 46 M2 pools, which means that 5 out of the 46 M2 pools yielded 2 different lines. 24 out of the 51 *se-3* suppressor lines were selected for further backcrossing to the parental *se-3* background (2-3 times), in order to clean the background of the line from unspecific EMS polymorphisms. The 24 suppressor lines were randomly selected for further analysis, although lines that showed stronger root and shoot suppression were prioritized.

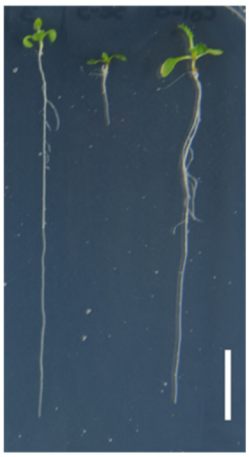
Figure 4.1: Outline of the EMS mutagenesis process to generate the *se-3* suppressor screen

(A) Schematic representation of the mutagenesis procedure for the generation of the *se-3* suppressor lines. *se-3* seeds were mutagenized with EMS. The M1 progeny were grown on soil and left to self-pollinate to generate the M2 seeds. M2 seed stocks were pooled for screening. (B) Image showing post-embryonic root phenotype of Col-0, *se-3*, and a representative *se-3* suppressor plant (from left to right). (C) Schematic representation of the genetic interactions of *SE/HD-ZIP III* with putative *se-3* suppressor genes, such as *Gene X* upstream of *SE*, and/or *Genes Y* and *Z* that function downstream or as a co-factor of *HD-ZIP III*, respectively.

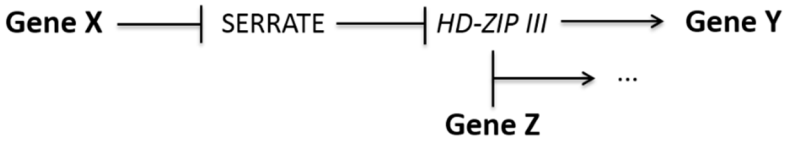
A


se-3
EMS
mutagenesis
M1 Plants
Mutant
sectors
Self pollination
M2 Plants
suppressors

B



C


Gene X
SERRATE
HD-ZIP III
Gene Y
...
Gene Z

Remarkably, shoot suppression has been observed in the majority of the 51 suppressor lines that were isolated from the M2 pools as suppressors of the short root phenotype of *se-3*. Only 2 out of the 51 lines had the *se-3* shoot phenotype and restored root phenotype (data not shown). These 2 lines were excluded from further analysis due to difficulties in subsequent crossing procedures for the generation of the mapping strains. There is a variety of root and shoot phenotypes detected amongst the 24 selected *se-3* suppressors. The mutant lines can be grouped in classes of complete or intermediate root suppression, and in classes of mild, intermediate, to almost complete suppression of the *se-3* shoot phenotype (Figure 4.3). Most of the suppressor lines showed complete suppression of the root phenotype of *se-3* (17 out of the 24 lines), and the rest showed intermediate suppression (Figure 4.3). Suppression of the shoot phenotype of *se-3*, although to variable extents, has been detected in all of those lines (Figure 4.3).

As depicted on graph G in Figure 4.3, the most common combinations of shoot/root suppression detected amongst the 24 suppressor lines are the ones with complete root suppression/intermediate shoot suppression, and complete root/shoot suppression (Figure 4.3). In other words, it seems that most of the mutations that alleviate the *se-3* root phenotype suppress also the shoot phenotype of *se-3*. There are two possible hypotheses for this observation. One possibility could be that the genes that are mutated in these suppressors are implicated in *SE*-dependent pathways that directly regulate both root and shoot patterning. Alternatively, these genes may function in patterning events that take place in either the root or the shoot, ultimately affecting development of both organs via possible cross-communication mechanism(s). These hypotheses require further testing and possible elaboration of grafting experiments, which is not part of this thesis.

After backcrossing to *se-3* (2-3 times), the selected lines were crossed with various strains, such as *SE::GUS* and *phb-1d/+*, to gain insights into the function of the genes that underlie the suppressors, and also with a *se-3* (L*er)* strain for mapping (Figure 4.2). Details about these experiments are described in the following chapters.

Figure 4.2: Outline of the *se-3* suppressor screening process

1125 mutagenized M1 *se-3* plants were grouped in 225 M2 pools. Of these, 190 pools were screened for plants that have longer roots than *se-3*. 51 lines have been isolated and 24 of those lines have been backcrossed to the *se-3* parental genotype (2 or 3 times). To identify suppressors that are upstream or downstream of the *SE/HD-ZIP III* pathway, individual lines were crossed to *SE::GUS* and *phb-1d/+* strains, respectively. These lines were also crossed with *se-3 (*L*er)* strains and the F2 progeny of those crosses were used for mapping. Selected backcrossed lines were used for whole genome sequencing (WGS) for identification of SNPs.

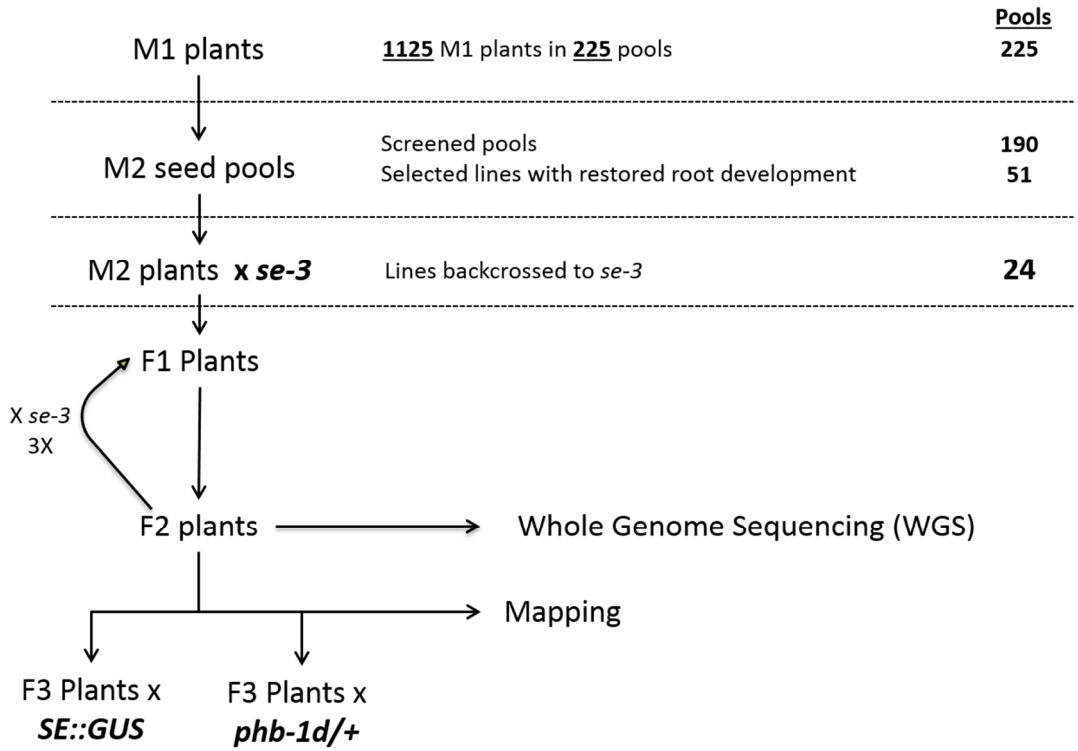
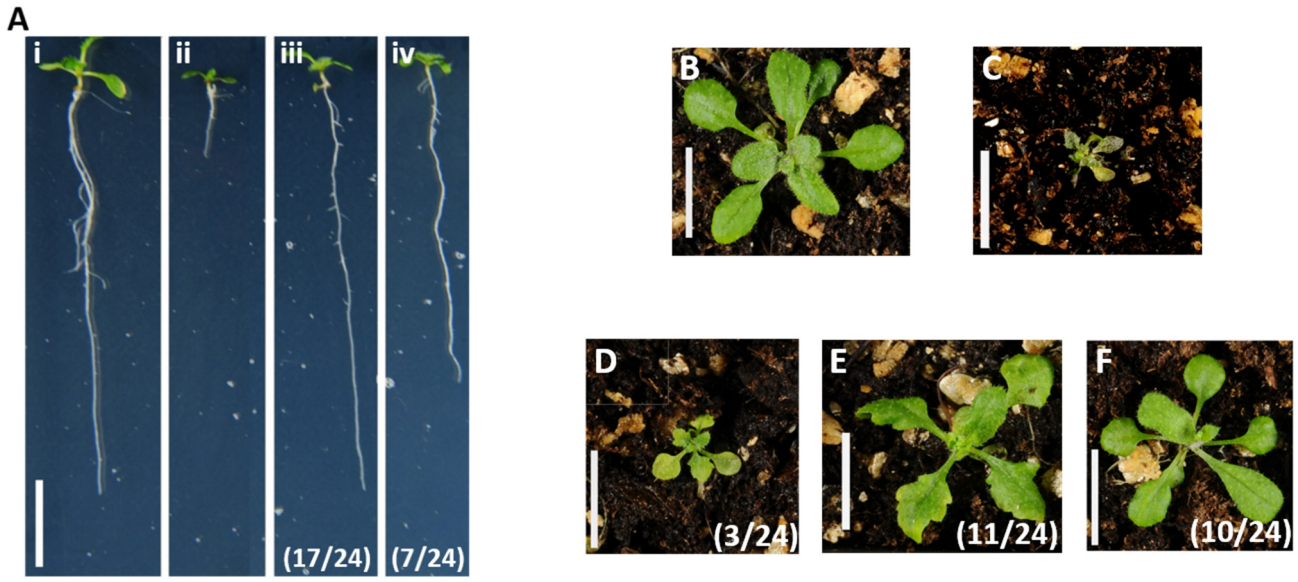
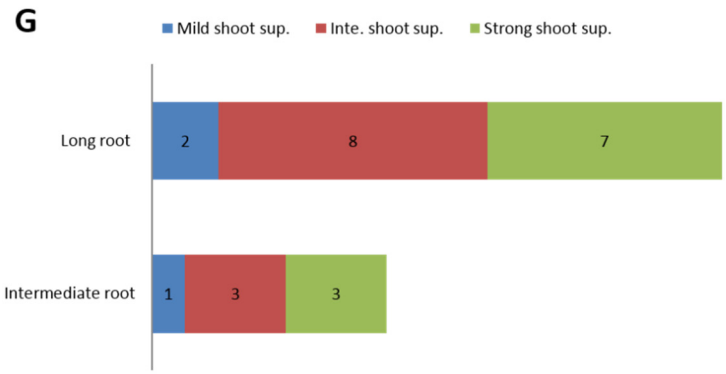

Pools
M1 plants
1125 M1 plants in 225 pools
225
M2 seed pools
Screened pools
190
Selected lines with restored root development
51
M2 plants x se-3
Lines backcrossed to se-3
24
F1 Plants
X se-3
3X
F2 plants
Whole Genome Sequencing (WGS)
Mapping
F3 Plants x
SE::GUS
F3 Plants x
phb-1d/+

Figure 4.3: Shoot and root phenotypic classes observed amongst the selected *se-3* suppressor lines

Image showing classes of root phenotype (Aiii-Aiv) and shoot phenotype (D-F) that were observed amongst the selected *se-3* suppressor lines. From left to right, Col-0 (Ai), *se-3* (Aii), representative suppressor with complete suppression (Aiii), and representative suppressor with intermediate suppression (Aiv) of the *se-3* short root phenotype. Col-0 (B), *se-3* (C), representative suppressor with mild suppression (D), intermediate suppression (E), and almost complete suppression (F) of the *se-3* shoot defects. In both cases, the ratios in brackets indicate the number of individual lines that have the respective phenotype to the total number of lines. (G) Bar graph showing the distribution of the 24 *se-3* suppressor lines along the various combinations of shoot and root phenotypes detected amongst the suppressors. On the x axis, "Long root" and "intermediate root" correspond to the root phenotypes in images Aiii and Aiv, respectively. On the y axis, "Mild shoot suppression" (blue) corresponds to the shoot phenotype in image D, "Intermediate shoot suppression" corresponds to the phenotype in image E, and "Strong shoot suppression" corresponds to the phenotype in image F. The numbers in the bars indicate the number of lines that share the respective combination of shoot and root phenotypes. The most common combinations of shoot/ root phenotypes that are detected in the 24 suppressor lines are the ones with complete root suppression/ intermediate or complete shoot suppression. The table below the bar graph shows the root and shoot phenotypes for each of the 24 *se-3* suppressor lines (shaded in grey) and the inheritance of the suppressor mutation. The column titles of the table correspond to the labels of the bar graph that is described above. Scale bars: 1 cm.





Inheritance	*se-3* sup. #	Inte. root	Long root	Mild shoot sup.	Inte. shoot sup.	Strong shoot sup.
Recessive	1		■		■	
Recessive	3		■		■	
Recessive	8	■			■	
Dominant	19		■		■	
Dominant	23		■		■	
Recessive	50		■		■	
Dominant	76		■			■
Recessive	77		■			■
Recessive	89	■				■
Recessive	99	■		■		
Dominant	117	■		■		
Recessive	120	■		■		
Recessive	125	■				■
Dominant	126	■			■	
Dominant	139		■		■	
Dominant	140		■		■	
Recessive	144	■				■
Recessive	145		■			■
Recessive	146	■			■	
Dominant	148		■			■
Dominant	196		■			■
Dominant	197	■				■
Dominant	198		■			■
Recessive	204		■		■	

■ Dominant

■ Recessive

4.2.2 Analysis of *se-3* suppressors crossed with *SE::GUS* reveals genes upstream of *SE*

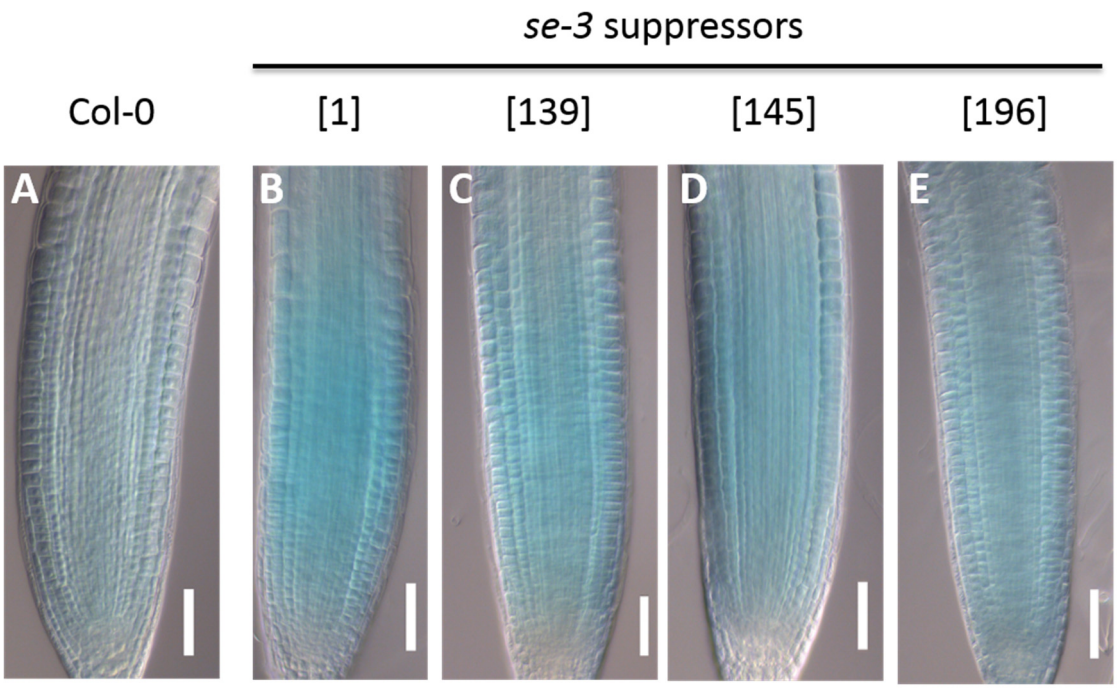
To identify suppressors that function upstream of *SE*, I assayed for *SE::GUS* expression in the 24 suppressor lines (Figures 4.1C and 4.2). I crossed all 24 suppressor lines (having the *se-3* mutation in the background) with the *SE::GUS* transgenic strain generating the *se-3/+;sup/+;SE::GUS/+* F1 plants. From a large number of segregating populations, I isolated heterozygous *se-3/+* individuals for each line and genetically analyzed the F3 generation of those lines to validate that the parental line was homozygous for both the suppressor mutation and the *SE::GUS* transgene. From these F3 populations, I selected homozygous individuals for the suppressor mutation and the *SE::GUS* transgene, but negative for the *se-3* allele. I followed this approach to separate the *se-3* parental mutation from the background of the 24 suppressor lines, given that the majority of the suppressors do not have any obvious phenotype without *se-3* in the background. These lines were used for further analysis.

The *SE::GUS* reporter is expressed everywhere in the seedling, but its expression is much stronger in highly proliferating tissues, such as young leaves and root and shoot meristems (data not shown). Due to the amenability of roots to GUS staining, I chose staining of root tips as the system to screen for suppressors that regulate SE transcription. The 24 suppressor lines (with the *SE::GUS* reporter) were assayed for 30 min at 37^{o}C using the SE::GUS strain as control. Analysis of these revealed that only *se-3* suppressor lines [1], [139], [145], and [196] have increased GUS activity at the root tip in comparison to the *SE::GUS* control (Figure 4.4). The rest of the 24 lines had comparable expression to that of the control (data not shown). This observation indicates that the genes that are mutated in the four suppressors are upstream of *SE*. A possible explanation of how these genes may function in the pathway may be by negatively

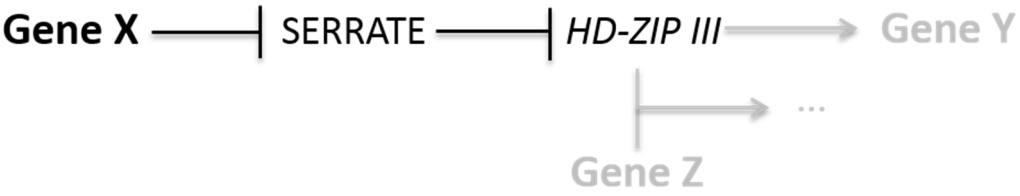
regulating *SE* transcription (Figure 4.4). So, knocking down those genes in the *se-3* allows for increased *SE* transcription which compensates for the reduced SE activity in this background.

Figure 4.4: *se-3* suppressors upstream of SE revealed by *SE::GUS* staining assays

(A-E) Root meristem images of Col-0 (A), se-3 suppressor line [1] (B), [139] (C), [145] (D), and [196] (E) stained for *SE::GUS*. (F) Schematic representation of the *SE/HD-ZIP III* genetic pathway highlighting upstream interactions with genes that negatively regulate *SE* expression, like "*Gene X*". Scale bars: 1 cm.


se-3 suppressors
Col-0
[1]
[139]
[145]
[196]
A
B
C
D
E

F


Gene X
SERRATE
HD-ZIP III
Gene Y
...
Gene Z

4.2.3 A *se-3* suppressor functioning downstream or as a cofactor of the *HD-ZIP III*

Although SE is a miRNA biogenesis component regulating correct processing of a variety of miRNAs that subsequently regulate many developmentally important transcription factors, it is remarkable that a great deal of the *se-3* root and shoot phenotypes are suppressed by knocking down two *HD-ZIP III* members, *PHB* and *PHV* (Grigg *et al.*, 2005). As such, we would expect genes that function downstream or as cofactors of *HD-ZIP III* to be present amongst the suppressors of the screen.

A straightforward genetic assay that can be used to identify such suppressors is crossing the *se-3* suppressor strains with gain-of-function *HD-ZIP III* mutants and assess to what extent the suppressor mutations can also suppress the phenotype of these alleles. Thus, I have crossed the 24 *se-3* suppressor lines with the *phb-d/+* strain (introgressed into Col-0 from the original L*er* strain of (McConnell et al., 2001)), which is a gain-of-function allele of the *HD-ZIP III* gene *PHB*. The *phb-d/+* segregating plants show a variety of phenotypes that are dependent on the gene dosage of the *phb-d* allele. In homozygous condition the *phb-d* seedlings form fully radialized cotyledons and leaves, and are infertile (data not shown). Development of the *phb-d/+* heterozygotes, however, show less severe phenotypes with plants that form trumpet or up-curled leaves, and manage to produce some inflorescences (Figure 4.5 B, B'). By crossing the 24 *se-3* suppressor lines with *phb-d/+* I wanted to assess whether and to what extend *se-3* suppressors can repress the *phb-d* phenotype, which would indicate that the gene behind the suppressor is putatively implicated in patterning processes that involve the HD-ZIP III PHB.

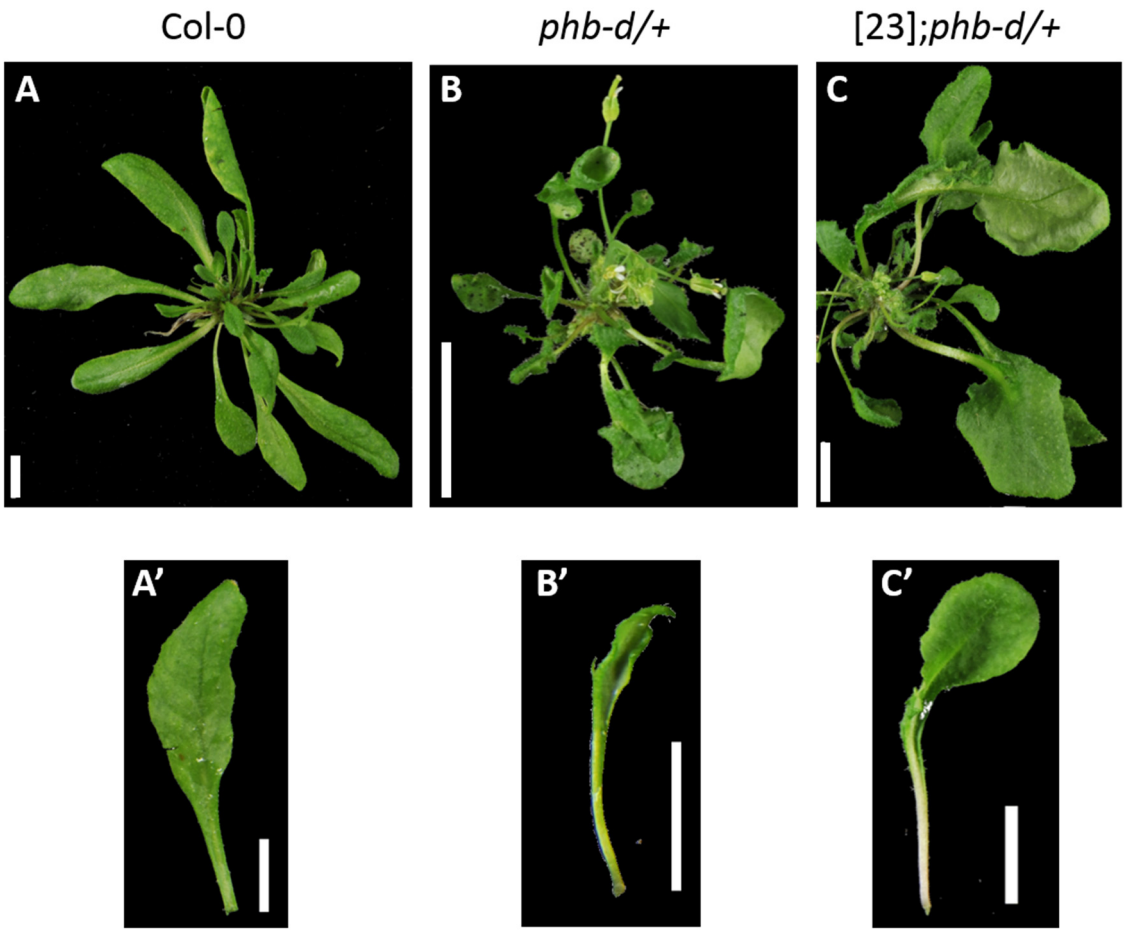
Analysis of the segregating F2 generation of those strains revealed that only suppressor line [23] can at least partially rescue the *phb-d/+* phenotype (Figure 4.5), whilst all other

lines are indistinguishable from *phb-d/+*. Although shoot development of the *se-3* suppressor[23];phb-d/+ plants was still defective with non-canonical phyllotactic patterns, trumpet-shaped leaves were rarely observed and many leaves developed larger and less up-curled blades (Figure 4.5). These results indicate that the mutated gene in suppressor [23] is a possible candidate acting either downstream or as a co-factor of PHB. Nonetheless, it has to be noted that the suppressor [23] mutation did not rescue any of the *phb-d* homozygote phenotypes, which were observed in 25% of the plants of *se-3* suppressor [23];*phb-d/+* segregating populations. This suggests a possible PHB dosage dependent mechanism also affecting the gene in suppressor [23]. Mutation in this gene can partially suppress the *phb-d/+* leaf phenotype, but with further increase in PHB levels this effect disappears. This may further hint towards a putative role of the suppressor gene as a co-factor of PHB. Alternatively, the gene in suppressor [23] may be only one of the downstream components of the genetic network that is regulated by HD-ZIP IIIs, with other components in the network compensating for the loss of gene [23] in high levels of PHB protein.

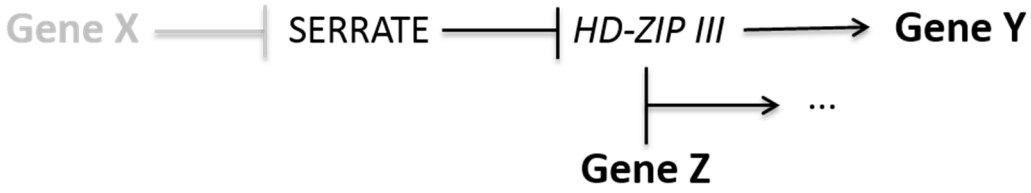
The fact that only *se-3* suppressor [23] mutation can partially suppress the phb-d/+ mutant phenotype does not necessarily mean that it is unlikely for any of the other 23 suppressor genes to function upstream of *PHB* or as a cofactor. The *phb-d* is a strong mutation that is suppressed only by a few other mutations. This agrees also with the observation that even *se-3* suppressor [23] can not suppress the phenotype of the *phb-d* homozygous plants.

Figure 4.5: *se-3* suppressor [23] suppresses the *phb-d/+* phenotype

(A-C) Rosette images of Col-0 (A), *phb-d/+* (B), and *se-3 suppressor [23];phb-d/+* (C) plants. (A'-C') Representative leaf images of A-C, respectively. (D) Schematic representation of the *SE/HD-ZIP III* genetic pathway highlighting genetic interactions with downstream genes, like "*Gene Y*", and *HD-ZIP III* co-factors like "*Gene Z*". Scale Bars: 1 cm.


Col-0
phb-d/+
[23];phb-d/+
A
B
C
A'
B'
C'

F


Gene X
SERRATE
HD-ZIP III
Gene Y
...
Gene Z

4.2.4 *se-3* suppressors resistant to hormonal treatments reveal a possible role in CK pathways

Plant development involves integration of external as well as endogenous signals that in coordination with the genetic network regulate plant form. Phytohormones play important roles in regulating these morphogenetic processes. Recent work links CK-dependent patterning processes in the root with the HD-ZIP III transcription factors and miR165 (Dello Ioio et al., 2012). More specifically, the HD-ZIP III transcription factor PHB promotes biogenesis of CK, which in turn negatively regulates both PHB and its regulator, miR165 (Dello Ioio et al., 2012). It has been suggested that this incoherent feedback loop mechanism confers robustness on the establishment of the transition zone of the root (Dello Ioio et al., 2012), which determines root meristem size and consequently root length. Given that the *se-3* mutant has a short root phenotype and that the *se-3* suppressors rescue this phenotype, it is conceivable that amongst the suppressors there are candidates mutated in genes involved in CK-related pathways.

In order to reveal the identity of CK-related *se-3* suppressors, I have performed CK-treatment assays on the 24 selected suppressors. Resistance to external application of CK will reveal whether any of the lines is mutated in a gene that is involved in CK-dependent pathways. Thus, I treated all 24 suppressor lines, which were homozygosed for the suppressor mutation without the *se-3* T-DNA insertion, with dihydrozeatin (DHz) and counted the root meristem cell number (root meristem size) to assess for resistance in external CK application. DHz is one of the CKs that is preferably recognized by the membrane receptor HISTIDINE KINASE3 (AHK3), which has been shown to trigger downstream signal transduction pathways that regulate root growth and meristem size

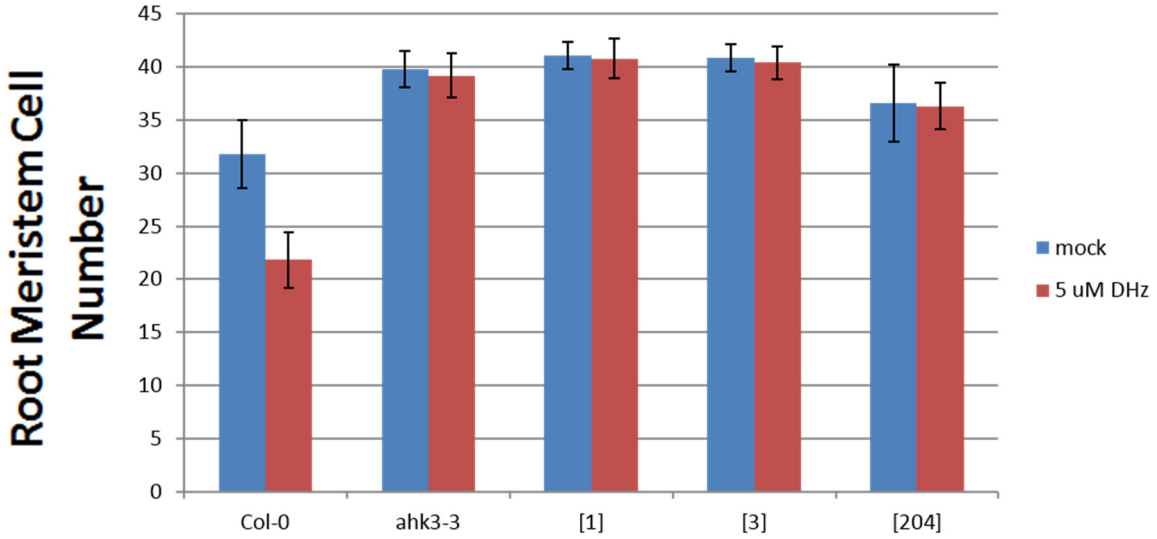
(Spichal et al., 2004; Romanov et al., 2006; Dello Ioio et al., 2007). Root meristem cell number is defined as the number of cortex cells from the stem cell niche until the first elongated cell of the transition zone (Dello Ioio et al., 2007), (Figure 4.6). Col-0 plants were used as negative control and *ahk3-3*, which is a loss-of-function mutant of the AHK3 receptor of DHz, as a positive control. Col-0 and *se-3* suppressors that are not resistant to DHz application are expected to have smaller root meristems with fewer cortex cells. On the contrary, the *ahk3-3* positive control and resistant suppressors are expected to have a constant number of meristematic cortex cells before and after treatment.

From the 24 suppressor lines that were subjected to external application of DHz, only lines [1], [3], and [204] showed insensitivity to CK application (Figure 4.6) as the meristem cell number did not change after CK treatment, similarly to the *ahk3-3* positive control. As expected, in the Col-0 plants the root meristem cell number decreased significantly after DHz application (Figure 4.6). These results indicate that the genes that underlie those three suppressors may have a role in CK-dependent pathways, involving SE and HD-ZIP IIIs.

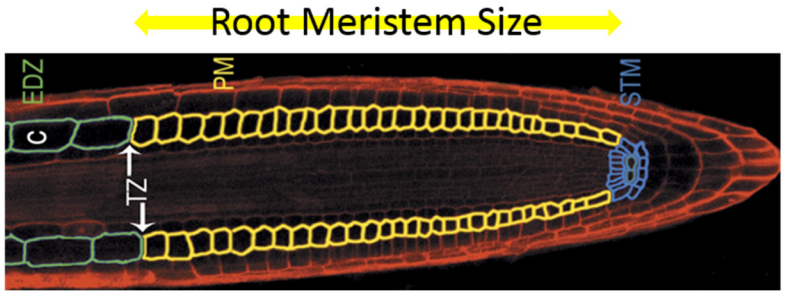
Figure 4.6: *se-3* suppressors resistant to CK application

(A) Root meristem size of Col-0, ahk3-3, and se-3 suppressor lines [1], [3], and [204] before (blue bars) and after treatment with 5uM Dihydrozeatin (DHz) (red bars). (B) Root meristem size is defined as the number of cortex cells between the cortex stem cell and the first elongated cortex cell (image modified from (Dello Ioio et al., 2007)). Error bars represent SD.

A


Root Meristem Cell Number
45
40
35
30
25
20
15
10
5
0
Col-0
ahk3-3
[1]
[3]
[204]
mock
5 uM DHz

B


Root Meristem Size
EDZ
C
TZ
PM
STM

4.3 Discussion

Since the miRNA mediated regulation of the HD-ZIP III by SE has been involved in a variety of developmental processes in Arabidopsis, I was interested in unveiling novel genetic interactions in the SE/ HD-ZIP III regulatory pathway. Novel genetic interactions of complex developmental processes can be revealed by second-site modifier screens. Thus, I conducted a second-site suppressor screen, screening for mutants that suppress the short root phenotype of the non-embryo lethal *se-3* mutation. The fact that shoot and root patterning is defective in both the *se-3* and the null *se-5* alleles (Grigg et al., 2009) and that *se-3* shows some mild embryonic defects (Grigg et al., 2005), suggest that genetic pathways involving SE may underlie both embryonic and post-embryonic patterning processes.

Although the screen was not saturated, it yielded a large number of candidate suppressor lines. 51 independent suppressor lines were isolated out of 190 M2 pools (Figure 4.2). This is possibly attributable to the fact that the *se-3* T-DNA insertion does not completely nullify the activity of SE (Grigg et al., 2005). As such, even the smallest of changes in interacting genes might be enough to permit some residual activity of SE, an effect that might have not been revealed if a stronger allele of SE was used for the screen. For practical reasons, I focused on 24 out of the 51 of the isolated se-3 suppressors for further analysis.

Phenotypic analysis of the 24 suppressor lines revealed a wide spectrum of shoot and root suppression phenotypes. However, several phenotypic classes were more common amongst the 24 suppressors. These include suppressors with complete root and shoot suppression, and suppressors with complete root and intermediate shoot suppression

(Figure 4.3). In both cases, although to variable extents, both shoot and root defects are strongly suppressed. This suggests that the genes that are mutated in these lines are involved in SE-dependent patterning mechanisms that coordinate both root and shoot development, either directly or via a possible genetic cross-communication between these organs.

To get insights in how the "suppressor genes" interact with the SE/HD-ZIP III pathway, I crossed the 24 *se-3* suppressors with the *SE::GUS* reporter and the *phb-d* allele. Analysis of those strains revealed four suppressors upstream of *SE* and one suppressor downstream or as a co-factor of the *HD-ZIP III PHB*. Concerning the upstream suppressors, the GUS assays revealed "suppressor genes" that negatively regulate transcription of *SE* (Figure 4.4). Thus, knocking down the function of those genes, in the context of the *se-3* suppressor lines, permits increased SE transcription and consequently increased SE activity. Analysis of the *phb-d/+;suppressor* strains revealed only *se-3* suppressor [23] as suppressor of the *phb-d/+* phenotype (Figure 4.5), which strongly suggests that the underlying gene is interacting with the *HD-ZIP III*. Given that most of the *se-3* phenotypes are largely attributed to HD-ZIP III misregulation, it is conceivable that this suppressor may affect expression of the *phb-d* phenotype by functioning upstream of the SE/HD-ZIP III pathway regulating SE. However, since the mutation in this suppressor does not increase *SE::GUS* activity, this excludes such a possibility, at least at the transcriptional level. This positions the suppressor gene [23] downstream of SE, likely to function as a co-factor or downstream of the HD-ZIP IIIs.

Although the identity of those suppressor genes is currently unknown, recent work in the field has shed some light on possible candidate genes. Dello Ioio *et al*., 2012, revealed a

novel role for the HD-ZIP III PHB upstream of the CK biosynthesis pathway, promoting CK production (Dello Ioio et al., 2012). Furthermore, they show that ARR transcription factors directly regulate expression of *PHB* and *MIR165* (Dello Ioio et al., 2012). Remarkably, plants with increased CK levels have a short root phenotype, reminiscent of *phb-d* and *se-3* plants. Thus, it is conceivable that genes in the CK signalling pathway are possible candidates as "*se-3* suppressor genes". To identify such suppressors, I treated the 24 suppressor lines with CK to assay for lines that are resistant to the treatment, similar to loss-of-function mutants in the CK signal transduction pathway. These experiments revealed three suppressor lines as putative mutants in the CK signalling pathway (Figure 4.6). It is noteworthy that one of those suppressors, *se-3* suppressor [1], was also identified as an upstream regulator of *SE*. This observation hints that the suppressor gene [1] may have an *ARR*-like function regulating *SE* in a feedback mechanism similar to the one that has been proposed by Dello Ioio *et al,.* 2012 (Dello Ioio et al., 2012).

Chapter 5

Whole genome sequencing (WGS) and mapping

of selected *se-3* suppressors

5.1 Introduction

After isolating and analyzing the 24 *se-3* suppressor lines, as described in chapter 4, I set out to identify which genes are mutated in a subset of lines. There are several methods by which mutations linked to a phenotype can be identified, from the more conventional method of mapping of the causal mutation to more recent methodologies utilizing next generation sequencing technologies. Although conventional mapping techniques utilizing linkage maps generated by analysis of polymorphic DNA markers have proven to be an invaluable tool in identifying mutations, it is usually a time consuming and laborious process. In the model organism Arabidopsis, complete sequencing of the genome paved the way for the development of powerful next generation sequencing technologies that can facilitate rapid identification of mutations. Such technologies can be used on unidentified mutants and strain-specific polymorphisms can be detected by comparison with the reference genome.

To rapidly delimit the genomic region of the mutation in selected *se-3* suppressors, I used next generation sequencing to identify the SNPs in three *se-3* suppressors. In parallel, I performed conventional linkage mapping for two lines in order to delimit the interval of where the suppressor mutations reside in the genome. In this chapter, I discuss the results of the WGS analysis of three *se-3* suppressor lines that have been selected from the assays described in the previous chapter, and also show the progress in the mapping of two of those lines.

5.2 Results

5.2.1 Whole genome sequencing (WGS): a rapid method for identifying putative mutations

To speed up the identification of the causal mutation in the *se-3* suppressors, I decided to use next generation sequencing technologies. Sequencing the genome of selected suppressor lines and then comparing that to the reference genome, I aim to identify line-specific SNPs. Further analysis of those SNPs will reveal whether any of those polymorphisms is the mutation that suppresses *se-3* phenotype.

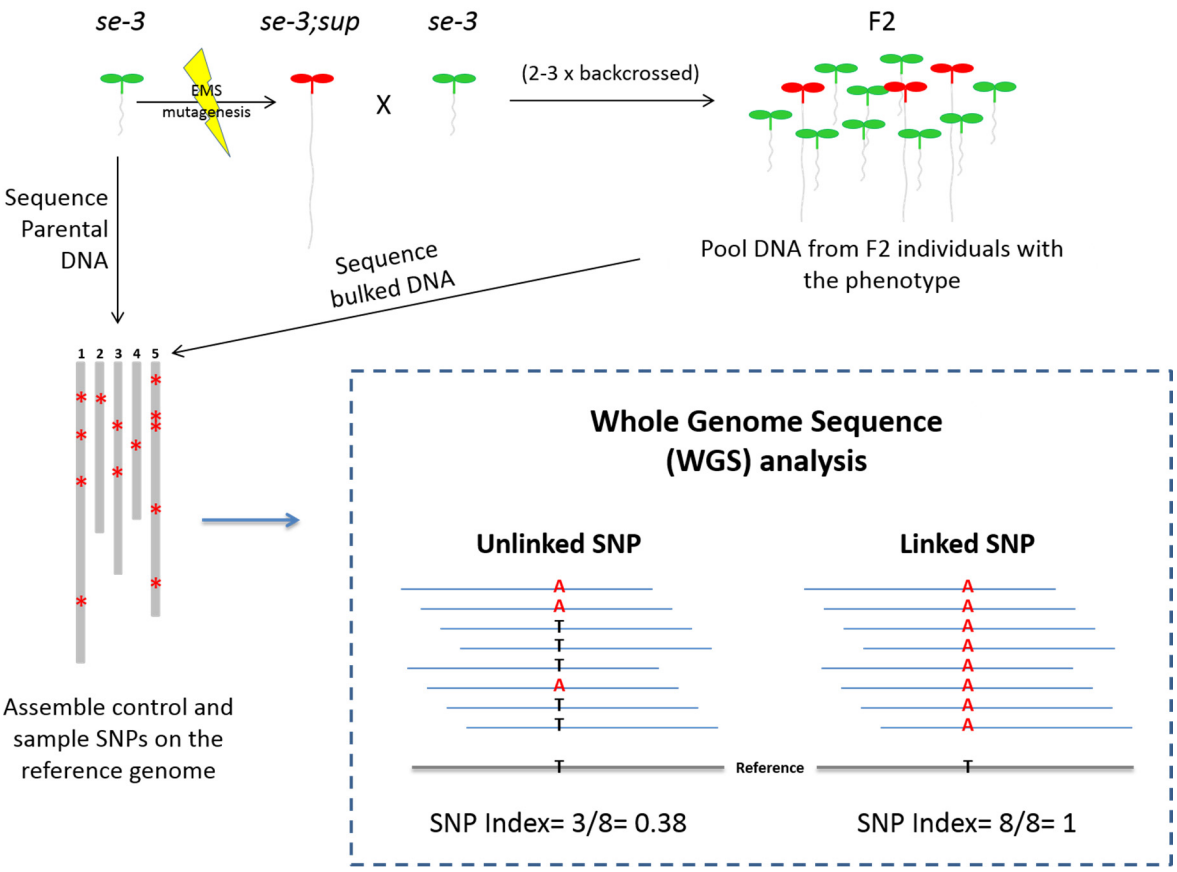
Because it is impractical and expensive to apply this method in all 24 suppressor lines, I selected three independent *se-3* suppressor lines. These are the recessive suppressors [1] and [3], and the dominant suppressor [23]. Line [1] derived as a candidate from the *SE::GUS* (Chapter 4.2.2) and CK treatment assays (Chapter 4.2.4), line [3] from the CK treatment assay (Chapter 4.2.4), and line [23] from the *phb-d/+* genetic assay (Chapter 4.2.3).

As depicted in figure 5.1, after mutagenization with EMS and selection, the *se-3* suppressor lines have been backcrossed 2-3 times to the parental *se-3* background. After backcrossing, the F2 segregating populations were analyzed and approximately 50 individuals with a long root were pooled for each line. DNA was extracted from each pool and also from the reference *se-3* pool. These DNA samples were sent to and BGI TECH SOLUTIONS (HONGKONG) CO., LIMITED for generation of libraries and illumina sequencing, using 30X sequencing depth. The short reads generated by the sequencing of those DNAs were aligned and assembled by BGI TECH SOLUTIONS (HONGKONG) CO., LIMITED along the Col-0 sequenced genome, which was used as a scaffold. Comparison of

the assembled genomes of the samples with the reference genome generated the lists of SNPs that are detected in each sample but excluded from the reference. In other words, SNPs that are present in all lists have been excluded from the analysis. This part of the analysis has been performed by and BGI TECH SOLUTIONS (HONGKONG) CO., LIMITED.

Figure 5.1: Whole genome sequencing (WGS) analysis of se-3 suppressors for rapid identification of the causal mutation

Schematic representation of the outline of the WGS analysis of *se-3* suppressor lines for identification of the causal mutation. *se-3* plants were mutagenized with EMS and *se-3* suppressor lines have been identified. Selected suppressor lines were backcrossed to the parental *se-3* strain and after 2-3 backcrosses ~50 F2 individuals that share the suppression phenotype (long root) were pooled together. Short sequence reads were generated from the parental *se-3* DNA and the *se-3* suppressor bulked DNA. The reads were assembled along the sequenced Col-0 genome and a list of SNPs was generated by comparison of the *se-3* suppressor and control genomes. The dashed box shows examples of unlinked and linked SNPs. Red letters represent point mutations detected in the *se-3* suppressor genome, whereas black letters indicates the reference genome. SNP index value is defined as the number of reads that differ from the reference genome to the total number of reads in this genomic position.


se-3
se-3;sup
se-3
F2
EMS
mutagenesis
X
(2-3 x backcrossed)
Sequence
Parental
DNA
Sequence
bulked DNA
Pool DNA from F2 individuals with
the phenotype
1 2 3 4 5
Assemble control and
sample SNPs on the
reference genome
Whole Genome Sequence
(WGS) analysis
Unlinked SNP
Linked SNP
Reference
SNP Index= 3/8= 0.38
SNP Index= 8/8= 1

To further delimit the number of SNPs included in each list, I used the SNP index value (see Figure 5.1). The SNP index value is the "Depth of the variation" value divided by the "Total depth" value in any given SNP location. "Total depth" is defined as the number of reads around any given SNP and "Depth of the variation" is defined as the number of these reads that are different from the reference sequence. Thus, the higher the SNP index value is the higher the reliability of that SNP. In other words, polymorphisms that are detected in most of the sequencing reads are more reliable than polymorphisms detected in a few reads along the SNP region. With SNP index value 1.0 being the maximum and 0.2 being the minimum value, I set the SNP index value threshold to 0.7 for recessive suppressors and 0.45 for dominant suppressors, as hits below those values are not sufficiently significant to be considered candidates. The threshold value for a dominant mutation is lower than the one for a recessive mutation, due to the fact that the phenotype of dominant mutations is not always clearly distinguishable amongst heterozygous and homozygous plants, and the SNP index value will be affected accordingly by non-mutant SNPs present in the heterozygous plants. SNPs with "Total depth" value below 10 were excluded from the analysis, because this coverage is not sufficient for this analysis. Furthermore, SNPs in intergenic regions were excluded from the lists, because they are less likely to affect gene function.

Filtering the SNP lists of the three suppressor lines using the parameters described above yielded a manageable number of candidate SNPs for further manual verification (see Tables 5.1-5.3). To identify which of those SNPs are linked to the phenotype, I performed "derived cleaved amplified polymorphic sequence" (dCAP)/ "cleaved amplified polymorphic sequence" (CAP) profiling on markers designed for those polymorphisms and sequencing of the predicted mutagenized region.

se-3 suppressor [3] SNP verification

se-3 suppressor [3] WGS analysis and SNP verification	
Before filtering	
Initial no. of SNPs	1337
Filtering for	
No. of SNPs with SNP index above 0.7	146
No. after excluding intragenic SNPs	21
After filtering	
Candidate SNPs	21
Real SNPs	11
Linked SNPs	2

Table 5.1: Table summarizing the results obtained by the WGS analysis and SNP verification for *se-3* suppressor [3]. Before filtering the SNP list contained 1337 SNPs. These are unique SNPs for *se-3* suppressor [3]. Exclusion of SNPs that had a SNP index value lower than 0.7 reduced the number to 165. Further filtering of the SNP list by excluding intragenic SNPs reduced the number of candidates to 21. These 21 candidates were verified by dCAP/CAP linkage analysis and only 2 of them are linked to the suppressor. Both candidate SNPs are located on chromosome II at positions 10422834 (in the AT2G24530 locus) and 11923505 (in the AT2G27990 locus). For further information concerning filtering and details about the candidate SNPs refer to the text.

dCAP/CAP marker analysis of the *se-3* suppressor [3] SNPs shown in Table 5.1 revealed that 11 out of the 21 SNPs are real, indicating that almost 50% of the candidate SNPs are false positive. This is likely attributable to possible complications in the sequencing process or to defective alignment of the sequencing reads of the suppressor along the scaffold. Further linkage analysis of the 11 real SNPs revealed two SNPs linked to suppressor [3]. One of these SNPs is located in the BELL homeobox gene *BEL1-LIKE HOMEODOMAIN8 (BLH8*) (AT2G27990) and the other is located in an unknown protein-coding gene (AT2G24530). These genes are located on chromosome II having a distance

interval of approximately 1.5 Mb. Both SNPs change the amino acid sequence of the respective genes. In the case of *BLH8*, the mutation in the first exon of the gene causes an amino acid change at residue 133 R (Arginine) to Q (Glutamine). Although both amino acids are polar, R is positively charged whereas Q is not. Such changes in amino acid charge usually cause misfolding of proteins, which may subsequently affect protein function. In the case of AT2G24530, the EMS mutation in the single exon of the gene changes the amino acid P (Proline) at residue 81 into the polar amino acid S (Serine). Similarly to the *BLH8* mutation, this mutation might also affect protein folding and function. Although not described in this thesis, I am currently assessing if any or both mutations suppress *se-3*, by complementation tests and by determining whether independent mutations in these genes are allelic to the *se-3* suppressor [3] mutation.

WGS analysis of se-3 suppressor [1] and [23]

se-3 suppressor [1] WGS analysis	
Before filtering	
Initial no. of SNPs	1238
Filtering for	
No. of SNPs with SNP index above 0.7	142
No. after excluding intragenic SNPs	23
After filtering	
Candidate SNPs	23

Table 5.2: Table summarizing the results obtained by the WGS analysis of *se-3* suppressor [1]. The original list of SNPs derived from the WGS analysis of *se-3* suppressor [1] contained 1238 SNPs. These are unique SNPs for *se-3* suppressor [1]. Exclusion of SNPs that had a SNP index value lower than 0.7 reduced the number to 142. Further filtering of the SNP list by excluding intragenic SNPs reduced the number of candidates to 23.

se-3 suppressor [23] WGS analysis	
Before filtering	
Initial no. of SNPs	449
Filtering for	
No. of SNPs with SNP index above 0.45	36
No. after excluding intragenic SNPs	15
After filtering	
Candidate SNPs	15

Table 5.3: Table summarizing the results obtained by the WGS analysis of *se-3* suppressor [23]. The original list of SNPs derived from the WGS analysis of *se-3* suppressor [23] contained 449 SNPs. These are unique SNPs for *se-3* suppressor [23]. Exclusion of SNPs that had a SNP index value lower than 0.45 reduced the number to 36. Further filtering of the SNP list by excluding intragenic SNPs reduced the number of candidates to 15.

Comparison of the values in Tables 5.1-5.3, shows that WGS analysis for *se-3* suppressors C[1] and [3] generated similar results concerning the number of SNPs before and after filtering. Although, the *se-3* suppressor [23] sample had less SNPs in total, it had proportionally more SNPs in coding sequences and less SNPs in intergenic regions (Tables 5.1-5.3). Nevertheless, filtering of all three samples generated similar results in the context of candidate SNP numbers. The 23 and 15 candidate SNPs for *se-3* suppressor [1] and [23], respectively, are currently verified by dCAP/CAP profiling and sequencing.

5.2.2 Mapping of the *se-3* suppressor lines [1] and [3]

To aid identification of candidate SNPs, I also followed conventional mapping for suppressor lines [1] and [3]. A combination of linkage mapping with WGS analysis aims to quickly delimit the mapping interval in which the causal SNP should be searched. In this section, I address the progress in mapping of *se-3* suppressors [1] and [3], and also explain implications faced with the mapping and WGS analysis of line [3].

The first step in any mapping is the generation of the mapping populations, which will be used for recombination analysis of polymorphic DNA markers in relation to the causal mutation. These populations are usually generated by crossing the mutant in study with an ecotype that is highly homologous with, yet divergent enough from the ecotype of the mutant, hence highly polymorphic. Given that both *se-3* suppressor lines [1] and [3], as well as, most of the suppressors in the screen, do not have any obvious phenotype without *se-3* in the background, I generated the se-3 (L*er*) strain, after eight consecutive outcrosses of *se-3* (Col-0) into L*er*. The *se-3* suppressor lines (2x backcrossed to *se-3*) were crossed with these strains and the generated mapping populations were used for mapping. Mapping analysis of the *se-3* suppressor lines [1] an [3] was conducted in a population of approximately 100 F2 long root individuals (suppressed *se-3* phenotype) per line.

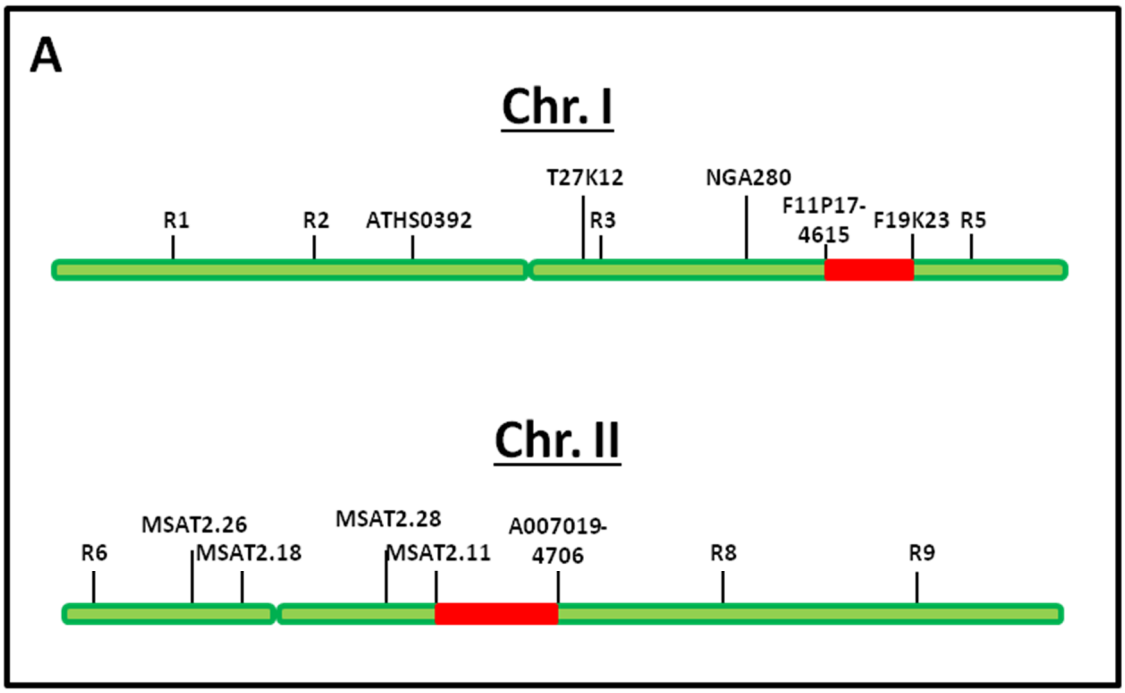
As shown in Figure 5.2 A, mapping analysis of the *se-3* suppressor [1] revealed linkage in two distinct regions of the genome. The suppressor [1] mutation(s) map in a ~1.5 Mb interval of the right arm of chromosome I and, also, in a ~2 Mb interval of the right arm of chromosome II. This interval is bordered by markers F11P17-4615 (5 cM) and F19K23 (7 cM) on chromosome I, and markers MSAT2.11 (8 cM) and A007019-4706 (7 cM) on

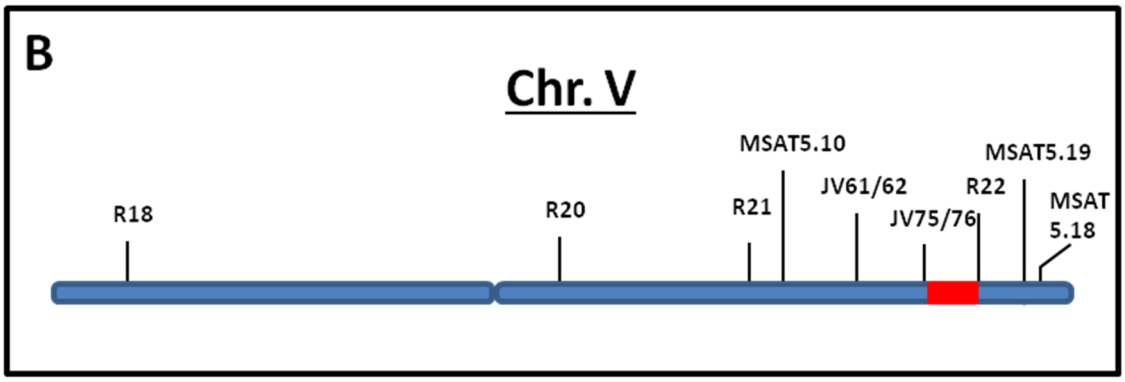
chromosome II. This dual linkage suggests that the *se-3* suppressor [1] phenotype is possibly attributed to 2 different mutations. However, the segregation rate of the mutant phenotype follows the expected Mendelian values, which argues against such possibility.

Concerning *se-3* suppressor [3], mapping analysis positions the causal mutation in a ~1 Mb interval at the end of the right arm of chromosome V (Figure 5.2 B). This interval is bordered by markers JV75/76 and R22, which are 5 cM away from the mutation each. Surprisingly, the location of the mutation on chromosome V does not agree with the WGS sequencing experiment. dCAP analysis of the SNPs generated from the WGS analysis (see Chapter 5.2.1) shows that there are no significant SNPs located in that region of the genome. There are several possibilities that could explain this paradox. For example, this could be attributed to low quality of sequencing and alignment of reads that were generated by the WGS analysis, which consequently affects the final output of candidate SNPs. The fact that the mapping populations were generated by crossing the suppressors with an introgressed *se-3* (L*er*) strain may also contribute to this paradox. Effects of false positive linkage can be detected in introgressed mapping strains, usually caused by fixed regions of the donor genome (in this case Col-0) into the genome of the host (in this case L*er*). The fact that 2 of the SNPs from the WGS analysis are linked to the suppressor suggests that at least one of them is likely to be the causal mutation. These SNPs are currently undergoing further verification with complementation and allelism tests, to clarify whether any of them is the causal mutation to *se-3* suppressor [3].

Figure 5.2: Mapping of the *se-3* suppressor [1] and [3] mutations

(A) Mapping interval of suppressor [1] mutation(s) (marked in red). *se-3* suppressor [1] mutation(s) map in a ~1.5 Mb interval of the right arm of chromosome I and, also, in a ~2 Mb interval of the right arm of chromosome II. This interval is bordered by markers *F11P17-4615* (5 cM) and *F19K23* (7 cM) on chromosome I, and markers *MSAT2.11* (8 cM) and *A007019-4706* (7 cM) on chromosome II. (B) Mapping interval of suppressor [3] mutation (marked in red). *se-3* suppressor [3] mutation maps in a ~1 Mb interval at the end of the right arm of chromosome V. This interval is bordered by marker *JV75/76* (5 cM) and *R22* (5 cM).


A
Chr. I
R1
R2
ATHS0392
T27K12
R3
NGA280
F11P17-
4615
F19K23
R5
Chr. II
R6
MSAT2.26
MSAT2.18
MSAT2.28
MSAT2.11
A007019-
4706
R8
R9


B
Chr. V
R18
R20
R21
MSAT5.10
JV61/62
JV75/76
R22
MSAT5.19
MSAT
5.18

5.3 Discussion

There are several approaches for identifying causal mutations that underlie mutant phenotypes, from the more traditional linkage mapping, to more current methodologies that involve next generation sequencing. Both approaches have their pros and cons. Conventional linkage mapping is more precise but it is time laborious. Whole genome sequencing, on the other hand, is a faster approach but usually less precise in identifying the causal mutation. Taking into account both advantages and disadvantages of both approaches, I decided to follow both, since they complement each other well and a combination can be a powerful tool in the identification of the causal mutation.

As such, for practical reasons three out of the 24 suppressor lines were selected for WGS and linkage mapping. This selection was informed by the assays described in the previous chapter (Chapter 4). *se-3* suppressor [1] was selected as an upstream regulator of SE and also as a candidate in CK signalling pathways, suppressor [3] as a candidate in CK signalling pathways, and *se-3* suppressor [23] as a co-factor/downstream target of PHB.

DNA extracted from plants with the phenotype from segregating populations for all three *se-3* suppressors was subjected to WGS sequencing analysis. The reads generated per sample were aligned using the annotated Col-0 sequenced genome as scaffold in order to identify sample unique SNPs. The list of SNPs that was generated for each sample was filtered with various algorithmic values to exclude noise SNPs, which usually derive from poor alignment of the sequencing reads in some regions of the genome. I have also excluded from these lists SNPs detected in transposable element loci and intergenic regions that are more than 3 kb upstream of genes, since these mutations are less likely to cause a phenotype. This significantly reduced the number of candidate SNPs to a few

dozen per sample that could be further analyzed. SNPs that were detected in coding sequences and especially the ones causing protein sequence alterations were prioritized.

The WGS analysis and subsequent verification of SNPs for *se-3* suppressor [3] revealed 2 out of the 21 candidate SNPs as putative causal mutation(s). Both of those SNPs are located on chromosome II and are approximately 1.5Mb away from each other. Both SNPS cause amino acid alterations. The corresponding affected loci are the AT2G24530 gene that encodes for an unknown protein, and the AT2G27990 gene that encodes for the BELL homeobox protein BLH8/ PNF (POUND-FOOLISH). BELL homeobox proteins, which homo- and hetero-dimerize with the class I KNOTTED1-LIKE HOMEOBOX (KNOX I) transcription factors, have been implicated in the development of the vegetative and reproductive meristems (Kanrar et al., 2006; Kanrar et al., 2008; Rutjens et al., 2009). If the SNP in the *PNF* gene is the actual causal mutation of *se-3* suppressor [3], it would be intriguing to decipher how genes implicated in pathways of the shoot affect also patterning in the root. Although *KNOX I* genes are not expressed in the Arabidopsis root, there is another family of KNOX transcription factors that it has been speculated may have a role in root development. These are the class II *KNOX* genes (*KNAT 3, 4*, and *5)*. This hypothesis is supported by the fact that all three genes have homeotic expression patterns in the root, and also from the fact that their expression is modulated by hormones that affect root growth (Truernit and Haseloff, 2007). If BELL proteins interact with class II KNOX proteins, this could explain a plausible mechanism by which PNF could regulate root patterning. This *se-3* suppressor is currently verified with complementation and allelism tests, to clarify whether the causal mutation actually resides in this *BELL* gene.

Chapter 6

General discussion

6.1 Introduction

Pattern formation is the process by which relatively simple structures develop in space and time to give rise to more complex structures. In plants, patterning begins with embryogenesis and continues post-embryonically by the function of the meristems. Meristems are populations of pluripotent cells that fuel post-embryonic shoot and root organs with a continuous supply of cells. The shoot and root meristems are formed during embryogenesis, at the apices of the embryonic body, after a series of axial patterning events.

Amongst the various factors contributing to embryonic patterning, the SE/ HD-ZIP III regulatory pathway is known to play important roles in embryonic axiality. Failure to restrict *HD-ZIP III* mRNAs at the apical pole of the embryo, via a SE-dependent miRNA regulatory mechanism, perturbs elaboration of all embryonic axial patterns and results in embryo lethality (Grigg et al., 2009). This observation suggests that miRNA regulation is integral for embryonic patterning and viability. This notion is supported by two lines of evidence. Firstly, many miRNA-regulated genes are central in several patterning events during embryogenesis (Aida et al., 1997; Emery et al., 2003; Dharmasiri et al., 2005a; Prigge et al., 2005). Secondly, loss-of-function mutants in genes that are required for miRNA biogenesis, such as *SE* and *DCL1*, show severe patterning defects and embryo lethality (Lobbes et al., 2006; Grigg et al., 2009; Nodine and Bartel, 2010).

6.2 Investigation of cell-specific SE activities reveals its non-cell autonomous functions

To understand the role of miRNAs at the tissue-specific level, I dissected the tissue-specific role of SE during embryogenesis. I focused on the miRNA biogenesis protein SE, because null *se-5* embryos show severe patterning defects, reflecting the fact that SE via regulation of the HD-ZIP IIIs is required for correct patterning along all embryonic developmental axes (Grigg et al., 2009). To that end, I expressed SE in different domains of the *se-5* embryo-lethal strain and assessed to what extent re-constitution of SE activity in these domains can rescue embryo lethality in that mutant. The expression domains chosen for the purposes of this thesis aimed to cover key compartments of the Arabidopsis pro-embryo (Figure 6.1). *CUC2* is expressed in the upper tier, *PLT2* is expressed in the lower tier complementary to *CUC2*, and the *SHR*, *P7*, and *P19* domains further dissect the lower tier of the pro-embryo, in central, peripheral-basal, and basal subdomains, respectively (Figure 6.1).

Analysis of those tissue specific expression lines revealed that the activity of SE in all the cells of the lower tier and basal pole of the embryo is sufficient to fully rescue patterning defects and viability of *se-5* mutants (Chapter 3, Figure 6.1). However, further restriction of SE activity at the lower tier to cells of the central zone, or cells at the peripheral-basal domain of the embryo was not sufficient to fully rescue *se-5* embryogenesis (Chapter 3, Figure 6.1). These findings indicate that activity of SE, and by implication miRNAs, is required in the lower tier/basal pole of the embryo, and that more restricted expression of SE within this domain is insufficient to support correct embryonic patterning.

Intriguingly, expressing SE in the upper tier of the embryo, within the CUC2 domain, was also sufficient to fully rescue *se-5* embryogenesis (Chapter 3, Figure 6.1). Collectively

these results indicate that although SE is expressed everywhere in the Arabidopsis embryo, more restricted expression either at the upper and/ or lower tier of the embryo is sufficient to permit correct patterning throughout the embryonic body. This observation further suggests that SE may influence patterning in domains in which it is not expressed, via non-cell autonomous mechanisms. Given that both PLT2 and CUC2 tissue-specific expression experiments yielded the same result, this is most likely to be a bi-directional mechanism.

A valid argument that arises from these observations is whether SE itself can move from cell to cell to regulate patterning in a non-cell autonomous manner. Nonetheless, there are several observations that do not support such functionalities for SE. Firstly, even if SE was mobile, for which we do not have any indication, the vYFP:SE fusion is too large (more than 85 kDa) to move from cell to cell via PD. This is supported by the work of Kim *et al.*, 2005 who show that cell-to-cell mobility of proteins more than 80 kDa is significantly restricted during embryonic development (Kim et al., 2005b). Secondly, the tissue-specific CLSM experiments performed in chapter 3 reveal that SE expression is strictly localized in the cellular context of the domain that it`s expression was driven. This is clearly seen in the tissue-specific expression of SE in domains that contain just a few files of cells, such as *p7* and *p19*, where SE is limited only in ground-tissue cells and the progeny of the hypophysis, respectively (Figure 3.6). Lastly, expression analysis of the *PLT2::vYFP:SE;se-5/+* lines at the post-embryonic stage also shows that SE is restricted in the root tip, where *PLT2* is active, and is not detected in other organs of the plant (Figure 3.3). Collectively these indicate that SE is unlikely to move, and possibly influences patterning by regulating a mobile factor.

It is intriguing that broad SE expression in the apical and/or the basal pole is sufficient for correct embryogenesis, whereas expression of SE in subdomains of the basal pole is insufficient. There are several hypotheses that could explain this observation, and they can relate to either spatial and/or temporal considerations.

a. Spatial aspects of the SE-dependent non-cell autonomous patterning mechanism(s)

Differences in the effectiveness to rescue embryogenesis may be attributed to the spatial differences of these expression domains. To put it simply, expression of SE in restricted regions, such as that of SHR (see Frigure 6.1), may be insufficient to support patterning of the whole embryo, and as long as SE is active in broader domains (e.g. PLT2, see Figure 6.1) correct axial patterning can take place. This is a valid argument given that both *SHR*, *p7*, and *p19* domains are considerably smaller than *PLT2* and *CUC2*, especially since both *SHR*, *p7*, and *p19* tissue-specific SE expressions can partially rescue *se-5* embryogenesis (see Chapter 3). However, this automatically assumes that lower levels of SE within the *PLT2* and/or *CUC2* domain should also be less effective in rescuing *se-5* embryogenesis. Although investigation of those arguments requires further experimentation, several observations from the initial analysis may argue against dosage effects having a crucial role in the SE-dependent patterning processes. Firstly, heterozygous *PLT2::vYFP:SE/+;se-5* plants weren't less potent in suppressing the *se-5* phenotype and the strength of their vYFP expression was similar to that of homozygous lines (data not shown). Secondly, similar effects were also observed amongst lines with single or multiple T-DNA insertions (data not shown). Thus, it seems that the dosage of SE is not as crucial as the domain where SE is expressed for correct embryogenesis.

To that end, it has to be noted that there was one subdomain in the periphery of the embryo that has been excluded from the tissue-specific SE analysis, and that is the epidermal domain. That was an educated choice, given that protoderm is the only tissue that seems to develop correctly in the null *se-5* embryos (Grigg et al., 2009), thus less likely to play a significant role in the SE-dependent patterning processes. However, it should be stated that both the *CUC2* and *PLT2* genes are expressed in the epidermis, which is the only common cell type amongst those domains, and might explain why SE from either of those domains can rescue *se-5* embryogenesis. This is not implausible, given that the integrity of the epidermal identity in *se-5* embryos was verified by expression analysis only of the *AtML1* gene (Grigg et al., 2009), which of course is not the only marker of the epidermal cell fate.

Another reasonable hypothesis that derives from studies of plasmodesmata development encompasses both spatial and temporal aspects, but it is centered on spatial/transport routes in the developing embryo. Plasmodesmata are subcellular channels that connect the cytoplasm of neighboring plant cells and serve in the exchange of micro- and macromolecules, such as proteins and RNAs (Zambryski and Crawford, 2000; Lucas and Lee, 2004; Liarzi and Epel, 2005; Christensen et al., 2009). Although plasmodesmata development has not been extensively studied in early embryogenesis, they seem to play important roles in embryonic patterning. Mutants that affect plasmodesmata development have severe patterning defects and they are embryo lethal (Kobayashi et al., 2007; Burch-Smith and Zambryski, 2010; Xu et al., 2012), similarly to what is observed in *se-5* and *dcl-1* embryos (Grigg et al., 2009; Nodine and Bartel, 2010).

Recent work in the field shows that the size exclusion limit of plamodesmata channels changes during embryogenesis, with earlier stage embryos having cells with larger plasmodesmata, whereas in later embryonic stages plasmodesmata openings get smaller (Kim et al., 2005a; Kim and Zambryski, 2005; Xu et al., 2012). This distribution plays a role in how effectively molecules move from cell to cell, and it is believed to affect patterning. The pioneering work of Kim *et al*., 2005 (Kim et al., 2005a) links plasmodesmata development and apical-basal axial patterning in Arabidopsis. In this study, they show that the embryonic body is separated in regions of potent symplastic movement of macromolecules (Kim et al., 2005a). The central zone of the heart to late torpedo stage embryo is less potent for macromolecule exchanges than the neighboring meristematic areas (Kim et al., 2005a). Notably, this central zone is where SHR promoter is active (Figure 6.1). Assuming that SE coordinates patterning via a mobile agent that moves through plasmodesmata, this might explain why expression of SE in the SHR domain is not sufficient to rescue *se-5* embryogenesis.

b. Temporal aspects of the SE-dependent non-cell autonomous patterning mechanism(s)

Another hypothesis that could explain the differences observed in the tissue-specific SE expression experiments considers temporal aspects of the expression domains. Both *PLT2* and *CUC2* promoters are active much earlier than the *SHR*, *P7*, and *P19* promoters. *PLT2* and *CUC2* are active before the 16-cell stage embryo, whereas *SHR*, *P7*, and *P19* are active from early globular stage onwards (data not shown). Therefore, it is not only important where SE is expressed, but also at what embryonic stage SE is active. In other words, expression of SE during early embryogenesis is sufficient to promote correct axial

patterning, but delayed SE expression (from the globular stage onwards) is not sufficient to compensate for the absence of SE in early patterning events. Such early requirements for miRNA function have recently been revealed by Nodine and Bartel, 2010, who showed that DCL1 and miR156 are required at the 16-cell stage embryo to block expression of the SPL transcription factors and prevent premature developmental transitions (Nodine and Bartel, 2010). Given that regulation of HD-ZIP IIIs by miR165/6 requires SE function early in embryogenesis (Grigg et al., 2005; Grigg et al., 2009), it is possible that similar temporal mechanisms may also govern the SE/HD-ZIP III regulatory pathway.

6.3 Novel genetic interactions in the SE/HD-ZIP III pathway revealed by a second-site suppressor screen of the *se-3* mutation

6.3.1 Upstream and downstream genes in the SE/HD-ZIP III pathway

Because the miRNA-mediated SE/HD-ZIP III regulation is involved in various developmental processes in Arabidopsis, I was interested in identifying novel genes in this regulatory pathway. Thus, I performed a second site suppressor screen on the non-embryo lethal *se-3* mutant strain. Although *se-3* does not cause embryo lethality, *se-3* plants show post-embryonic defects in their root and shoot development and mild embryonic phenotypes (Grigg et al., 2005). Defective root and shoot patterning is also observed in *se-5* mutant embryos (Grigg et al., 2009), which hints towards common genetic mechanisms during embryonic and post-embryonic development. Thus, I performed the mutagenesis on the *se-3* strain and screened for restored root development. Although the screen was not saturated (~1000 M1 plants), it yielded many

independent suppressor lines. Such a result is not surprising, given that the *se-3* mutants have residual SE activity (Grigg et al., 2005), and even modest changes in the activity of interacting genes might improve SE efficiency and revert the short root phenotype of *se-3* back to wild type.

Phenotypic analysis of the lines isolated from the screen revealed a diversity of shoot and root phenotypes. These ranged from mild to complete shoot suppression, and intermediate to complete root suppression of the *se-3* phenotypes (Chapter 4). It is noteworthy that most of the lines isolated from the screen as suppressors of the root phenotype of *se-3*, also strongly suppress the shoot phenotypes observed in this strain (Chapter 4). This observation suggests that the underlying genes in the suppressors may be involved in patterning mechanisms that regulate both root and shoot development, either directly or via cross-communication between these organs. To uncouple such possibilities further work, including grafting experiments, is required.

Given that regulation of the HD-ZIP III transcription factors requires the activity of SE (Grigg et al., 2005; Grigg et al., 2009), a screen for *se-3* suppressors can potentially reveal interactors of both SE and the HD-ZIP IIIs. To understand the how the "suppressor genes" function in the SE/ HD-ZIP III pathway, I performed a series of genetic tests. As expected, these tests revealed not only mutants in genes upstream of SE, but also mutants in genes that likely function downstream of or in parallel to the *HD-ZIP IIIs* (Chapter 4). I selected two of those lines for whole genome sequencing to identify the candidate mutations. Further verification and complementation tests are ongoing to identify the causal mutation.

6.3.2 PNF, a novel component of the SE/HD-ZIP III pathway, plays a role in CK signalling

Treatment of the suppressor lines with CK revealed three lines that are mutated in genes of CK-dependent pathways (Chapter 4). Such suppressors are expected, given that the miR165/HD-ZIP III regulatory pathway is linked with the CK-biosynthesis and signalling pathways that regulate root development (Dello Ioio et al., 2012). The *se-3* suppressor [3] was identified by next generation sequencing and linkage analysis as a putative mutant in the BELL homeobox gene *BLH8/PNF* (Chapter 4, and 5). The BELL homeobox proteins, which dimerize with KNOX I transcription factors, are required for SAM and floral meristem development (Kanrar et al., 2006; Kanrar et al., 2008; Rutjens et al., 2009). While it is not known whether *BELL* genes may play any role in root development, it is intriguing to speculate about mechanisms by which this might be happening. Although *KNOX I* genes are not expressed in the Arabidopsis root, the *KNOX II* genes, *KNAT 3, 4,* and *5*, show homeotic expression patterns at the root tips. Furthermore, the expression of these genes is modulated by hormones that affect root development (Truernit and Haseloff, 2007). Assuming *BELL* and *KNOX II* genes interact, this could give a plausible explanation as to how PNF may affect root patterning.

An alternative explanation for this putative function of PNF in root development derives from several genetic observations. For example, *bp-1;blr(van-1);rev-6* triple mutant of the *KNOX I* gene *BREVIPEDICELLUS* (*BP)*, the *BELL* gene *BELLRINGER* (*BLR)* and the *HD-ZIP III* gene *REV* enhances the phenotype of the *bp-1;blr(van-1)* double mutant (Etchells et al., 2012). All three mutants were also shown to enhance the phenotypes of weak *stm* alleles (Otsuga et al., 2001; Byrne et al., 2002; Bhatt et al., 2004). These observations collectively indicate that *KNOX I*, *BELL*, and *HD-ZIP III* genes may have overlapping functions.

Specifically, the link between *HD-ZIP III* and *KNOX I* genes is also supported from the observations that weak *se* loss-of-function and *phb-d* gain-of-function alleles suppress phenotypes observed in *stm* loss-of-function mutants (McConnell and Barton, 1998; Grigg et al., 2005). Given that HD-ZIP III transcription factors are also involved in root development by promoting CK production (Dello Ioio et al., 2012), it is possible that PNF and KNOX I to regulate root development by promoting CK production in concert with the HD-ZIP IIIs.

6.4 Future work and perspectives

This work contributes to the understanding of the tissue-specific role of miRNAs during embryogenesis, by dissecting the domains in which SE activity is required in the Arabidopsis embryo. Nonetheless, there are still many questions the answers to which remain elusive. A fundamental question that requires investigation is whether the patterning mechanism by which SE functions in the tissue-specific level is a general mechanism of miRNA function, or is a mechanism associated only with SE activity. To answer this question, similar tissue-specific expression experiments should be conducted with other components of the miRNA biogenesis pathway, such as DCL1. If such experiments reveal that DCL1 rescues *dcl1* embryogenesis in the same domains that SE rescues *se-5* embryogenesis, this would be a strong indication that the mechanism by which SE regulates axial patterning is most likely mediated by miRNAs and that it involves both SE and DCL1 proteins.

Another important point would be to get insights into the nature of the mechanism by which SE coordinates patterning. Is this non-cell autonomous and bi-directional SE-

dependent mechanism mediated by miRNAs or is it independent of miRNA function? Given that miRNAs have been reported to function in non-cell autonomous patterning processes (Marin-Gonzalez and Suarez-Lopez, 2012) and that SE is an important component of miRNA biogenesis, it is reasonable to assume that this SE-dependent mechanism is mediated by miRNAs. If that is the case, then this mechanism likely involves the miR165-6/HD-ZIP III regulation, which requires the function of SE (Grigg et al., 2005; Grigg et al., 2009). Investigating the differences of miR165/6-activity sensors amongst the various tissue-specific SE rescue lines that I have generated, will reveal whether SE regulates patterning via miR165/6 from those domains. Alternatively, expression of mimicry constructs, which sequester complementary miRNAs, in the domains where SE rescues embryogenesis, would also reveal whether SE regulates patterning from these domains via miR165/6. Furthermore, utilization of inducible-expression constructs of SE in the *CUC2* and *PLT2* domains at different developmental stages would distinguish between temporal and special aspects of the SE function in these domains.

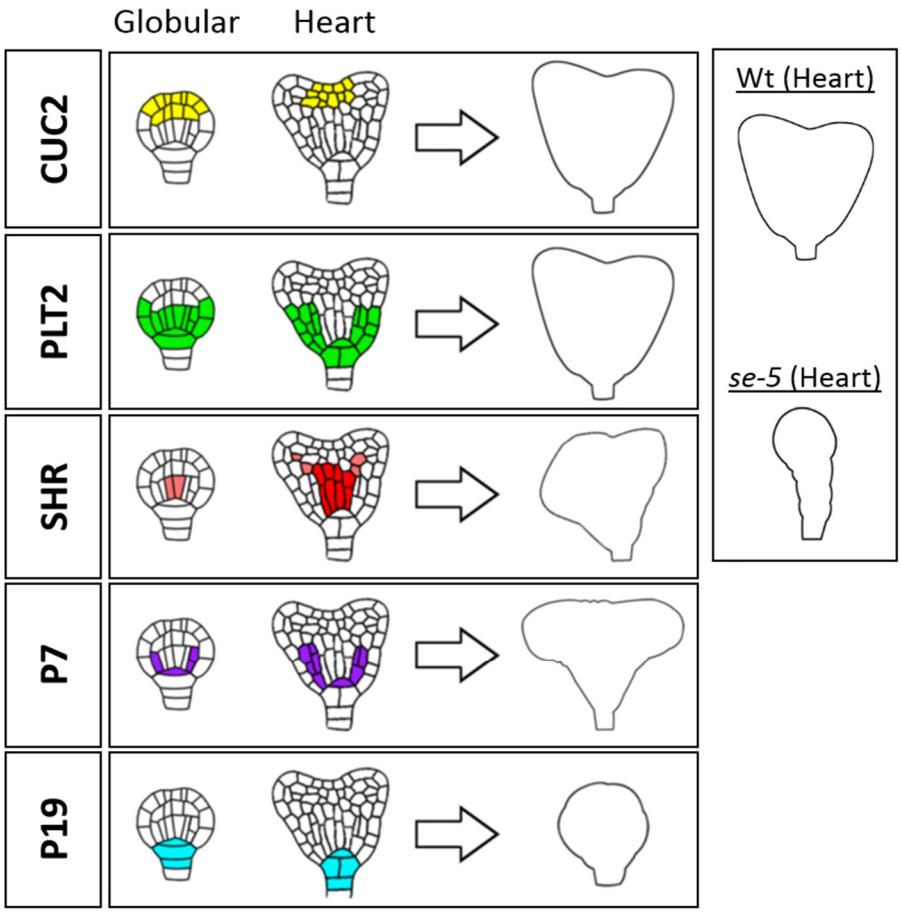
Finally, it is important to investigate the routes by which SE-dependent non-cell autonomous mechanisms regulate axial patterning. This could be achieved by blocking the flow through the plasmodesmata in specific tissues and assessing to what extent the embryonic patterning is perturbed. Tissue-specific expression of plasmodesmata-modifying proteins, such as the callose synthetase CalS3 (Sevilem et al., 2013)(reviewed by Sevilem *et al*., 2013), could be used to achieve such localized manipulation of the plasmodesmatal connections.

Figure 6.1: Graphical representation of the embryonic domains where SE was expressed for the purposes of this thesis

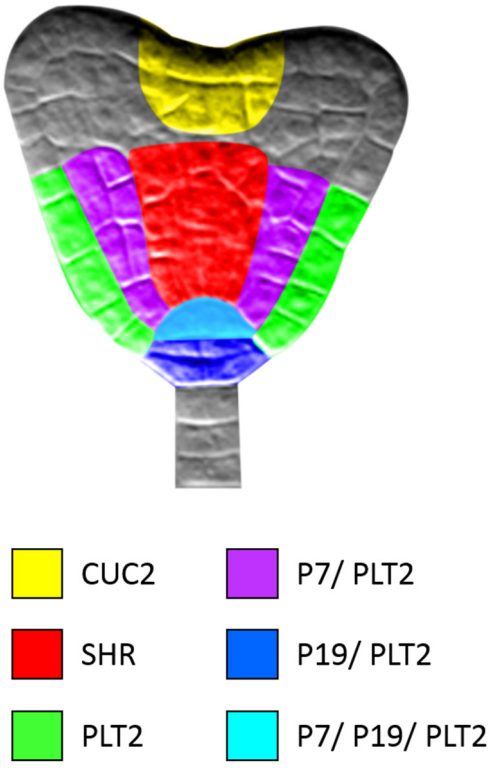
(A) Table summarizing the domains where SE was expressed in *se-5* embryos. These are *CUC2* (Yellow), *PLT2* (Green), *SHR* (Red), *P7* (Magenta), and *P19* (Cyan). The wild-type expression pattern for each domain is shown in globular (left) and heart (right) embryonic stages. The shapes shown after the arrowheads represent the shape of a heart stage *se-5* embryo that expresses SE in the indicated domains. For comparison, the panel on the right side of the figure shows the shape of a wild-type and a *se-5* embryo at the heart stage. SE expression in the *CUC2* and *PLT2* domains fully rescues the patterning of *se-5* embryos, whereas expression of SE only in the *SHR*, *P7*, and *P19* domains is insufficient.

(B) DIC image of a wild-type heart stage embryo showing how the various expression domains overlap at the heart stage. These are *CUC2* (Yellow), *SHR* (Red), *PLT2* (Green), overlap of *P7* and *PLT2* (Magenta), overlap of *P19* and *PLT2* (Dark Blue), and overlap of *P7*, *P19*, and *PLT2* (Cyan).

A


Globular
Heart
CUC2
PLT2
SHR
P7
P19
Wt (Heart)
se-5 (Heart)

B


CUC2
SHR
PLT2
P7/ PLT2
P19/ PLT2
P7/ P19/ PLT2

References

Abe, M., Katsumata, H., Komeda, Y., and Takahashi, T. (2003). Regulation of shoot epidermal cell differentiation by a pair of homeodomain proteins in Arabidopsis. Development **130,** 635-643.

Aida, M., Ishida, T., and Tasaka, M. (1999). Shoot apical meristem and cotyledon formation during Arabidopsis embryogenesis: interaction among the CUP-SHAPED COTYLEDON and SHOOT MERISTEMLESS genes. Development **126,** 1563-1570.

Aida, M., Ishida, T., Fukaki, H., Fujisawa, H., and Tasaka, M. (1997). Genes involved in organ separation in Arabidopsis: an analysis of the cup-shaped cotyledon mutant. Plant Cell **9,** 841-857.

Aida, M., Vernoux, T., Furutani, M., Traas, J., and Tasaka, M. (2002). Roles of PIN-FORMED1 and MONOPTEROS in pattern formation of the apical region of the Arabidopsis embryo. Development **129,** 3965-3974.

Aida, M., Beis, D., Heidstra, R., Willemsen, V., Blilou, I., Galinha, C., Nussaume, L., Noh, Y.S., Amasino, R., and Scheres, B. (2004). The PLETHORA genes mediate patterning of the Arabidopsis root stem cell niche. Cell **119,** 109-120.

Alvarez, J., and Smyth, D.R. (1999). CRABS CLAW and SPATULA, two Arabidopsis genes that control carpel development in parallel with AGAMOUS. Development **126,** 2377-2386.

Andreu-Agullo, C., Maurin, T., Thompson, C.B., and Lai, E.C. (2011). Ars2 maintains neural stem-cell identity through direct transcriptional activation of Sox2. Nature **481,** 195-198.

Aukerman, M.J., and Sakai, H. (2003). Regulation of flowering time and floral organ identity by a MicroRNA and its APETALA2-like target genes. Plant Cell **15,** 2730-2741.

Bao, N., Lye, K.W., and Barton, M.K. (2004). MicroRNA binding sites in Arabidopsis class III HD-ZIP mRNAs are required for methylation of the template chromosome. Dev Cell **7,** 653-662.

Bartel, D.P. (2004). MicroRNAs: genomics, biogenesis, mechanism, and function. Cell **116,** 281-297.

Barton, M.K., and Poethig, R.S. (1993). Formation of the shoot apical meristem in Arabidopsis thaliana: an analysis of development in the WT and *shoot meristemless* mutant. . Development**,** 823-831.

Bhatt, A.M., Etchells, J.P., Canales, C., Lagodienko, A., and Dickinson, H. (2004). VAAMANA--a BEL1-like homeodomain protein, interacts with KNOX proteins BP and STM and regulates inflorescence stem growth in Arabidopsis. Gene **328,** 103-111.

Blilou, I., Xu, J., Wildwater, M., Willemsen, V., Paponov, I., Friml, J., Heidstra, R., Aida, M., Palme, K., and Scheres, B. (2005). The PIN auxin efflux facilitator network controls growth and patterning in Arabidopsis roots. Nature **433,** 39-44.

Borsani, O., Zhu, J., Verslues, P.E., Sunkar, R., and Zhu, J.K. (2005). Endogenous siRNAs derived from a pair of natural cis-antisense transcripts regulate salt tolerance in Arabidopsis. Cell **123,** 1279-1291.

Bowman, J.L., and Floyd, S.K. (2008). Patterning and Polarity in Seed Plant Shoots. Annual Review of Plant Biology **59,** 67-88.

Brennecke, J., Stark, A., Russell, R.B., and Cohen, S.M. (2005). Principles of MicroRNAâ€“Target Recognition. PLoS Biol **3,** e85.

Breuninger, H., Rikirsch, E., Hermann, M., Ueda, M., and Laux, T. (2008). Differential Expression of WOX Genes Mediates Apical-Basal Axis Formation in the Arabidopsis Embryo. Developmental Cell **14,** 867-876.

Brodersen, P., Sakvarelidze-Achard, L., Bruun-Rasmussen, M., Dunoyer, P., Yamamoto, Y.Y., Sieburth, L., and Voinnet, O. (2008). Widespread translational inhibition by plant miRNAs and siRNAs. Science (New York, N.Y.) **320,** 1185-1190.

Burch-Smith, T.M., and Zambryski, P.C. Loss of INCREASED SIZE EXCLUSION LIMIT (ISE)1 or ISE2 increases the formation of secondary plasmodesmata. Curr Biol **20,** 989-993.

Burch-Smith, T.M., and Zambryski, P.C. (2010). Loss of INCREASED SIZE EXCLUSION LIMIT (ISE)1 or ISE2 increases the formation of secondary plasmodesmata. Curr Biol **20,** 989-993.

Byrne, M.E. (2006). Shoot meristem function and leaf polarity: the role of class III HD-ZIP genes. PLoS Genet **2,** e89.

Byrne, M.E., Simorowski, J., and Martienssen, R.A. (2002). ASYMMETRIC LEAVES1 reveals knox gene redundancy in Arabidopsis. Development **129,** 1957-1965.

Carlsbecker, A., Lee, J.Y., Roberts, C.J., Dettmer, J., Lehesranta, S., Zhou, J., Lindgren, O., Moreno-Risueno, M.A., Vaten, A., Thitamadee, S., Campilho, A., Sebastian, J., Bowman, J.L., Helariutta, Y., and Benfey, P.N. (2010). Cell signalling by microRNA165/6 directs gene dose-dependent root cell fate. Nature **465,** 316-321.

Chandler, J., Nardmann, J., and Werr, W. (2008). Plant development revolves around axes. Trends in Plant Science **13,** 78-84.

Chellappan, P., Xia, J., Zhou, X., Gao, S., Zhang, X., Coutino, G., Vazquez, F., Zhang, W., and Jin, H. (2010). siRNAs from miRNA sites mediate DNA methylation of target genes. Nucleic acids research **38,** 6883-6894.

Chen, E.J., and Kaiser, C.A. (2003). LST8 negatively regulates amino acid biosynthesis as a component of the TOR pathway. J Cell Biol **161,** 333-347.

Chen, X. (2009). Small RNAs and Their Roles in Plant Development. Annual Review of Cell and Developmental Biology **25,** 21-44.

Christensen, N.M., Faulkner, C., and Oparka, K. (2009). Evidence for unidirectional flow through plasmodesmata. Plant Physiol **150,** 96-104.

Cui, H., Hao, Y., Kovtun, M., Stolc, V., Deng, X.W., Sakakibara, H., and Kojima, M. (2011). Genome-wide direct target analysis reveals a role for SHORT-ROOT in root vascular patterning through cytokinin homeostasis. Plant Physiol **157,** 1221-1231.

Cui, H., Levesque, M.P., Vernoux, T., Jung, J.W., Paquette, A.J., Gallagher, K.L., Wang, J.Y., Blilou, I., Scheres, B., and Benfey, P.N. (2007). An evolutionarily conserved mechanism delimiting SHR movement defines a single layer of endodermis in plants. Science (New York, N.Y.) **316,** 421-425.

De Rybel, B., van den Berg, W., Lokerse, A., Liao, C.Y., van Mourik, H., Moller, B., Peris, C.L., and Weijers, D. (2011). A versatile set of ligation-independent cloning vectors for functional studies in plants. Plant Physiol **156,** 1292-1299.

Dello Ioio, R., Linhares, F.S., Scacchi, E., Casamitjana-Martinez, E., Heidstra, R., Costantino, P., and Sabatini, S. (2007). Cytokinins determine Arabidopsis root-meristem size by controlling cell differentiation. Curr Biol **17,** 678-682.

Dello Ioio, R., Nakamura, K., Moubayidin, L., Perilli, S., Taniguchi, M., Morita, M.T., Aoyama, T., Costantino, P., and Sabatini, S. (2008). A genetic framework for the control of cell division and differentiation in the root meristem. Science (New York, N.Y.) **322,** 1380-1384.

Dello Ioio, R., Galinha, C., Fletcher, A.G., Grigg, S.P., Molnar, A., Willemsen, V., Scheres, B., Sabatini, S., Baulcombe, D., Maini, P.K., and Tsiantis, M. (2012). A PHABULOSA/cytokinin feedback loop controls root growth in Arabidopsis. Curr Biol **22,** 1699-1704.

Dharmasiri, N., and Estelle, M. (2004). Auxin signalling and regulated protein degradation. Trends Plant Sci **9,** 302-308.

Dharmasiri, N., Dharmasiri, S., and Estelle, M. (2005a). The F-box protein TIR1 is an auxin receptor. Nature **435,** 441-445.

Dharmasiri, N., Dharmasiri, S., Weijers, D., Lechner, E., Yamada, M., Hobbie, L., Ehrismann, J.S., Jurgens, G., and Estelle, M. (2005b). Plant development is regulated by a family of auxin receptor F box proteins. Dev Cell **9,** 109-119.

Djupedal, I., and Ekwall, K. (2009). Epigenetics: heterochromatin meets RNAi. Cell Res **19,** 282-295.

Dong, Z., Han, M.H., and Fedoroff, N. (2008). The RNA-binding proteins HYL1 and SE promote accurate in vitro processing of pri-miRNA by DCL1. Proceedings of the National Academy of Sciences of the United States of America **105,** 9970-9975.

Dunoyer, P., and Voinnet, O. (2008). Mixing and matching: the essence of plant systemic silencing? Trends Genet **24,** 151-154.

Dunoyer, P., Schott, G., Himber, C., Meyer, D., Takeda, A., Carrington, J.C., and Voinnet, O. Small RNA duplexes function as mobile silencing signals between plant cells. Science (New York, N.Y.) **328,** 912-916.

Emery, J.F., Floyd, S.K., Alvarez, J., Eshed, Y., Hawker, N.P., Izhaki, A., Baum, S.F., and Bowman, J.L. (2003). Radial patterning of Arabidopsis shoots by class III HD-ZIP and KANADI genes. Curr Biol **13,** 1768-1774.

Eshed, Y., Baum, S.F., and Bowman, J.L. (1999). Distinct mechanisms promote polarity establishment in carpels of Arabidopsis. Cell **99,** 199-209.

Eshed, Y., Baum, S.F., Perea, J.V., and Bowman, J.L. (2001). Establishment of polarity in lateral organs of plants. Curr Biol **11,** 1251-1260.

Eshed, Y., Izhaki, A., Baum, S.F., Floyd, S.K., and Bowman, J.L. (2004). Asymmetric leaf development and blade expansion in Arabidopsis are mediated by KANADI and YABBY activities. Development **131,** 2997-3006.

Etchells, J.P., Moore, L., Jiang, W.Z., Prescott, H., Capper, R., Saunders, N.J., Bhatt, A.M., and Dickinson, H.G. (2012). A role for BELLRINGER in cell wall development is supported by loss-of-function phenotypes. BMC Plant Biol **12,** 1471-2229.

Fahlgren, N., Montgomery, T.A., Howell, M.D., Allen, E., Dvorak, S.K., Alexander, A.L., and Carrington, J.C. (2006). Regulation of AUXIN RESPONSE FACTOR3 by TAS3 ta-siRNA affects developmental timing and patterning in Arabidopsis. Curr Biol **16,** 939-944.

Farh, K.K., Grimson, A., Jan, C., Lewis, B.P., Johnston, W.K., Lim, L.P., Burge, C.B., and Bartel, D.P. (2005). The widespread impact of mammalian MicroRNAs on mRNA repression and evolution. Science (New York, N.Y.) **310,** 1817-1821.

Faure, J.-E., Rotman, N., Fortuné, P., and Dumas, C. (2002). Fertilization in Arabidopsis thaliana wild type: Developmental stages and time course. The Plant Journal **30,** 481-488.

Friml, J., Vieten, A., Sauer, M., Weijers, D., Schwarz, H., Hamann, T., Offringa, R., and Jurgens, G. (2003). Efflux-dependent auxin gradients establish the apical-basal axis of Arabidopsis. Nature **426,** 147-153.

Furutani, M., Vernoux, T., Traas, J., Kato, T., Tasaka, M., and Aida, M. (2004). PIN-FORMED1 and PINOID regulate boundary formation and cotyledon development in Arabidopsis embryogenesis. Development **131,** 5021-5030.

Fusaro, A.F., Matthew, L., Smith, N.A., Curtin, S.J., Dedic-Hagan, J., Ellacott, G.A., Watson, J.M., Wang, M.B., Brosnan, C., Carroll, B.J., and Waterhouse, P.M. (2006). RNA interference-inducing hairpin RNAs in plants act through the viral defence pathway. EMBO Rep **7,** 1168-1175.

Galinha, C., Hofhuis, H., Luijten, M., Willemsen, V., Blilou, I., Heidstra, R., and Scheres, B. (2007). PLETHORA proteins as dose-dependent master regulators of Arabidopsis root development. Nature **449,** 1053-1057.

Galweiler, L., Guan, C., Muller, A., Wisman, E., Mendgen, K., Yephremov, A., and Palme, K. (1998). Regulation of polar auxin transport by AtPIN1 in Arabidopsis vascular tissue. Science (New York, N.Y.) **282,** 2226-2230.

Gandikota, M., Birkenbihl, R.P., Höhmann, S., Cardon, G.H., Saedler, H., and Huijser, P. (2007). The miRNA156/157 recognition element in the 3′ UTR of the Arabidopsis SBP box gene SPL3 prevents early flowering by translational inhibition in seedlings. The Plant Journal **49,** 683-693.

Geldner, N., Anders, N., Wolters, H., Keicher, J., Kornberger, W., Muller, P., Delbarre, A., Ueda, T., Nakano, A., and Jurgens, G. (2003). The Arabidopsis GNOM ARF-GEF mediates endosomal recycling, auxin transport, and auxin-dependent plant growth. Cell **112,** 219-230.

Gendrel, A.V., and Colot, V. (2005). Arabidopsis epigenetics: when RNA meets chromatin. Curr Opin Plant Biol **8,** 142-147.

Giraldez, A.J., Mishima, Y., Rihel, J., Grocock, R.J., Van Dongen, S., Inoue, K., Enright, A.J., and Schier, A.F. (2006). Zebrafish MiR-430 promotes deadenylation and clearance of maternal mRNAs. Science (New York, N.Y.) **312,** 75-79.

Grigg, S.P., Canales, C., Hay, A., and Tsiantis, M. (2005). SERRATE coordinates shoot meristem function and leaf axial patterning in Arabidopsis. Nature **437,** 1022-1026.

Grigg, S.P., Galinha, C., Kornet, N., Canales, C., Scheres, B., and Tsiantis, M. (2009). Repression of Apical Homeobox Genes Is Required for Embryonic Root Development in Arabidopsis. Current Biology **19,** 1485-1490.

Hadfi, K., Speth, V., and Neuhaus, G. (1998). Auxin-induced developmental patterns in Brassica juncea embryos. Development **125,** 879-887.

Haecker, A., Gross-Hardt, R., Geiges, B., Sarkar, A., Breuninger, H., Herrmann, M., and Laux, T. (2004). Expression dynamics of WOX genes mark cell fate decisions during early embryonic patterning in Arabidopsis thaliana. Development **131,** 657-668.

Hamann, T., Benkova, E., Baurle, I., Kientz, M., and Jurgens, G. (2002). The Arabidopsis BODENLOS gene encodes an auxin response protein inhibiting MONOPTEROS-mediated embryo patterning. Genes Dev **16,** 1610-1615.

Han, X., Kumar, D., Chen, H., Wu, S., and Kim, J.Y. (2013). Transcription factor-mediated cell-to-cell signalling in plants. Journal of experimental botany **2013,** 17.

Hardtke, C.S., and Berleth, T. (1998). The Arabidopsis gene MONOPTEROS encodes a transcription factor mediating embryo axis formation and vascular development. Embo J **17,** 1405-1411.

Hardtke, C.S., Ckurshumova, W., Vidaurre, D.P., Singh, S.A., Stamatiou, G., Tiwari, S.B., Hagen, G., Guilfoyle, T.J., and Berleth, T. (2004). Overlapping and non-redundant functions of the Arabidopsis auxin response factors MONOPTEROS and NONPHOTOTROPIC HYPOCOTYL 4. Development **131,** 1089-1100.

Heidstra, R., Welch, D., and Scheres, B. (2004). Mosaic analyses using marked activation and deletion clones dissect Arabidopsis SCARECROW action in asymmetric cell division. Genes Dev **18,** 1964-1969.

Helariutta, Y., Fukaki, H., Wysocka-Diller, J., Nakajima, K., Jung, J., Sena, G., Hauser, M.T., and Benfey, P.N. (2000). The SHORT-ROOT gene controls radial patterning of the Arabidopsis root through radial signalling. Cell **101,** 555-567.

Hofhuis, H., Laskowski, M., Du, Y., Prasad, K., Grigg, S., Pinon, V., and Scheres, B. (1013). Phyllotaxis and rhizotaxis in Arabidopsis are modified by three PLETHORA transcription factors. Curr Biol **23,** 956-962.

Izhaki, A., and Bowman, J.L. (2007). KANADI and class III HD-Zip gene families regulate embryo patterning and modulate auxin flow during embryogenesis in Arabidopsis. Plant Cell **19,** 495-508.

Jenik, P.D., Gillmor, C.S., and Lukowitz, W. (2007). Embryonic patterning in Arabidopsis thaliana. Annu Rev Cell Dev Biol **23,** 207-236.

Jones-Rhoades, M.W., Bartel, D.P., and Bartel, B. (2006). MicroRNAS and their regulatory roles in plants. Annu Rev Plant Biol **57,** 19-53.

Kanrar, S., Onguka, O., and Smith, H.M. (2006). Arabidopsis inflorescence architecture requires the activities of KNOX-BELL homeodomain heterodimers. Planta **224,** 1163-1173.

Kanrar, S., Bhattacharya, M., Arthur, B., Courtier, J., and Smith, H.M. (2008). Regulatory networks that function to specify flower meristems require the function of homeobox

genes PENNYWISE and POUND-FOOLISH in Arabidopsis. The Plant journal : for cell and molecular biology **54,** 924-937.

Karginov, F.V., Cheloufi, S., Chong, M.M.W., Stark, A., Smith, A.D., and Hannon, G.J. (2010). Diverse Endonucleolytic Cleavage Sites in the Mammalian Transcriptome Depend upon MicroRNAs, Drosha, and Additional Nucleases. Molecular cell **38,** 781-788.

Kerstetter, R.A., Bollman, K., Taylor, R.A., Bomblies, K., and Poethig, R.S. (2001). KANADI regulates organ polarity in Arabidopsis. Nature **411,** 706-709.

Kidner, C.A., and Martienssen, R.A. (2004). Spatially restricted microRNA directs leaf polarity through ARGONAUTE1. Nature **428,** 81-84.

Kim, I., and Zambryski, P.C. (2005). Cell-to-cell communication via plasmodesmata during Arabidopsis embryogenesis. Curr Opin Plant Biol **8,** 593-599.

Kim, I., Kobayashi, K., Cho, E., and Zambryski, P.C. (2005a). Subdomains for transport via plasmodesmata corresponding to the apical-basal axis are established during Arabidopsis embryogenesis. Proceedings of the National Academy of Sciences of the United States of America **102,** 11945-11950.

Kim, I., Cho, E., Crawford, K., Hempel, F.D., and Zambryski, P.C. (2005b). Cell-to-cell movement of GFP during embryogenesis and early seedling development in Arabidopsis. Proceedings of the National Academy of Sciences of the United States of America **102,** 2227-2231.

Kim, J.Y. (2005). Regulation of short-distance transport of RNA and protein. Curr Opin Plant Biol **8,** 45-52.

Kim, Y.J., Zheng, B., Yu, Y., Won, S.Y., Mo, B., and Chen, X. (2011). The role of Mediator in small and long noncoding RNA production in Arabidopsis thaliana. EMBO J **30,** 814-822.

Kobayashi, K., Otegui, M.S., Krishnakumar, S., Mindrinos, M., and Zambryski, P. (2007). INCREASED SIZE EXCLUSION LIMIT 2 encodes a putative DEVH box RNA helicase involved in plasmodesmata function during Arabidopsis embryogenesis. Plant Cell **19,** 1885-1897.

Kurihara, Y., Takashi, Y., and Watanabe, Y. (2006). The interaction between DCL1 and HYL1 is important for efficient and precise processing of pri-miRNA in plant microRNA biogenesis. Rna **12,** 206-212.

Laubinger, S., Sachsenberg, T., Zeller, G., Busch, W., Lohmann, J.U., RÃ¤tsch, G., and Weigel, D. (2008). Dual roles of the nuclear cap-binding complex and SERRATE in pre-mRNA splicing and microRNA processing in Arabidopsis thaliana. Proceedings of the National Academy of Sciences **105,** 8795-8800.

Laubinger, S., Zeller, G., Henz, S.R., Buechel, S., Sachsenberg, T., Wang, J.-W., RÃ¤tsch, G., and Weigel, D. (2010). Global effects of the small RNA biogenesis machinery on the Arabidopsis thaliana transcriptome. Proceedings of the National Academy of Sciences **107,** 17466-17473.

Laux, T., Mayer, K.F., Berger, J., and Jurgens, G. (1996). The WUSCHEL gene is required for shoot and floral meristem integrity in Arabidopsis. Development **122,** 87-96.

Lenhard, M., Jurgens, G., and Laux, T. (2002). The WUSCHEL and SHOOTMERISTEMLESS genes fulfil complementary roles in Arabidopsis shoot meristem regulation. Development **129,** 3195-3206.

Lewis, B.P., Shih, I.h., Jones-Rhoades, M.W., Bartel, D.P., and Burge, C.B. (2003). Prediction of Mammalian MicroRNA Targets. Cell **115,** 787-798.

Li, S., Liu, L., Zhuang, X., Yu, Y., Liu, X., Cui, X., Ji, L., Pan, Z., Cao, X., Mo, B., Zhang, F., Raikhel, N., Jiang, L., and Chen, X. (2013). MicroRNAs Inhibit the Translation of Target mRNAs on the Endoplasmic Reticulum in Arabidopsis. Cell **153,** 562-574.

Liarzi, O., and Epel, B.L. (2005). Development of a quantitative tool for measuring changes in the coefficient of conductivity of plasmodesmata induced by developmental, biotic, and abiotic signals. Protoplasma **225,** 67-76.

Lippman, Z., Gendrel, A.V., Black, M., Vaughn, M.W., Dedhia, N., McCombie, W.R., Lavine, K., Mittal, V., May, B., Kasschau, K.D., Carrington, J.C., Doerge, R.W., Colot, V., and

Martienssen, R. (2004). Role of transposable elements in heterochromatin and epigenetic control. Nature **430,** 471-476.

Liu, C., Xu, Z., and Chua, N.H. (1993). Auxin Polar Transport Is Essential for the Establishment of Bilateral Symmetry during Early Plant Embryogenesis. Plant Cell **5,** 621-630.

Lobbes, D., Rallapalli, G., Schmidt, D.D., Martin, C., and Clarke, J. (2006). SERRATE: a new player on the plant microRNA scene. EMBO Rep **7,** 1052-1058.

Long, J.A., Moan, E.I., Medford, J.I., and Barton, M.K. (1996). A member of the KNOTTED class of homeodomain proteins encoded by the STM gene of Arabidopsis. Nature **379,** 66-69.

Long, J.A., Ohno, C., Smith, Z.R., and Meyerowitz, E.M. (2006). TOPLESS regulates apical embryonic fate in Arabidopsis. Science (New York, N.Y.) **312,** 1520-1523.

Long, J.A., Woody, S., Poethig, S., Meyerowitz, E.M., and Barton, M.K. (2002). Transformation of shoots into roots in Arabidopsis embryos mutant at the TOPLESS locus. Development **129,** 2797-2806.

Lu, P., Porat, R., Nadeau, J.A., and O'Neill, S.D. (1996). Identification of a meristem L1 layer-specific gene in Arabidopsis that is expressed during embryonic pattern formation and defines a new class of homeobox genes. The Plant Cell Online **8,** 2155-2168.

Lucas, W.J., and Lee, J.Y. (2004). Plasmodesmata as a supracellular control network in plants. Nat Rev Mol Cell Biol **5,** 712-726.

Lucas, W.J., Bouche-Pillon, S., Jackson, D.P., Nguyen, L., Baker, L., Ding, B., and Hake, S. (1995). Selective trafficking of KNOTTED1 homeodomain protein and its mRNA through plasmodesmata. Science (New York, N.Y.) **270,** 1980-1983.

Lukowitz, W., Roeder, A., Parmenter, D., and Somerville, C. (2004). A MAPKK Kinase Gene Regulates Extra-Embryonic Cell Fate in Arabidopsis. Cell **116,** 109-119.

Lund, E., Liu, M., Hartley, R.S., Sheets, M.D., and Dahlberg, J.E. (2009). Deadenylation of maternal mRNAs mediated by miR-427 in Xenopus laevis embryos. Rna **15,** 2351-2363.

Machida, S., Chen, H.Y., and Yuan, Y.A. (2011). Molecular insights into miRNA processing by Arabidopsis thaliana SERRATE. Nucleic acids research **39,** 7828-7836.

Mallory, A.C., and Bouché, N. (2008). MicroRNA-directed regulation: to cleave or not to cleave. Trends in Plant Science **13,** 359-367.

Mallory, A.C., Reinhart, B.J., Jones-Rhoades, M.W., Tang, G., Zamore, P.D., Barton, M.K., and Bartel, D.P. (2004). MicroRNA control of PHABULOSA in leaf development: importance of pairing to the microRNA 5' region. Embo J **23,** 3356-3364.

Manavella, P.A., Hagmann, J., Ott, F., Laubinger, S., Franz, M., Macek, B., and Weigel, D. (2012). Fast-forward genetics identifies plant CPL phosphatases as regulators of miRNA processing factor HYL1. Cell **151,** 859-870.

Marin-Gonzalez, E., and Suarez-Lopez, P. (2012). "And yet it moves": cell-to-cell and long-distance signalling by plant microRNAs. Plant Sci **196,** 18-30.

Mattsson, J., Ckurshumova, W., and Berleth, T. (2003). Auxin signalling in Arabidopsis leaf vascular development. Plant Physiol **131,** 1327-1339.

Mayer, K.F., Schoof, H., Haecker, A., Lenhard, M., Jurgens, G., and Laux, T. (1998). Role of WUSCHEL in regulating stem cell fate in the Arabidopsis shoot meristem. Cell **95,** 805-815.

McConnell, J.R., and Barton, M.K. (1998). Leaf polarity and meristem formation in Arabidopsis. Development **125,** 2935-2942.

McConnell, J.R., Emery, J., Eshed, Y., Bao, N., Bowman, J., and Barton, M.K. (2001). Role of PHABULOSA and PHAVOLUTA in determining radial patterning in shoots. Nature **411,** 709-713.

Mette, M.F., Aufsatz, W., van der Winden, J., Matzke, M.A., and Matzke, A.J. (2000). Transcriptional silencing and promoter methylation triggered by double-stranded RNA. EMBO J **19,** 5194-5201.

Meyers, B.C., Axtell, M.J., Bartel, B., Bartel, D.P., Baulcombe, D., Bowman, J.L., Cao, X., Carrington, J.C., Chen, X., Green, P.J., Griffiths-Jones, S., Jacobsen, S.E., Mallory, A.C.,

Martienssen, R.A., Poethig, R.S., Qi, Y., Vaucheret, H., Voinnet, O., Watanabe, Y., Weigel, D., and Zhu, J.K. (2008). Criteria for annotation of plant MicroRNAs. Plant Cell **20,** 3186-3190.

Miyashima, S., Koi, S., Hashimoto, T., and Nakajima, K. (2011). Non-cell-autonomous microRNA165 acts in a dose-dependent manner to regulate multiple differentiation status in the Arabidopsis root. Development **138,** 2303-2313.

Moss, E.G., Lee, R.C., and Ambros, V. (1997). The cold shock domain protein LIN-28 controls developmental timing in C. elegans and is regulated by the lin-4 RNA. Cell **88,** 637-646.

Muller, B., and Sheen, J. (2008). Cytokinin and auxin interaction in root stem-cell specification during early embryogenesis. Nature **453,** 1094-1097.

Nakajima, K., Sena, G., Nawy, T., and Benfey, P.N. (2001). Intercellular movement of the putative transcription factor SHR in root patterning. Nature **413,** 307-311.

Nodine, M.D., and Bartel, D.P. MicroRNAs prevent precocious gene expression and enable pattern formation during plant embryogenesis. Genes Dev **24,** 2678-2692.

Nodine, M.D., and Bartel, D.P. (2010). MicroRNAs prevent precocious gene expression and enable pattern formation during plant embryogenesis. Genes & Development **24,** 2678-2692.

Otsuga, D., DeGuzman, B., Prigge, M.J., Drews, G.N., and Clark, S.E. (2001). REVOLUTA regulates meristem initiation at lateral positions. The Plant journal : for cell and molecular biology **25,** 223-236.

Pagnussat, G.C., Alandete-Saez, M., Bowman, J.L., and Sundaresan, V. (2009). Auxin-Dependent Patterning and Gamete Specification in the Arabidopsis Female Gametophyte. Science (New York, N.Y.) **324,** 1684-1689.

Petrasek, J., Mravec, J., Bouchard, R., Blakeslee, J.J., Abas, M., Seifertova, D., Wisniewska, J., Tadele, Z., Kubes, M., Covanova, M., Dhonukshe, P., Skupa, P., Benkova, E., Perry, L., Krecek, P., Lee, O.R., Fink, G.R., Geisler, M., Murphy, A.S., Luschnig, C., Zazimalova, E., and Friml, J. (2006). PIN proteins perform a rate-limiting function in cellular auxin efflux. Science (New York, N.Y.) **312,** 914-918.

Prigge, M.J., Otsuga, D., Alonso, J.M., Ecker, J.R., Drews, G.N., and Clark, S.E. (2005). Class III homeodomain-leucine zipper gene family members have overlapping, antagonistic, and distinct roles in Arabidopsis development. Plant Cell **17,** 61-76.

Rajagopalan, R., Vaucheret, H., Trejo, J., and Bartel, D.P. (2006). A diverse and evolutionarily fluid set of microRNAs in Arabidopsis thaliana. Genes Dev **20,** 3407-3425.

Ramachandran, V., and Chen, X. (2008). Small RNA metabolism in Arabidopsis. Trends Plant Sci **13,** 368-374.

Raven, P.H., Evert, R.F., and Eichhorn, S.E. (2005). Biology of Plants (Seventh Edition). W. H. Freeman and Company Publishers.

Reinhart, B.J., Slack, F.J., Basson, M., Pasquinelli, A.E., Bettinger, J.C., Rougvie, A.E., Horvitz, H.R., and Ruvkun, G. (2000). The 21-nucleotide let-7 RNA regulates developmental timing in Caenorhabditis elegans. Nature **403,** 901-906.

Rogers, K., and Chen, X. (2013). Biogenesis, Turnover, and Mode of Action of Plant MicroRNAs. Plant Cell **25,** 2383-2399.

Romanov, G.A., Lomin, S.N., and Schmulling, T. (2006). Biochemical characteristics and ligand-binding properties of Arabidopsis cytokinin receptor AHK3 compared to CRE1/AHK4 as revealed by a direct binding assay. Journal of experimental botany **57,** 4051-4058.

Rutjens, B., Bao, D., van Eck-Stouten, E., Brand, M., Smeekens, S., and Proveniers, M. (2009). Shoot apical meristem function in Arabidopsis requires the combined activities of three BEL1-like homeodomain proteins. The Plant journal : for cell and molecular biology **58,** 641-654.

Ruzicka, K., Simaskova, M., Duclercq, J., Petrasek, J., Zazimalova, E., Simon, S., Friml, J., Van Montagu, M.C., and Benkova, E. (2009). Cytokinin regulates root meristem activity via

modulation of the polar auxin transport. Proceedings of the National Academy of Sciences of the United States of America **106,** 4284-4289.

Sabatini, S., Heidstra, R., Wildwater, M., and Scheres, B. (2003). SCARECROW is involved in positioning the stem cell niche in the Arabidopsis root meristem. Genes Dev **17,** 354-358.

San-Bento, R., Farcot, E., Galletti, R., Creff, A., and Ingram, G. (2013). Epidermal identity is maintained by cell-cell communication via a universally active feedback loop in Arabidopsis thaliana. The Plant journal : for cell and molecular biology.

Sarkar, A.K., Luijten, M., Miyashima, S., Lenhard, M., Hashimoto, T., Nakajima, K., Scheres, B., Heidstra, R., and Laux, T. (2007). Conserved factors regulate signalling in Arabidopsis thaliana shoot and root stem cell organizers. Nature **446,** 811-814.

Scheres, B., Wolkenfelt, H., Willemsen, V., Terlouw, M., Lawson, E., Dean, C., and Weisbeek, P. (1994). Embryonic origin of the Arabidopsis primary root and root meristem initials. Development **120,** 2475-2487.

Scheres, B., Di Laurenzio, L., Willemsen, V., Hauser, M.T., Janmaat, K., Weisbeek, P., and Benfey, P.N. (1995). Mutations affecting the radial organisation of the Arabidopsis root display specific defects throughout the embryonic axis. Development **121,** 53-62.

Schlereth, A., Moller, B., Liu, W., Kientz, M., Flipse, J., Rademacher, E.H., Schmid, M., Jurgens, G., and Weijers, D. (2010). MONOPTEROS controls embryonic root initiation by regulating a mobile transcription factor. Nature **464,** 913-916.

Sevilem, I., Miyashima, S., and Helariutta, Y. (2013). Cell-to-cell communication via plasmodesmata in vascular plants. Cell adhesion & migration **7,** 27-32.

Shin, C., Nam, J.-W., Farh, K.K.-H., Chiang, H.R., Shkumatava, A., and Bartel, D.P. (2010). Expanding the MicroRNA Targeting Code: Functional Sites with Centered Pairing. Molecular cell **38,** 789-802.

Smith, Z.R., and Long, J.A. (2010). Control of Arabidopsis apical-basal embryo polarity by antagonistic transcription factors. Nature **464,** 423-426.

Souter, M., and Lindsey, K. (2000). Polarity and signalling in plant embryogenesis. Journal of experimental botany **51,** 971-983.

Spichal, L., Rakova, N.Y., Riefler, M., Mizuno, T., Romanov, G.A., Strnad, M., and Schmulling, T. (2004). Two cytokinin receptors of Arabidopsis thaliana, CRE1/AHK4 and AHK3, differ in their ligand specificity in a bacterial assay. Plant Cell Physiol **45,** 1299-1305.

Stadler, R., Wright, K.M., Lauterbach, C., Amon, G., Gahrtz, M., Feuerstein, A., Oparka, K.J., and Sauer, N. (2005). Expression of GFP-fusions in Arabidopsis companion cells reveals non-specific protein trafficking into sieve elements and identifies a novel post-phloem domain in roots. The Plant journal : for cell and molecular biology **41,** 319-331.

Steinmann, T., Geldner, N., Grebe, M., Mangold, S., Jackson, C.L., Paris, S., Galweiler, L., Palme, K., and Jurgens, G. (1999). Coordinated polar localization of auxin efflux carrier PIN1 by GNOM ARF GEF. Science (New York, N.Y.) **286,** 316-318.

Szemenyei, H., Hannon, M., and Long, J.A. (2008). TOPLESS mediates auxin-dependent transcriptional repression during Arabidopsis embryogenesis. Science (New York, N.Y.) **319,** 1384-1386.

Takada, S., Hibara, K., Ishida, T., and Tasaka, M. (2001). The CUP-SHAPED COTYLEDON1 gene of Arabidopsis regulates shoot apical meristem formation. Development **128,** 1127-1135.

Tanaka, H., Watanabe, M., Watanabe, D., Tanaka, T., Machida, C., and Machida, Y. (2002). ACR4, a Putative Receptor Kinase Gene of Arabidopsis thaliana, that is Expressed in the Outer Cell Layers of Embryos and Plants, is Involved in Proper Embryogenesis. Plant and Cell Physiology **43,** 419-428.

Tanaka, H., Onouchi, H., Kondo, M., Hara-Nishimura, I., Nishimura, M., Machida, C., and Machida, Y. (2001). A subtilisin-like serine protease is required for epidermal surface formation in Arabidopsis embryos and juvenile plants. Development **128,** 4681-4689.

Tanaka, H., Watanabe, M., Sasabe, M., Hiroe, T., Tanaka, T., Tsukaya, H., Ikezaki, M., Machida, C., and Machida, Y. (2007). Novel receptor-like kinase ALE2 controls shoot development by specifying epidermis in Arabidopsis. Development **134,** 1643-1652.

Todesco, M., Rubio-Somoza, I., Paz-Ares, J., and Weigel, D. (2010). A collection of target mimics for comprehensive analysis of microRNA function in Arabidopsis thaliana. PLoS Genet **6,** e1001031.

Treml, B.S., Winderl, S., Radykewicz, R., Herz, M., Schweizer, G., Hutzler, P., Glawischnig, E., and Ruiz, R.A. (2005). The gene ENHANCER OF PINOID controls cotyledon development in the Arabidopsis embryo. Development **132,** 4063-4074.

Truernit, E., and Haseloff, J. (2007). A Role for KNAT Class II Genes in Root Development. Plant signalling & behavior **2,** 10-12.

Ueda, M., Zhang, Z., and Laux, T. (2011). Transcriptional Activation of Arabidopsis Axis Patterning Genes WOX8/9 Links Zygote Polarity to Embryo Development. Developmental Cell **20,** 264-270.

Vaucheret, H. (2008). Plant ARGONAUTES. Trends in Plant Science **13,** 350-358.

Vazquez, F. (2006). Arabidopsis endogenous small RNAs: highways and byways. Trends Plant Sci **11,** 460-468.

Vieten, A., Vanneste, S., Wisniewska, J., Benkova, E., Benjamins, R., Beeckman, T., Luschnig, C., and Friml, J. (2005). Functional redundancy of PIN proteins is accompanied by auxin-dependent cross-regulation of PIN expression. Development **132,** 4521-4531.

Voinnet, O. (2009). Origin, biogenesis, and activity of plant microRNAs. Cell **136,** 669-687.

Vroemen, C.W., Mordhorst, A.P., Albrecht, C., Kwaaitaal, M.A., and de Vries, S.C. (2003). The CUP-SHAPED COTYLEDON3 gene is required for boundary and shoot meristem formation in Arabidopsis. Plant Cell **15,** 1563-1577.

Walbot, V. (1985). On the life strategies of plants and animals. Trends in genetics : TIG **1,** 165-169.

Wang, H., Ngwenyama, N., Liu, Y., Walker, J.C., and Zhang, S. (2007). Stomatal Development and Patterning Are Regulated by Environmentally Responsive Mitogen-Activated Protein Kinases in Arabidopsis. The Plant Cell Online **19,** 63-73.

Weijers, D., Schlereth, A., Ehrismann, J.S., Schwank, G., Kientz, M., and Jurgens, G. (2006). Auxin triggers transient local signalling for cell specification in Arabidopsis embryogenesis. Dev Cell **10,** 265-270.

Weijers, D., Benkova, E., Jager, K.E., Schlereth, A., Hamann, T., Kientz, M., Wilmoth, J.C., Reed, J.W., and Jurgens, G. (2005). Developmental specificity of auxin response by pairs of ARF and Aux/IAA transcriptional regulators. Embo J **24,** 1874-1885.

Werner, D., Gerlitz, N., and Stadler, R. (2011). A dual switch in phloem unloading during ovule development in Arabidopsis. Protoplasma **248,** 225-235.

Wightman, B., Ha, I., and Ruvkun, G. (1993). Posttranscriptional regulation of the heterochronic gene lin-14 by lin-4 mediates temporal pattern formation in C. elegans. Cell **75,** 855-862.

Willemsen, V., and Scheres, B. (2004). MECHANISMS OF PATTERN FORMATION IN PLANT EMBRYOGENESIS. Annual Review of Genetics **38,** 587-614.

Williams, L., Grigg, S.P., Xie, M., Christensen, S., and Fletcher, J.C. (2005). Regulation of Arabidopsis shoot apical meristem and lateral organ formation by microRNA miR166g and its AtHD-ZIP target genes. Development **132,** 3657-3668.

Wisniewska, J., Xu, J., Seifertova, D., Brewer, P.B., Ruzicka, K., Blilou, I., Rouquie, D., Benkova, E., Scheres, B., and Friml, J. (2006). Polar PIN localization directs auxin flow in plants. Science (New York, N.Y.) **312,** 883.

Wu, G., Park, M.Y., Conway, S.R., Wang, J.W., Weigel, D., and Poethig, R.S. (2009). The sequential action of miR156 and miR172 regulates developmental timing in Arabidopsis. Cell **138,** 750-759.

Wu, X., Chory, J., and Weigel, D. (2007). Combinations of WOX activities regulate tissue proliferation during Arabidopsis embryonic development. Developmental Biology **309,** 306-316.

Wysocka-Diller, J.W., Helariutta, Y., Fukaki, H., Malamy, J.E., and Benfey, P.N. (2000). Molecular analysis of SCARECROW function reveals a radial patterning mechanism common to root and shoot. Development **127,** 595-603.

Xie, Z., Allen, E., Fahlgren, N., Calamar, A., Givan, S.A., and Carrington, J.C. (2005). Expression of Arabidopsis MIRNA Genes. PLANT PHYSIOLOGY **138,** 2145-2154.

Xu, M., Cho, E., Burch-Smith, T.M., and Zambryski, P.C. (2012). Plasmodesmata formation and cell-to-cell transport are reduced in decreased size exclusion limit 1 during embryogenesis in Arabidopsis. Proceedings of the National Academy of Sciences of the United States of America **109,** 5098-5103.

Yang, L., Wu, G., and Poethig, R.S. (2012). Mutations in the GW-repeat protein SUO reveal a developmental function for microRNA-mediated translational repression in Arabidopsis. Proceedings of the National Academy of Sciences of the United States of America **109,** 315-320.

Yang, X., Murthy, V., Schultz, K., Tatro, J.B., Fitzgerald, K.A., and Beasley, D. (2006). Toll-like receptor 3 signalling evokes a proinflammatory and proliferative phenotype in human vascular smooth muscle cells. Am J Physiol Heart Circ Physiol **291,** H2334-2343.

Yoshikawa, M., Peragine, A., Park, M.Y., and Poethig, R.S. (2005). A pathway for the biogenesis of trans-acting siRNAs in Arabidopsis. Genes Dev **19,** 2164-2175.

Zambryski, P., and Crawford, K. (2000). Plasmodesmata: gatekeepers for cell-to-cell transport of developmental signals in plants. Annu Rev Cell Dev Biol **16,** 393-421.

Zeng, Y., Yi, R., and Cullen, B.R. (2003). MicroRNAs and small interfering RNAs can inhibit mRNA expression by similar mechanisms. Proceedings of the National Academy of Sciences **100,** 9779-9784.

Zhang, J., Liu, W., Yang, X., Gao, A., Li, X., Wu, X., and Li, L. (2011). Isolation and characterization of two putative cytokinin oxidase genes related to grain number per spike phenotype in wheat. Molecular biology reports **38,** 2337-2347.

Zheng, X., Zhu, J., Kapoor, A., and Zhu, J.K. (2007). Role of Arabidopsis AGO6 in siRNA accumulation, DNA methylation and transcriptional gene silencing. EMBO J **26,** 1691-1701.

Zilberman, D., Cao, X., and Jacobsen, S.E. (2003). ARGONAUTE4 control of locus-specific siRNA accumulation and DNA and histone methylation. Science (New York, N.Y.) **299,** 716-719.